Optical and Radar Remotely Sensed Data for Large-area Wildlife Habitat Mapping

A Thesis Submitted to the College of

Graduate Studies and Research

in Partial Fulfillment of the Requirements

for the Degree of Doctor of Philosophy

in the Department of Geography and Planning

University of Saskatchewan

Saskatoon

By

KAI WANG

PERMISSION TO USE

In presenting this thesis in partial fulfillment of the requirements for a Postgraduate degree from the University of Saskatchewan, I agree that the Libraries of the University may make it freely available for inspection. I further agree that permission for copying of this thesis in any manner, in whole or in part, for scholarly purposes may be granted by the professors who supervised my thesis work or, in their absence, by the Head of the Department or the Dean of the College in which my thesis work was completed. It is understood that any copying or publication of use of this thesis or parts thereof for financial gain shall not be allowed without my written permission. It is also understood that due recognition shall be given to me and to the University of Saskatchewan in any scholarly use which may be made of any material in my thesis.

Requests for permission to copy or to make any other use of the material in this thesis in whole or in part should be addressed to:

Head of the Department of Geography and Planning

University of Saskatchewan

Saskatoon, Saskatchewan, S7N 5C8, Canada

ABSTRACT

Wildlife habitat mapping strongly supports applications in natural resource management, environmental conservation, impacts of anthropogenic activity, perturbed ecosystem restoration, species-at-risk recovery and species inventory. Remote sensing has long been identified as a feasible and effective technology for large-area wildlife habitat mapping. However, existing and future uncertainties in remote sensing will definitely have a significant effect on relevant scientific research, such as the limitation of Landsat-series data; the negative impact of cloud and cloud shadows (CCS) in optical imagery; and landscape pattern analysis using remote sensing classification products. This thesis adopted a manuscript-style format; it addresses these challenges (or uncertainties) and opportunities through exploring the state-of-the-art optical and radar remotely sensed data for large-area wildlife habitat mapping, and investigating their feasibility and applicability primarily by comparison either on the level of direct remote sensing products (e.g. classification accuracy) or indirect ecological model (e.g. presence/absence and frequency of use model based on landscape pattern analysis). A framework designed to identify and investigate the potential remotely sensed data, including Disaster Monitoring Constellation (DMC), Landsat Thematic Mapper (TM), Indian Remote Sensing (IRS), and RADARSAT-2, has been developed. The chosen DMC and RADARSAT-2 imagery have acceptable capability of addressing the existing and potential challenges (or uncertainties) in remote sensing of large-area habitat mapping, in order to produce cloud-free thematic maps for the study of wildlife habitat. A quantitative comparison between Landsat-based and IRS-based analyses showed that the characteristics of remote sensing products play an important role in landscape pattern analysis to build grizzly bear presence/absence and frequency of use models.

ACKNOWLEDGEMENTS

I am truly blessed to have Dr. Xulin Guo and Dr. Steven Franklin as my co-supervisors. To me, they both are my best mentors, advisors, research partners and friends. Without their priceless support and shelter, I could never ever have completed this dissertation, and accomplished my Ph.D. program. I would like to thank my committee members, Dr. Marc Cattet, Dr. Dirk de Boer, Dr. Scott Bell, Dr. Mohammad Kamal, and Dr. Gregory McDermid for their valuable help and guidance through my Ph.D. study. I am also grateful to my external reviewer, Dr. Jinfei Wang for devoting her precious time to serve on my dissertation, and providing pertinent comments on the revision. I wish to express my gratitude to Dr. Yuhong He, who helps me go through the first but the hardest year in my Ph.D. program.

I would like to acknowledge Zhaoqin Li, Xiaohui Yang, Sarah Lowe, Erica Kovach, David Oh, Erica Keet, Dr. Zhangbao Ma, Li Shen, Meng Li, and Carmen Finnigan for their help and advice on thesis proposal, data processing, manuscript preparation, and proof reading.

Thanks go to the Foothills Research Institute Grizzly Bear Program (FRIGBP), the Natural Sciences and Engineering Research Council of Canada (NSERC), the Department of Geography and Planning at the University of Saskatchewan for funding me, and DMC International Imaging Ltd. and SOAR-E of Canadian Space Agency (CSA) for sponsoring imagery.

Finally, I am deeply grateful to my parents, Qinxiang Zhang and Gui Wang, and my brother-like friends in China. Without your love, support and encouragement, any of my achievements would not have been possible. This dissertation also belongs to you all.

TABLE OF CONTENTS

LIST OF TABLES

LIST OF FIGURES

CHAPTER 1 - INTRODUCTION

The concept of habitat is a cornerstone in wildlife ecology (Hall et al., 1997; Morrison et al., 2006). Hall et al. (1997) defined that "habitats are the resources and conditions present in an area that produce occupancy, including survival and reproduction, by a given organism, and, as such, imply more than vegetation and vegetation structure. A habitat is the sum of the specific resources that are needed by an organism". The definition of habitat should refer to three principal concepts (Mitchell, 2005): 1) Where an organism lives; 2) Environment in its physical and chemical aspects; and 3) Community concepts. Mapping and monitoring wildlife habitat has become the key component used to interpret organism distribution, evaluate population dynamics, and predict abundance/biomass of organisms.

Remote sensing has become an indispensable tool for habitat mapping applications because of its broad spatial extents that cannot be obtained using field-based methods (Kerr and Ostrovsky, 2003). Aplin (2005) pointed out that the field-based approaches generate measurements with high accuracy, but it is generally impractical for any studies beyond local scale due to its labor and time intensity. Remote sensing data and techniques observe the target or area of interest at scales ranging from individual landscapes (local scale) to the entire world (global scale) (Kerr and Ostrovsky, 2003). Besides the advantage in scale, others should be underlined including the practical integration of remote sensing (RS) and geographic information system (GIS) (Campbell, 2007; Foody, 2008), the capability of long-term change detection (Rindfuss et al., 2004, Warner et al., 2009), the data fusion of different sources (Pohl and van Genderen, 1998; Gamba and Chanussot, 2008), non-disturbance of object or area of interest

(Jensen, 2007), public communication (i.e. remote sensed data are highly persuasive, and therefore can be easily used to reveal scientific results to the public) (Sohl, 1999), etc.

Grizzly bear (*Ursus arctos* L.) is a species widely recognized as an indicator of ecosystem health in west-central Alberta (Maehr et al., 2001). The Foothills Research Institute Grizzly Bear Program (FRIGBP, formerly called Foothills Model Forest Grizzly Bear Research Program), initiated in 1999, focuses on the relationships between landscape conditions, landscape change (human-caused), and health in grizzly bears (Stenhouse, 2008). More specifically, this program is meant to provide knowledge and planning tools to the land and resource managers in order to ensure the long-term conservation of grizzly bears in Alberta (McDermid, 2005). 2010/11 marks the eleventh year in which remote sensing specialists have contributed products and services to the FRIGBP.

However, both present and future uncertainties in remote sensing (RS) will definitely have a significant effect on scientific research regarding large-area habitats, such as the limitation of Landsat-series data; the negative impact of cloud and cloud shadows (CCS) in optical imagery; and landscape pattern analysis using RS classification products (Wang et al., 2009). Therefore, the main purpose of this research is to identify and investigate potential remotely sensed data sources and methods to address the aforementioned uncertainties (including both challenges and opportunities) in large-area habitat mapping, especially in the grizzly bear habitat mapping.

1.1 Research objectives

1.1.1 Research hypothesis

The overall hypothesis of this research is that optical and radar remote sensing can reliably and effectively generate wildlife-habitat information over large-areas.

More specifically,

- The alternative imagery with medium spatial resolution can be used as the primary resource for large-area habitat mapping.
- The alternative imagery with medium spatial resolution can produce reliable products compared with those based on Landsat imagery.
- The landscape pattern analysis can be further characterized via the comparison of presence/absence and frequency of use models based on diverse remote sensing products.

1.1.2 Research objectives

In order to address these research gaps (see more detailed elucidation in Chapter 2), the aim of this study is to:

- Review problems in remote sensing of landscapes and habitats, and provide theoretically possible solutions;
- Investigate the applicability of Disaster Monitoring Constellation (DMC) and Radarsat-2 imagery for large-area wildlife habitat mapping; and
- Identify the response of landscape pattern analysis to diverse remote sensing products.

1.2 Thesis structure

There are seven chapters in this thesis (Figure 1.1). Chapter 1 is the brief introduction, which includes research background, research objectives and thesis structure. Chapter 2 identifies the current challenges and opportunities in remote sensing for large-area wildlife habitat mapping, and accordingly provides possible solutions and directions for further research. Chapter 3 compares the Landsat multispectral and Indian Remote Sensing (IRS) panchromatic imagery for landscape pattern analysis of grizzly bear habitat in agricultural areas of western Alberta. Chapter 4 examines the applicability of small-satellite constellation in classification for large-area habitat mapping: a case study of DMC multispectral imagery in west-central Alberta. The textural information on the application of Synthetic Aperture Radar (SAR) imagery under the environment of northern boreal forest is evaluated in Chapter 5. Chapter 6 is the summary of this thesis.

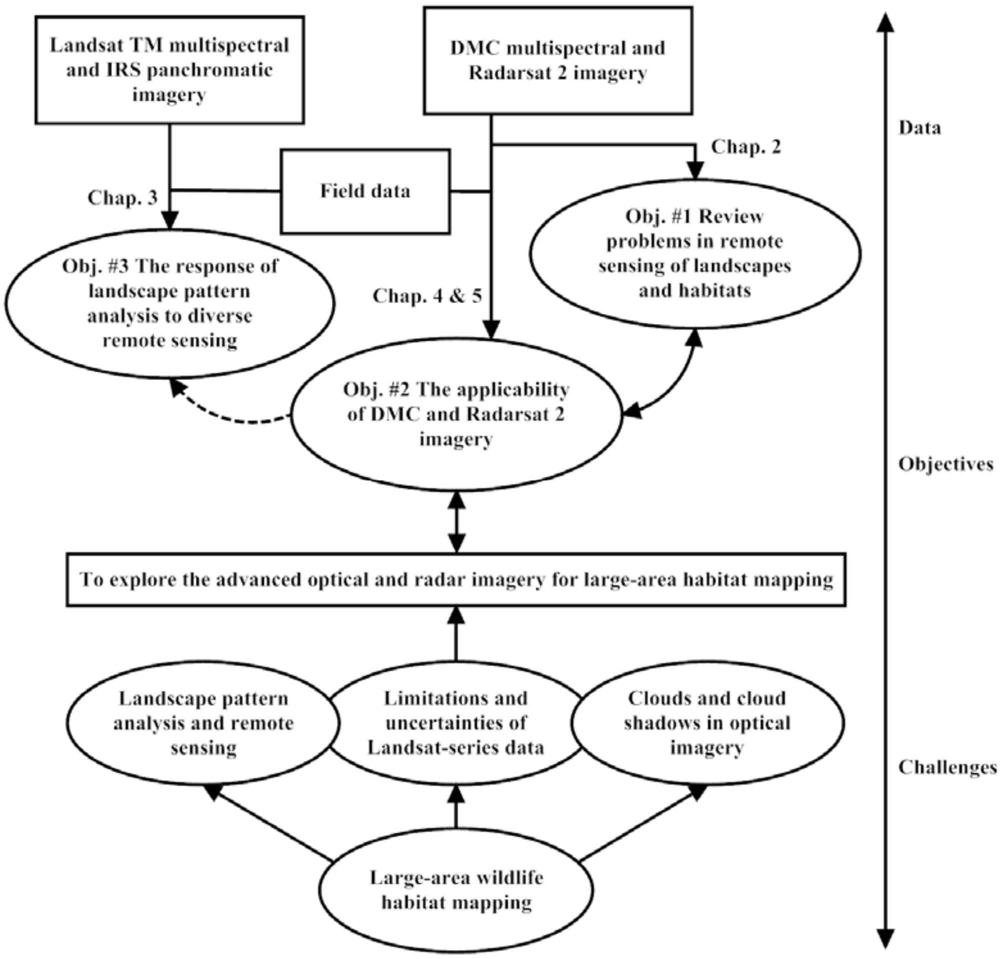

Figure 1.1 Framework of this thesis and thesis structure

1.3 References

Aplin, P. 2005: Remote sensing: ecology. *Progress in Physical Geography* 29, 104-13.

Campbell, J.B. 2007: *Introduction to remote sensing* (fourth edition). New York, NY: Guilford Press.

Foody, G.M. 2008: GIS: biodiversity applications. *Progress in Physical Geography* 32, 223-35.

Gamba, P. and Chanussot, J. 2008: Guest editorial: Foreword to the special issue on data fusion. *IEEE Transactions on Geoscience and Remote Sensing* 46, 1283-88.

Hall, L.S., Krausman, P.R. and Morrison, M.L. 1997: The habitat concept and a plea for standard terminology. *Wildlife Society Bulletin* 25, 173-82.

Jensen, J.R. 2007: *Remote sensing of the environment: An Earth resource perspective.* Second edition. Upper Saddle River, NJ: Pearson Prentice Hall, 4 and 291-294.

Kerr, J.T. and Ostrovsky, M. 2003: From space to species: ecological applications for remote sensing. *Trends in Ecology and Evolution* 18, 299-305.

Maehr, D.S., Noss, R.F. and Larkin, J.L. 2001: Large Mammal Restoration: Ecological and Sociological Challenges in the 21st Century. Island Press, Washington, D.C., pp. 71-72.

McDermid, G.J. 2005: Remote sensing for large-area, multi-jurisdictional habitat mapping. PhD thesis. Waterloo, ON: University of Waterloo.

Mitchell, S.C. 2005: How useful is the concept of habitat? – A critique. *Oikos* 110, 634-38.

Morrison, M.L., Marot, B.G. and Mannan, R.W. 2006: *Wildlife-habitat relationships: Concepts and application.* Third edition. Washington D.C.: Island Press, 3-128.

Pohl, C. and van Genderen, J.L.1998: Multisensor image fusion in remote sensing: concepts, methods and applications. *International Journal of Remote Sensing* 19, 823-54.

Rindfuss, R.R., S.J. Walsh, B.L. Turner, II, J. Fox, and V. Mishra, 2004. Developing a science of land change: challenges and methodological issues. Proceedings of the National Academics of Science, 101(39): 13976-13981. DOI: 10.1073/pnas.0401545101.

Sohl, T., 1999. Change analysis in the United Arab Emirates: an investigation of techniques. PE&RS, 65(4), 475-484.

Stenhouse, G. 2008: Introduction. In: Stenhouse, G., and K. Graham (eds), 2008. *Foothills Research Institute Grizzly Bear Program 2007 Annual Report.* Hinton, Alberta. 204pp.

Wang, K., Franklin, S.E., Guo, X., He, Y. and McDermid, G.J. 2009: Problems in remote sensing of landscapes and habitats. Progress in Physical Geography 33, 747-68.

Warner, T.A., A. Almutairi, and J.Y. Lee, 2009. Remote sensing of land cover change. In: T.A. Warner, M. Duane Nellis, and G.M. Foody (eds), The SAGE Handbook of Remote Sensing, SAGE Publications.

CHAPTER 2 - PROBLEMS IN REMOTE SENSING OF LANDSCAPES AND HABITATS[1]

2.1 Abstract

Wildlife habitat mapping strongly supports applications in natural resource management, environmental conservation, impacts of anthropogenic activity, perturbed ecosystem restoration, species-at-risk recovery and species inventory. Remote sensing has long been identified as a feasible and effective technology for large-area habitat mapping. However, existing and future uncertainties in remote sensing will definitely have a significant effect on the relevant scientific research. This article attempts to identify the current challenges and opportunities in remote sensing for large-area wildlife habitat mapping, and accordingly provide possible solutions and directions for further research.

2.2 Introduction

Wildlife habitat, representing the physical space within which an organism lives, and the applicable resources (including biotic and abiotic entities; Hall et al., 1997), are recognized as critical to the size of a wildlife population, playing a central role in basic and applied ecology (Mitchell, 2005). Mapping and monitoring wildlife habitat has become the key component used to interpret organism distribution, evaluate population dynamics, and predict abundance/biomass of organisms. It also strongly supports applications in natural resource management,

[1] The full citation of this published chapter is: Wang, K., Franklin, S.E., Guo, X., He, Y., and McDermid, G.J. 2009. Problems in remote sensing of landscapes and habitats. Progress in Physical Geography, 33(6): 747-768. This article is re-printed according to SAGE Publications copyright regulations.

environmental conservation, impacts of anthropogenic activity, perturbed ecosystem restoration, species-at-risk recovery and species inventory (Mitchell, 2005; Morrison et al., 2006). Most studies use physical environment characteristics when describing wildlife-habitat relationships or mapping wildlife habitat, for example land cover (Hansen et al., 2001; Collingwood, 2008; McDermid et al., 2008), canopy closure (Hyde, 2005), leaf area index (LAI) (Chen et al., 1992; Qi et al., 2000; Li et al., 2008), etc.

Jensen (2007: 4) suggested, 'Remote sensing is the noncontact recording of information from the ultraviolet, visible, infrared, and microwave regions of the electromagnetic spectrum by means of instruments such as cameras, scanners, lasers, linear arrays, and / or area arrays located on platforms such as aircraft or spacecraft, and the analysis of acquired information by means of visual and digital image processing'. Remote sensing has long been identified as a feasible and effective technology for large-area habitat mapping (Osborne et al., 2001; McDermid, 2005; Hyde, 2005), compared with in-situ observation which has obvious limitations in time, cost and labor. However, both present and future uncertainties in remote sensing (RS) will definitely have a significant effect on scientific research regarding large-area habitats, such as the limitation of Landsat-series data; the negative impact of cloud and cloud shadows (CCS) in optical imagery; and landscape pattern analysis using RS classification products. This review focuses on three aspects relating to present and anticipated sources of uncertainty: 1) current challenges and opportunities in remote sensing; 2) possible sensors and methods to deal with these challenges and opportunities; and 3) the application issue - landscape analysis and remote sensing.

2.3 Current challenges and opportunities in remote sensing

With the increasing abundance of RS products and RS techniques, more-and-more challenges and opportunities emerge. Here, we focus on three significant aspects of current challenges and opportunities: 1) the Landsat-series data in large-area habit mapping; 2) clouds and cloud shadows; and 3) data fusion.

2.3.1 The Landsat-series data in large-area habitat mapping

The first satellite of the Landsat series was launched in 1972, and until 2008 the Landsat program has provided a continuous record of earth observation data for 36 years (Landsat 5 and 7 sensors are also available for delivering data). The archived images from the program present the longest continual remotely-sensed datasets available for monitoring spaced-based environment (Draeger et al., 1997). Cohen and Goward (2004) have indicated that, of all remotely sensed data, data acquired by Landsat sensors have played the most pivotal role in modeling biogeochemical cycles, and also for characterizing land cover, vegetation biophysical attributes, forest structure, and fragmentation in relation to biodiversity. Franklin and Wulder (2002) argued that Landsat, due to the distinctive combination of spatial and spectral resolutions, is the best satellite sensor supporting management, monitoring, and scientific activities over large-areas. In the world-famous citation database – Web of Science - users can access 5675 articles on remote sensing subject areas if the search topic is set to remote sensing. Of these, there are 2857 articles referring to Landsat, which exceeds 50% of the total (search on 20 November 2008). Wulder et al. (2008) concluded that the reasons for the prevalence of Landsat series are: 1) the sensor characteristics adapt perfectly to ecological application over large areas with large amounts of detail, such as the combination of spatial, spectral and temporal resolutions, and reasonable image size; 2) a 36-year record of Landsat data makes long-term change detection commonplace; and 3) the Landsat data policy, covering data acquisition, processing, archiving, distribution, and pricing, facilitates the widespread use of data.

However, some of the Landsat characteristics restrict its application in large-area habitat mapping, including a 16-day temporal resolution, 180 km image size, and the gap of Landsat continuity. More specifically, the 16-day Landsat revisit cycle has limited Landsat's use for monitoring biodynamics (Ranson et al., 2003; Roy et al., 2008), and blocked the application for detecting rapid surface changes such as crop-growth monitoring and detecting intraseasonal ecosystem disturbance (Gao et al., 2006; Pape and Franklin, 2008). The 185 × 185 km image size is not always suitable for the large-area applications. For example, the Foothills Research Institute Grizzly Bear Program (FRIGBP, formerly called Foothills Model Forest Grizzly Bear Research Program), initiated in 1999, is using Landsat-based products to study the relationships between landscape conditions, landscape change (human-caused), and health in grizzly bears in Alberta, Canada (Stenhouse, 2008). But the total study area should cover 273,071 km^2 (Kansas, 2002), and the 185 × 185 km size is not big enough to cover the area in a study period. Therefore, the researchers developed mosaic methods (McDermid et al., 2008) to combine land cover maps from different years forming a large map of the whole study area (i.e. first divide the whole study area into several sub-units; then classify a sub-unit per year; finally combine all of the sub-units together). This classified map as a whole, cannot, however, present the updated situation of land cover, because the map of the first sub-unit was generated in 1999, and that of the last one in 2007 (McDermid et al., 2008). It is a major problem for subsequent users, such as resource managers, ecologists, etc.

In addition, after mapping the Earth's surface for over 30 years to meet a wide range of information needs (Chander, 2007), a gap in Landsat continuity appears unavoidable before the Landsat Data Continuity Mission data is potentially available in approximately December 2012 (as revealed by the National Aeronautics and Space Administration, NASA). The Landsat 5 TM (Thematic Mapper) sensor has been in orbit for more than 24 years, far exceeding its design life of four years, and continues to provide quality data products. Its duty cycle has been reduced and could systematically fail at any time because of the instruments age (Chander, 2007) – note problems with the solar array drive mechanism in 2005 (Wulder et al., 2008). The Landsat 7 ETM+ (Enhanced Thematic Mapper Plus) sensor failed the Scan Line Corrector (SLC) in 2003, and should have retired in 2004 (Chander, 2007). It is likely that both satellites will run out of fuel before the end of 2010 (Chander, 2007).

2.3.2 Clouds and cloud shadows

Remote sensing demonstrates a high quality of performance in many applications on account of global and repetitive measurement capability, such as scene analysis, land-use classification, landscape ecological change detection, terrain modeling, etc. However, regardless of the variety of uses for remote sensing images, the first goal is to extract landscape information from the satellite images (Tseng et al., 2008). Unfortunately, two-thirds of the Earth's surface is always covered by clouds throughout the year (Wang et al., 1999), causing serious problems in optical wavelength remote sensing (Wang et al., 1999). Esche et al. (2002) also stated that since approximately 50% of the earth is covered in cloud at any given time, one of the most significant challenges in creating repeatable and robust classifications is understanding and appropriately addressing cloud contamination. Since clouds and the shadows they cast blur the optical imagery, many of the applications are impeded. For example, cloud shadow affects the accuracy of vegetation estimates, and cloud cover affects the climate system over a broad range of time and space scales (Simpson and Stitt, 1998). Asner (2001) studied cloud cover in Landsat observations of the Brazilian Amazon and identified that clouds are a major obstacle to optical remote sensing of humid tropical regions.

Many researchers have attempted to detect clouds and the corresponding cloud shadows so as to eliminate cloud contamination producing cloud-free imagery, such as Tseng et al. (2008), Chen (2001), and Wang et al. (1999). However, numerous obstacles still exist. For example, Chen (2001) stated that the thin cloud and cloud shadow pixels had similar reflectance ranges to the cloud-free pixels; in particular, both cloud shadow and water pixels had a very similar reflectance range, and Griffin et al. (2003) indicated that bright surface features such as snow, ice and sand can easily be mistaken for cloud features in the visible portion of the spectrum. Even though the locations of clouds can be detected, it is still difficult to estimate the locations of their corresponding shadows (Want et al., 1999). This is because in some cases, the clouds and their shadows are likely to be separated by a considerable distance. The locations of shadows in the image depend on the distances of the corresponding clouds from the ground and the incidence angle of the sunlight at that time (Wang et al., 1999). In addition, Esche et al. (2002) pointed out that the location of clouds in the scene may have an impact on the classification algorithm.

2.3.3 Data fusion

Earth observation satellites provide data that covers different portions of the electromagnetic spectrum at different spatial, temporal and spectral resolutions. For the full exploitation of increasingly sophisticated multisource data, data fusion emerged as a new topic in the late 1980s (Gamba and Chanussot, 2008). Fused images may provide more information since data with different characteristics are combined, and consequently more reliable results obtained. A good example is the fusion of images acquired by optical sensors with data from radar sensors. Optical images reflect the spectral information of the target illuminated by sunlight, and radar intensities are sensitive to the target roughness (texture) and vertical characteristics. The fusion of these disparate data contributes to the understanding of the objects observed (Pohl and van Genderen, 1998).

A general definition of remotely sensed data (image) fusion is given as 'the combination of two or more different images to form a new image by using a certain algorithm' (Pohl and van Genderen, 1998: 825). Data fusion can be categorized into three groups according to the processing level where the fusion takes place: pixel, feature and interpretation level (Figure 2.1). Pixel level fusion refers to the merging of measured physical parameters at the lowest processing level. It requires raster data that are at least co-registered and geocoded. Fusion at the feature level is performed after the extraction of objects recognized in the various data sources. The recognized object is called a feature, which correspond to characteristics extracted from raw images. Interpretation level fusion uses value-added data to reinforce common interpretation and furnish a better understanding of the observed data. In this level, input images are processed individually for information extraction.

Apart from the processing levels, data fusion can be applied to various types of data sets:

- Single sensor for temporal, e.g. multitemporal analysis of ERS-1 (European Remote Sensing satellite) SAR (Synthetic Aperture Radar) images over land areas (Weydahl, 1993)
- Multi sensor for temporal, e.g. VIR / SAR image fusion (Pohl and van Genderen, 1995)
- Single sensor for spatial, e.g. pansharpening, i.e. high/low resolution panchromatic/multi-spectral images (Ranchin and Wald, 2000)
- Multi sensor for spatial, e.g. Landsat / MODIS (Moderate Resolution Imaging Spectroradiometer) (Gao et al., 2006)
- Multi sensor in single date, e.g. ERS-1 / ERS-2 (Guyenne, 1995)

- Remote sensing data with ancillary data, e.g. terrain data (Carpenter et al., 1997)

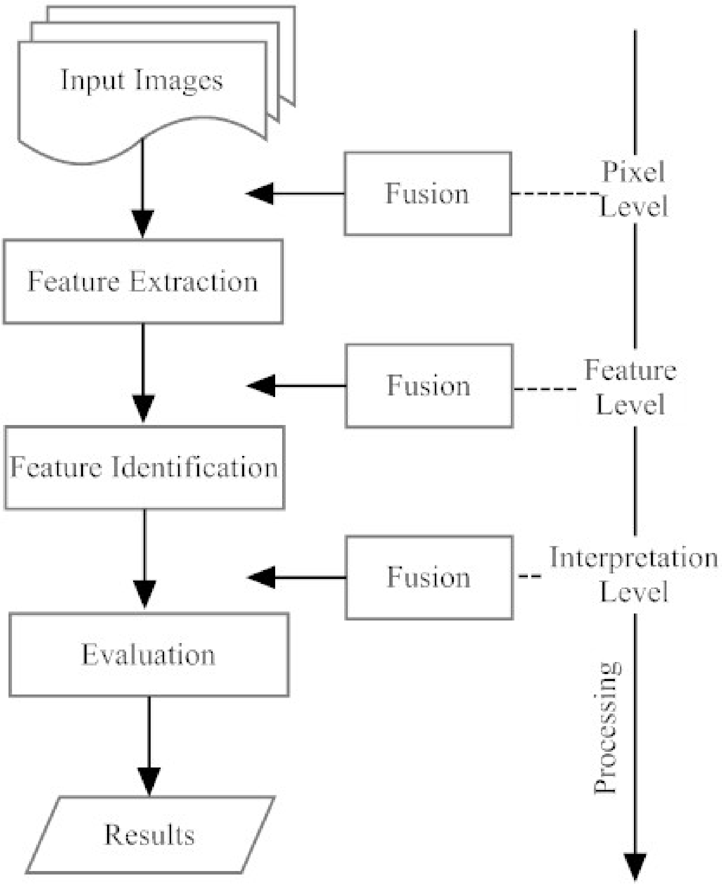

Figure 2.1 Processing level of data fusion (Pohl and van Genderen, 1998)

Data fusion is used to combine multisource image using certain fusion algorithms. It can integrate disparate and complementary data to improve image resolution in spatial, temporal or/and spectral aspects, and consequently to lead to more accurate data (Keys et al., 1990) and increased utility (Rogers and Wood, 1990). More specifically, the data fusion is applied to digital imagery in order to:

- Sharpen images (Ranchin and Wald, 2000)
- Improve co-registration (Leprince et al., 2007)

- Provide stereo-viewing capabilities for stereophotogrammetry (Bloom et al., 1988)
- Complement data sets for improving classification accuracy (Chanussot et al., 2006)
- Detect temporal change (Gao et al., 2006)
- Substitute missing information (e.g. cloud issue in MS image, or shadows in radar image)in one image with signals from another sensor image (Hegarat-Mascle et al., 1998)

The following points describe the purpose in more detail.

(1) Pansharpening: High-resolution panchromatic imagery is fused with low-resolution multispectral image data. These synthetic images looks like multispectral (MS) images observed with a sensor at the higher resolution (Ranchin and Wald, 2000).

(2) Improvement of co-registration: The input images might come from multiple platforms, multiple sensors onboard the same instrument, ancillary data sources, and so on. This situation usually requires the user to work on multisensor or multitemporal data sets simultaneously. The first problem encountered is co-registration, which remains a crucial step in numerous applications and still generates much critical attention (Wong and Clausi, 2007).

(3) Provide stereo-viewing capabilities for stereophotogrammetry: VIR/VIR (different spatial resolution), SAR/SAR (multiple incidence angles) and VIR/SAR were successfully fused to create stereo data sets. Bloom et al. (1988) demonstrated the stereophotogrammetry with combined SIR-B (Shuttle Imaging Radar-B) and Landsat TM images, and Gelautz et al. (2003) derived and compared radar stereo and interferometric DEMs (Digital Elevation Models) using a Radarsat stereo pair, and Radarsat and ERS-2 interferometric data.

(4) Improvement of classification accuracy: Images from microwave and optical sensors offer complementary information that helps in discriminating the different classes.

(5) Detection of temporal change: For example, Landsat's temporal resolution is 16 days, which is too long for detecting the vegetation change in temporal scale. Because MODIS has a daily revisit capability, fusion of Landsat and MODIS can help resolve this problem.

(6) Substitution of missing information: The image acquired by satellite sensors are influenced mainly by the carrier frequency of the electromagnetic waves. It is well known that the optical imagery is subject to interference from clouds, and thus the shadows of the clouds block the interpretability of the imagery. Radar imagery on the other hand suffers from severe geometric distortions and speckle due to its side-looking geometry. Therefore there is a big need and prospect to combine different images acquired by the same or by different instruments.

2.4 Possible sensors and methods for the challenges and opportunities

Newly advanced sensors and methods are increasing the probability of tackling the aforementioned problems, and providing great opportunities for new interpretative research and applications.

2.4.1 Possible sensors for large-area habitat mapping

As mentioned above, the limitations of Landsat suggest that alternative imagery should be tested for its suitability in wildlife habitat mapping. Currently available satellite-based imagery can be divided into three categories based on its relationship between scale and spatial resolution: low spatial resolution imagery (optical applications are most suitable for studying phenomena that varies over hundreds or thousands of meters (small scale), e.g. NOAA (National Oceanic and Atmospheric Administration) AVHRR (Advanced Very High Resolution Radiometer), EOS

(Earth Observing System) MODIS, and SPOT (Satellite Pour l'Observation de la Terre) VEGETATION sensor data); medium spatial resolution imagery (optical applications are most suitable for studying phenomena that varies over tens or hundreds of meters (medium scale), e.g. Landsat, SPOT, IRS (Indian Remote Sensing satellite) sensor data); and high spatial resolution imagery (optimal applications are suitable for studying phenomena that varies over centimeters to meters (large scale), e.g. aerial remote sensing platforms, IKONOS, and QUICKBIRD-2 sensor data; Franklin and Wulder, 2002).

Among these three categories of satellite imagery, Franklin and Wulder (2002) have pointed out that medium spatial resolution satellite imagery might be suitable for large-area land cover mapping. Medium spatial resolution imagery can provide detailed information to compare with coarse resolution imagery, and simultaneously guarantee large enough image size for large-area mapping to high resolution imagery. The challenge on Landsat-series data may be avoided if information from satellites such as those listed in Table 2.1 and 2.2 are tested and proven capable of delivering the information required. Figure 2.2 links the optical imagery properties listed in Table 2.1 to their specific habitat applications. Taking land cover classification as an example, spatial and spectral resolution can guarantee sufficient tone, size, shape and texture information for classification with required accuracy. In addition, image size can determine whether the image will cover the total study area. However, spatial resolution and image size have a negative relationship, which means that high spatial resolution corresponds to a small image size and vice versa. Therefore, users have to compromise according to their objectives. For radar sensors, polarization is an exclusive property as compared to optical sensors. It also provides useful information for a variety of applications (Table 2.3).

Table 2.1 Possible medium resolution optical sensors

Medium resolution sensors	Spatial resolution (m)[a]	Swath (km)	Spectral resolution (nm)	Temporal coverage	Revisit (day)
IRS-P6 (Resourcesat-1) (LISS III)	23.5	141	520-1700	2003-Present	24
SPOT 4 (HRVIR)	20	60	500-1750	1998-Present	1-3
SPOT 5 (HRG)	10 (MS); 20 (SWIR)	60	500-1730	2002-Present	1-3
CBERS -1 and -2	20	120	450-890	1999/2003-Present	3
Terra (ASTER)	15	60	530-1165	1999-Present	16
EO-1 (ALI)	10 (Pan); 30 (MS)	37	433-2350	2000-Present	16
ALOS (AVNIR-2)	10	70	420-890	2006-Present	2
DMC (SLIM-6)	22/32	600	520-990	2002-Present	1

[a] MS = multispectral, SWIR = shortwave infrared, Pan = panchromatic

Table 2.2 Possible radar sensors

Sensors	Spatial resolution (m)	Foot print (km^2)	Polarization	Temporal coverage	Revisit (day)
TerraSAR-X (X-band)	18	100*150	Single VV or HH	2007-Present	2.5
ERS-2 (C-band)	25	100*100	VV	1995-Present	12-20
Radarsat-1 (C-band)	25/30	100*100/ 150*150	HH	1995-Present	1-3
Radarsat-2 (C-band)	26.8-18.0*24.7 /40.0-19.2*24.7	100*100/ 150*150	Single (HH or VV or HV or VH) or Dual ((HH + HV) or (VV + VH))	2007-Present	1.5
ALOS PALSAR (L-band)	44-7/88-14	40-70* 40-70	(HH or VV) or (HH+HV or VV+VH)	2006-Present	2
ENVISAT ASAR (C-band)	30	100*100	(HH or VV) or (VV+HH or HH+HV or VV+VH)	2002-Present	4

Table 2.3 Radar polarization and potential application (adapted from Radarsat-2 Information, 2009a)

Polarization	**Application**		
	Forest	Hydrology	Agriculture
Single	Fire-scar mapping; low biomass estimation	Soil moisture; wetland detection; shoreline mapping	Crop canopy volume and structures; land use
Dual	Clear-cut mapping	Mapping of surficial deposits and rock units; tidal and near shore mapping	Crop discrimination
Quad	Stand age retrieval; forest structure estimation	Snow; wetland classification	Crop condition mapping; crop yield mapping

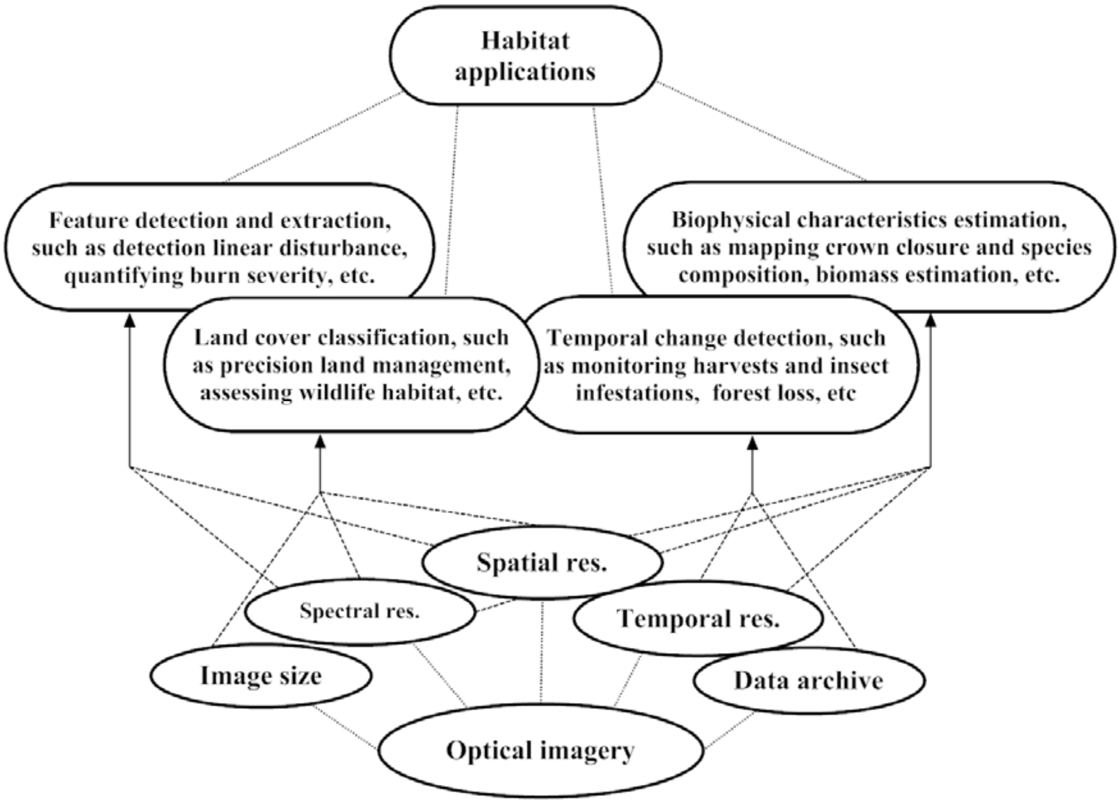

Figure 2.2 Linkage of optical imagery properties and habitat applications

The Disaster Monitoring Constellation (DMC) was designed as a proof of concept constellation (Table 2.4), capable of obtaining multispectral images of any part of the world every day. Surrey Linear Imager - 6 Channels (SLIM-6) is a dual bank linear push broom imager utilizing the orbital motion of the DMC platform to capture radiation reflected from the Earth's surface (Crowley, 2008). SLIM-6 has 3 bands, i.e. NIR (0.77-0.90 μm), Red (0.63-0.69 μm) and Green (0.52-0.60 μm), which are equivalent to Landsat TM or ETM+ band 4, band 3 and band 2 respectively. The combination of the above sensor characteristics can support DMC imagery to be used for extensive practical applications. For example, its 32 m spatial resolution and 3 spectral bands are analogous to the Landsat TM and ETM+ data, which allows image users to generate comparable remote sensing products used in existing habitat mapping and ecological models. A one-day temporal resolution can satisfy the application of detecting rapid surface changes such as crop-growth monitoring and detecting intraseasonal ecosystem disturbance. Meanwhile, the high temporal resolution also promotes acquisition of good-quality imagery with limited cloud-contamination. The sensor has been used in many applications including forest, agriculture, land cover and habitat mapping, and flood or fire monitoring. It is especially suitable for large area land cover mapping due to the 600 km swath width. The cost of purchasing DMC data ranges from 0.018-0.164 USD per km^2 depending on desired data types (DMC International Imaging Ltd, 2008). The further exploitation of DMC data likely provides an appropriate data source to traverse the coming Landsat gap.

Table 2.4 DMC on orbit (adapted from DMC International Imaging Ltd)

Designation	Type	Imager	Launch
Alsat-1	DMC	32m MS	2002
UK-DMC	DMC	32m MS	2003
Nigeriasat-1	DMC	32m MS	2003
Beijing-1	DMC+4	32m MS / 4m Pan	2005
Deimos-1	DMC	22m MS	2008
UK-DMC2	DMC	22m MS	2008

MS = Multispectral; Pan = Panchromatic

Radar, the acronym of radio detection and ranging, is based on the transmission of long-wavelength microwaves (e.g., 3 – 25 cm) through the atmosphere and then recording the amount of energy backscattered from the terrain (Jensen, 2007). Radar remote sensing uses the microwave portion of the electromagnetic spectrum, from a frequency of 0.3 GHz to 300 GHz, or in wavelength terms, from 1m to 1mm (Canada Center for Remote Sensing, 2008). Most remote sensing radars operate at wavelengths from 0.5 cm to 75 cm (Canada Center for Remote Sensing, 2008). The microwave frequencies have been arbitrarily assigned to different bands which are identified by letter. The most popular of these bands for use by imaging radars are included in Table 2.5 (Jensen, 2007). The capability to penetrate through cloud or into a surface layer is increased with longer wavelengths, e.g. L-band radar sensors have better penetration than the C-band sensors. However radars operating at wavelengths greater than 2 cm are not significantly affected by cloud cover (Canada Center for Remote Sensing, 2008). Jensen (2007) summarized the primary advantages of radar as follows:

(1) certain microwave frequencies will penetrate clouds, allowing all-weather remote sensing;

(2) it allows synoptic views of large areas for mapping from 1:10,000 to 1:400,000 and satellite coverage of cloud-shrouded countries is possible;

(3) coverage can be obtained at user-specified times, even at night;

(4) it permits imaging at shallow look angles, resulting in different perspectives that cannot

always be obtained using aerial photography;

(5) it senses in wavelengths outside the visible and infrared regions of the electromagnetic spectrum, providing information on surface roughness, dielectric properties, and moisture content.

Table 2.5 Bands for use by imaging radars

Band Designations (common wavelengths)	**Wavelength in cm**	**Frequency in GHz**	**Typical sensors**
X (3.0 and 3.2 cm)	2.4-3.8	12.5-8.0	CV-580 SAR
C (5.6 cm)	3.9-7.5	8.0-4.0	ERS-1 and RADARSAT
S (8.0, 9.6, 12.6 cm)	7.5-15.0	4.0-2.0	Almaz [a]
L (23.5, 24.0, 25.0 cm)	15.0-30.0	2.0-1.0	SEASAT and PALSAR
P (68.0 cm)	30.0-100	1.0-0.3	NASA/JPL AIRSAR

[a] The Almaz program was a series of military space stations (or "Orbital Piloted Station" - OPS) launched by Russia.

The Phased Array type L-band Synthetic Aperture Radar (PALSAR) onboard Advanced Land Observing Satellite (ALOS) is an enhanced version of the JERS-1 SAR (Japanese Earth Resources Satellite), launched in January 2006 by the Japanese Aerospace Exploration Agency (Rosenqvist et al., 2007). It is a fully polarimetric instrument, which operates in L-band with 1270-MHz (23.6 cm) center frequency and 14- and 28-MHz bandwidths. PALSAR operates in either single polarization (HH or VV), dual polarization (HH+HV or VV+VH), or quad-polarization mode, and the nominal ground resolution is ~10 and ~20 meters in the single- and dual-polarization modes, respectively, and ~30 meters in quad-pol mode (Rosenqvist et al., 2004). It can also operate in a coarse, 100 meter, resolution ScanSAR mode, with single polarization (HH or VV) and 250-350km swath width (Rosenqvist et al., 2004). Until now, PALSAR was the only available spaceborne L-band SAR with quad-pol mode to exist. Surface features can be readily discriminated if radar wavelength is matched to the size of the features (Canada Center for Remote Sensing, 2008). Consequently, the L-band is much better in geology mapping, and the corresponding low frequency is better for detecting water under closed canopies (Canada Center for Remote Sensing, 2008). In theory, quad-pol has more inherent information per pixel than dual- and single-pol, and so quad-pol data should produce more accurate products. PALSAR images have been successfully used for scientific research on earthquake (e.g. Lubis and Isezaki, 2009; Jin and Wang, 2009), ice sheet (e.g. Rignot, 2008), hydrology (e.g. Paillou et al., 2009), soil science (e.g. Takada et al., 2009), etc.

RADARSAT-2 (R-2) is the follow-on mission to RADARSAT-1 (R-1) designed to assure continuity of the supply of radar data, launched in December 2007 by the Canadian Space Agency (CSA) and MacDonald Dettwiler and Associates Ltd (MDA). However, the R-2 represents a significant evolution from R-1 in aspects of spatial resolution, polarization and look direction (table 6). With these advanced features, it is believed that R-2 can be used in many relevant application areas, such as resource management operations and the improvement of environmental quality (Morena et al., 2004). More specific to applications in forestry, R-2's array of beam modes and polarimetric capabilities is likely to provide significant steps forward in the detection of structural differences between forests, and offer greater potential for burn mapping. For example, ultra-fine beam mode provides increased accuracy of boundary placement; HV or VH single-pol likely provides the best potential for burn mapping since it is sensitive to structural damage incurred by the forest canopy (Radarsat-2 information, 2009a). High-resolution data from RADARSAT-2, such as 3 m ultra-fine mode data or 12 m fine quad-pol mode data, offers the potential to improve forest-type mapping using textural analysis (Radarsat-

2 information, 2009a). In the context of geology, R-2’s ultra-fine resolution and fully polarimetric capabilities can provide benefits such as more detailed mapping of terrain features or fine geological structures, better identification of structural features and improved discrimination of different geologic units (Radarsat-2 information, 2009a).

Table 2.6 RADARSAT-2 innovations (adapted from Radarsat-2 Information, 2009b)

Items	Characteristics	Specifics
Spatial resolution	3 to 100 meters	▪ Suite of spatial resolution options accommodates a wide range of applications ▪ Ultra-fine beam will improve object detection and recognition
Polarization	HH, HV, VV and VH	▪ Better discrimination of various surface types and improved object detection and recognition
Look direction	Routine left- and right-looking operation	▪ Increased re-visit time for improved monitoring efficiencies ▪ More responsive to user requests ▪ Antarctic mapping mission fully integrated

2.3.2 Methods for detection and removal of clouds and their shadows

In general, cloud cover is the unwanted information in optical images (Tseng et al., 2008). In this context, if complementary information can be found to replace clouds- and cloud shadow-contaminated areas, the problem will be resolved to generate cloud-free images or map products. Multi-temporal and radar images are considered as a good choice to provide the complementary information (Hegarat-Mascle, 1998; Wang et al., 1999; Tseng et al., 2008). The general steps of producing cloud-free images include: image preprocessing (co-registration, correction of brightness, and image enhancement), detection of clouds and cloud shadows, and removal of cloud and their shadows (replacement). Many approaches have been developed to tackle obstacles at every step, but here, we focus on reviewing the methods of detection and the removal of clouds and their shadows.

2.3.2.1 Detection of clouds and their shadows

Simpson and Stitt (1998) developed the pixel-by-pixel cross-track geometry of the scene and image analysis methods to detect cloud shadow in daytime AVHRR scenes over land. These methods are not suitable for removing clouds and their shadows in other satellite imagery (Meng et al., 2009). However, the mostly frequently used method is one based on a threshold, of which the values may vary for images acquired at different time (Meng et al., 2009). Chen (2001) stated clouds and their shadows can be detected using thresholds obtained from all five AVHRR (Advanced Very High Resolution Radiometer) channels as well as systematic mathematical expressions. The five channel involve the use of surface reflectance (channels 1 and 2) and thermal (channels 3, 4 and 5) data. Cloud detection is based on the characteristic that clouds are generally bright in the visible spectrum (channel 1) and/or cold in infrared spectrum (channel 2) (Gutman, 1992), and highly reflective in channel 3 and/or relative cold in channels 4 and 5 (Yamanouchi and Kawaguchi, 1992). Chen (2001) tested different thresholds for the detection of clouds and their shadows in AVHRR imagery, and used the thresholds of 0.27 for channel 1, 223 K for channel 4 and 0.8-1.6 for the ratio of channel 2 reflectance, to channel 1 reflectance. Finally, the contaminated pixels are classed into thick clouds, thin clouds, optical cirrus, cloud edges and cloud shadows according to their impacts on normalized difference vegetation index (NDVI). However, thermal bands are not available for many of the popular sensors, such as SPOT and IRS.

With Landsat imagery, Automatic Cloud Cover Assessment (ACCA) can detect clouds over most of the earth's surface by their high albedo in the visible spectrum and by their cold temperatures (Choi and Bindschadler, 2004). However, it is prone to mix up clouds and ice sheets because both targets are bright and temperature inversions commonly exist in the atmosphere above the ice sheets are common. This leaves the surface colder than the clouds (Choi and Bindschadler, 2004). Thus, an approach using the normalized difference snow index (NDSI) was developed by Choi and Bindschadler (2004). Besides cloud detection, Wang et al. (1999) suggested it is difficult to detect the shadow regions because of the similar brightness values between shadows and their neighbors or some other regions. Therefore, Wang et al. (1999) applied wavelet transforms to detect shadow regions, because shadows reduced the local contrasts of the image, and the wavelet co-efficients can measure the local contrasts of the image at different scales.

In addition, Griffin et al. (2003) developed a cloud cover algorithm for application to EO-1 (Earth Observer-1) Hyperion hyperspectral data. The algorithm successfully discriminated clouds from surface feature such as snow, ice, and desert sand only utilizing six bands in the reflected solar spectral regions. Tseng et al. (2008) used the linear spectral unmixing method (LSU) to extract all of the cloud cover pixels, but it can not handle thin-clouds and cloud shadow, and often confuses bright land surfaces as clouds.

2.3.2.2 Removal of clouds and their shadows

Adapted from the Tseng et al. (2008) research, the methods of removal can be categorized into four general classes according to the source of complementary information: 1) using image statistical information to interpolate or treat the cloud as noise to remove (e.g. Rossi et al., 1994; Feng et al., 2004); 2) using multi-spectral images to fuse and generate the cloud-free images (e.g.

Wang et al., 2005); 3) using multi-temporal images to fuse and generate the cloud-free images (e.g. Wang et al., 1999; Tseng et al., 2008; Meng et al., 2009); and 4) because radar images are not affected by clouds, using radar images can restore the cloud covered area (e.g. Thanh et al., 2008).

An example from the first-category, proposed by Feng et al. (2004), was called an improved homomorphism filtering method. This was based on the statistical characters of image information to remove cloud. Instead of filtering in the frequency field, it isolates the low frequency component of the image representing cloud information by calculating neighborhood averages in the spatial field. However, this method readily leads to the confusion of bright land cover area and clouds; moreover, theoretically the denoising methods can not completely recover the land covers blocked by the clouds (Tseng et al., 2008). An example from the second-category, proposed by Wang et al. (2005), encounters cloud contamination in all bands of multi-spectral images; in such a case, the clouds are also treated as noises and the similar results to these of the first-category methods are acquired (Tseng et al., 2008). As a result, neither classes of methods are likely to become mainstream in use.

More effort has gone into generating cloud-free composite images based on multi-temporal methods. Wang et al. (1999) developed a scheme to remove clouds and their shadows from remotely sensed images of Landsat TM. The scheme uses the image fusion technique to automatically recognize and remove contamination of clouds and their shadows, and integrate complementary information into the composite image from multi-temporal images. Tseng et al. (2008) generated cloud-free mosaic images from multi-temporal SPOT images based on multidisciplinary methods, such as multi-scale wavelet-based fusion method. Meng et al. (2009) proposed an efficient approach, called closest spectral fit. This technique can avoid the spectral inconsistency between the substitution and original image, and it does not depend on the areas, the thickness, and the density of clouds and cloud shadows in the images

The use of radar images to remove clouds and their shadows has rarely been studied, largely because optical and radar sensors fall into totally different genera (Jensen, 2007), which may result in more complicated processing than using multi-temporal methods. But the multi-temporal methods require that cloudy areas in the base image should be cloud-free in the complementary image. Frequently it is impossible or extremely difficult to obtain a cloud-free complementary image, especially in tropical or cloud-prone areas. Most importantly, the Landsat imagery, with its low temporal resolution (16 days) is further limited when research objects change dramatically in a short time period. Hence, radar imagery has exclusive advantages in addressing the cloud issue when compared with multi-temporal optical imagery. Thanh et al. (2008) achieved promising results on cloud removal of optical image using SAR data.

2.3.3 Fusion techniques of optical and radar imagery

Optical and radar image fusion is always at the leading edge of remotely sensed data fusion. The relevant technology has become progressively more systematic. Figure 2.3 indicates the outline of fusion between optical and radar images. Generally, system error will be corrected by the providers of the data, but the data need to be subject to further radiometric processing using a filter or other algorithms. Radar images have a strong “salt and pepper” phenomena (i.e. speckle). Therefore, speckle reduction is an elementary operation in processing, and some remote sensing professionals suggest first reducing speckle before geocoding (Dallemand et al., 1993). Optical imagery acquisition is strongly influenced by atmospheric conditions and therefore needs correction. The next step is geocoding, or co-registration, because the techniques are sensitive to misregistration (Pohl and van Genderen, 1999). Data can then be fused according to the fusion techniques described below. However, if the image data are very different in spatial resolution, resampling from low-resolution to high-resolution causes the data to appear blocky (Pohl and van Genderen, 1999). Therefore, Chavez (1987) recommended using a smoothing filter before image fusion - any spatial or spectral enhancement related to the application prior to image fusion will benefit the resulting fused image (Pohl and van Genderen, 1999).

In general, the fusion techniques can be categorized into two classes (Pohl and van Genderen, 1998): 1) Color-related techniques, such as color composites (RGB), intensity-hue-saturation (IHS); 2) Statistical or numerical methods, such as principal component analysis (PCA), band combinations using arithmetic operators and others. Table 2.7 indicates the most successful techniques for fusing images from Landsat, SPOT, ERS-1 and JERS-1 - Japanese Earth Resources Satellite; Pohl and van Genderen, 1999). Besides the typical techniques, more new techniques focus on the modeling and combination of fusion algorithms with the development of sensors and computation. For example, Farah et al. (2008) presented a semiautomatic approach based on case-based reasoning (CBR) to fuse images from ERS-2 and SPOT 4, and obtained encouraging results. Corbane et al. (2008) developed an algorithm consisting of a completely unsupervised procedure for processing pairs of co-registered SAR / optical images. Waske and van der Linden (2008) proposed a joint classification of multiple segmentation levels from multisensor imagery using SAR and optical data, and implemented this method based on a support vector machine (SVM). Garzelli (2002) proposed a method aiming to generate an integrated map which selects specific information from SAR data to be injected into the optical data based on the wavelet which is not referred to in classical IHS or PCS (Principal Component Substitution).

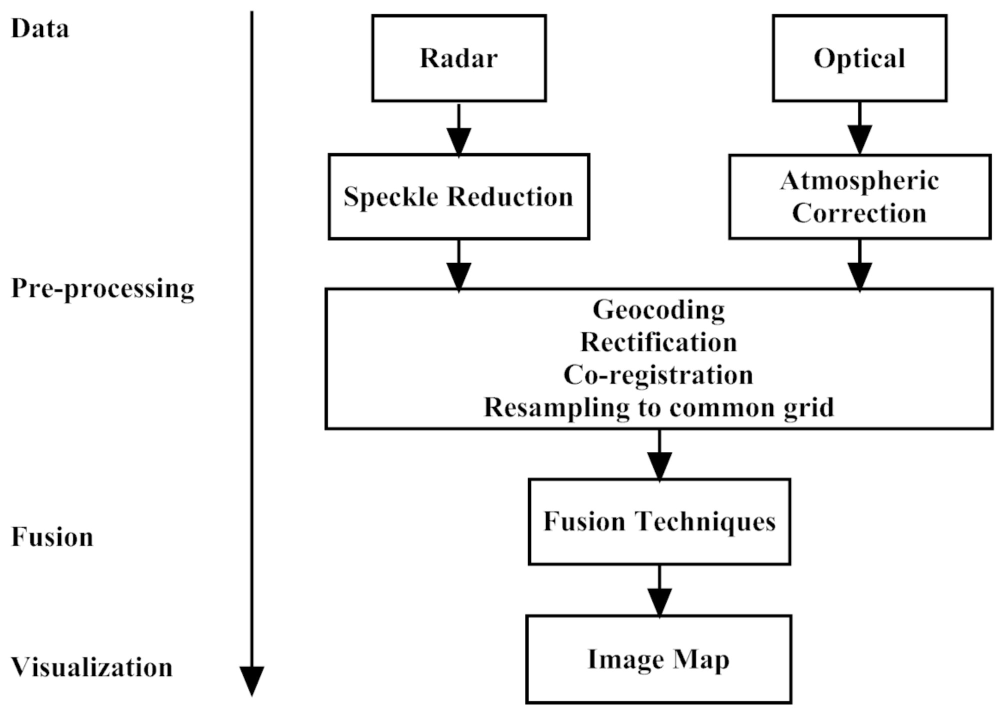

Figure 2.3 Outline of optical and radar image fusion (Pohl and van Genderen, 1998)

Table 2.7 Typical techniques testing on fusion from optical and radar sensors

Categorization	**Techniques**	**Results**
Color-related	RGB	Simple, and does not require CPU time-intensive computations. RGB overlay protects the contribution from optical imagery from being greatly affected by speckle from SAR.
	IHS	With the capability of allocating data from the SAR to cloud cover areas without having to identify the clouds at an earlier stage, but will reduce spatial detail.
Statistical or numerical	Band combinations	Improve the interpretation of the SAR data, but depend very much on the appearance and content of the SAR image. Don't solve the cloud-cover problem.
	Brovey transform	Successfully combine spectral information from the VIR with texture from the SAR data.
	PCA	Principal component SAR images show potential for topographic mapping, especially for the 3D impression of topography and change detection.

2.5 Application issue - landscape analysis and remote sensing

Landscape analysis refers to accurately quantifying landscape pattern, which has been commonly used in applications of resource management, environmental conservation and impacts of anthropogenic activity. A large number of metrics have been developed for quantifying landscape pattern since the seminal paper by O'Neill et al. (1988). Advances in remote sensing technologies have provided practical means for classified thematic maps which are the key inputs for most studies on landscape pattern analysis (Shao and Wu, 2008).

However, before using classification maps to calculate landscape metrics, classification accuracy should be assessed via analytically comparing satellite sensor derived products (e.g. land cover) to reference data, which is presumed to represent the target value (Justice et al., 2000). This is because the classification errors will be carried over or even propagated in subsequent landscape pattern analysis (Feng et al., 2006; Shao and Wu, 2008).

2.5.1 Accuracy assessment

Accuracy assessment is a critical step in analyzing any map created from remotely sensed data. Quantitative accuracy assessment is implemented to identify and measure map errors (Congalton and Plourde, 2002). The most widely used approaches in accuracy assessment are to calculate Root Mean Square Error (RMSE) for positional accuracy and to create an error matrix for classification accuracy. Before the assessment, one needs to learn about the source of errors (Powell et al., 2004). Besides the error gained from the method itself, other sources of errors include registration errors, processing errors, interpretation errors, and sampling errors, all of which will affect the accuracy of results (Lu and Weng, 2007).

RMSE is a measure of positional accuracy that encompasses both the effects of bias and random error. Because of the simplicity of RMSE calculation, it has long been utilized in accuracy assessments of remote sensing products (e.g. McDermid, 2005; Cohen et al., 2003; Xu et al., 2005).

The error matrix is currently at the core of the accuracy assessment literature (Foody, 2002). Congalton and Plourde (2002) stated that in order to correctly generate an error matrix, the following factors need to be considered: 1) reference data collection; 2) classification scheme; 3) sampling scheme; 4) spatial autocorrelation; and 5) sample size and sample unit. Afterward, one can calculate overall accuracy, user's accuracy (commission error), producer's accuracy (omission error), and kappa coefficient. The meaning and computation methods of an error matrix can be found in previous literature such as Congalton and Plourde (2002) and Foody (2002).

2.5.2 Landscape pattern analysis using remote sensing data

Landscape pattern is spatially correlated and scale-dependent (Wu, 2004), especially those measures linked with spatial heterogeneity in the landscape pattern, or of patch characteristics via metrics (Wu and Hobbs, 2002; Li and Wu, 2004; Wu, 2004; Kent, 2007). The term 'scale' may refer to any one or combinations of several concepts, including grain (spatial resolution), extent (geographic), lag (or spacing), and cartographic ratio (Wiens, 1989; Lam and Quatrochi, 1992; Wu, 2004), but the most commonly examined scales are grain or extent (Urban, 2005; Kent, 2007), which have previously been described as the 'Modifiable Areal Unit Problem' (MAUP) in Geographic Information Systems (GIS) (Kent, 2007). For remotely sensed data, grain and extent relate to image spatial resolution and footprint (image size) respectively. It is straightforward to deal with the extent issue via seamless image mosaicing. Accordingly, we focus on discussing the relationship of landscape metrics and image spatial resolution, and landscape metrics and thematic resolution. Furthermore, confronted with the limitations and uncertainties of Landsat-series data, it is important to examine what should be done at the application level. For instance, most ecological or resource-management models are Landsat-dependent, and if they must use other imagery to produce the mapping products, it will result in incompatibility, or even conflict with derived models because of distinct spectral and spatial resolution.

2.5.2.1 Landscape metrics and spatial resolution:

Benson and MacKenzie (1995) examined the effects of grain size (spatial resolution) on landscape parameters characterizing spatial structure, i.e. whether structural parameters remain constant from 20 m to 1100 m of grain size, and whether aggregation algorithms permit extrapolation within this range. Landscape parameters were used to quantify spatial structure including: percent water, number of lakes (patches), average lake area and perimeter, fractal dimension, and three measures of texture (homogeneity, contrast, and entropy). Results indicate that most measures were sensitive to changes in grain size. However, it was found that two texture measures were relatively invariant with grain size - homogeneity and entropy. The aggregation of the results indicated extrapolated values closely approximated the actual sensor values, and that interpolation between the grain sizes of different satellite sensors is possible when an approach involving an aggregation of pixels is applied.

However, considerable differences between aggregated values and actual sensor values were found by Saura (2004), who examined the effect of spatial resolution on six common fragmentation indices that are being used within the Third Spanish National Forest Inventory. Number of Patches (NP), Mean Patch Size (MPS), and Edge Length (EL) indicated that the aggregated values produced clearly more fragmented patterns than actual sensor ones. Different aggregation algorithms were tested in the context of forest fragmentation estimates across various spatial scales (Garcia-Gigorro and Saura, 2005). Thirty-meter Landsat-TM forest data were transferred to 188 m IRS-WiFS (Indian Remote Sensing Satellite-Wide Field Sensor) and compared with actual WiFS data. Sensor point spread function was found to greatly improve comparability of forest fragmentation indices. However, a poor performance of power scaling laws was observed at finer spatial resolutions, and accordingly Garcia-Gigorro and Saura (2005) suggested that the true accuracy and practical utility of these scaling functions may have been overestimated in previous literature. In addition, the sensitivity of each of the indices varied with the gradient of spatial resolution. But Cain et al. (1997) conducted a multivariate analysis of pattern metrics, and pointed out that measures of land cover diversity, texture, and fractal dimension were more consistent than measures of average patch shape or compaction among the land cover maps. Wu et al. (2002) summarized the responses of the 19 landscape metrics that fell into three general categories when calculated at the landscape level: Type I metrics showed predictable responses with changing scale, and their scaling relations could be represented by simple scaling equations (linear, power-law, or logarithmic functions); Type II metrics exhibited staircase-like responses that were less predictable; and Type III metrics behaved erratically in response to changing scale, suggesting no consistent scaling relations. Therefore, if metrics fall within category Type I, they can be readily and accurately extrapolated or interpolated across spatial scales, whereas if they fall in Type II or Type III categories, more explicit consideration of idiosyncratic details are required for successful scaling.

Proportion errors cannot be avoided when land-cover classification data are aggregated to coarser scales. Moody and Woodcock (1995) tested two statistical models, multiple-linear and tree-based regression techniques, to assess relationships between landscape spatial pattern and errors in the estimates of cover-type proportions. Results from a multiple-linear regression model suggest that as patch sizes, variance/mean ratio, and initial proportions of cover types increase, the proportion error moves in a positive direction and is governed by the interaction of the spatial characteristics and the scale of aggregation. However, the linear model does not explain the different directions of the proportion error. A regression tree model provided a much simpler fit to the complex scaling behavior through an interaction between patch size and aggregation scale. The understanding of proportion errors can help correct land-cover proportion estimates.

2.5.2.2 Landscape metrics and thematic resolution

The thematic resolution of remote sensing products is determined by the applied land-cover classification scheme. This represents the amount of detailed geospatial information, and influences on the various aspects of landscape classification and the relevance of the derived pattern attributes to particular ecological questions (Buyantuyev and Wu, 2007). Changing the thematic resolution of categorical maps may often alter the number of classes and their spatial pattern, thus resulting in differences in landscape metrics (Buyantuyev and Wu, 2007). Many research results have proven that thematic resolution had significant effects on most of the landscape metrics, such as Huang et al. (2006), Buyantuyev and Wu (2007), and Castilla et al. (2009). For example, Buyantuyev and Wu (2007) stated that three general response patterns emerged: increased, decreased, and little change. Most of the changes appear either linear or similar to a power-law. Additionally, Huang et al. (2006) pointed out that at lower class numbers, landscape metrics were most sensitive to increasing classification detail.

2.5.2.3 Solutions to the Landsat-gap on application level

It is necessary to generate Landsat-like classification maps using other alternative satellite images (e.g. SPOT, DMC or radar images), if the expected Landsat-gap happens. It is of vital importance for the subsequent landscape pattern analysis or relevant ecological models to be based on Landsat classification maps. As discussed, scale issues caused by spatial, thematic and spectral resolutions have a significant effect on classification, and consequently the calculation of landscape metrics. In general, three promising solutions are suggested to partly address this issue: 1) select approximate 30 m spatial resolution alternatives (e.g. DMC 32 m multispectral images); 2) adjust the procedural parameters of classification; 3) apply scaling relationships between landscape metrics and grain size to set up the model. The following points provide detailed information regarding these solutions.

- Solution 1: Landscape metrics are calculated based on classification maps with certain grain size. DMC imagery has 32 m spatial resolution, and 3 bands which are equivalent to Landsat TM or ETM+ band 2, 3 and 4. It is considered to be the closest sensor to Landsat TM or ETM+, and consequently it is likely to generate comparable classification maps.
- Solution 2: Franklin et al. (2009) tested the capability of SPOT and ASTER for replacing Landsat in an operational environment. An approach based on Definiens' Developer (also called eCognition; Definiens, 2008) was developed to diminish the dissimilarity between SPOT- and ASTER-based and Landsat-based classification as far as possible. The results indicated that if set Scale = 55, Shape = 0.2, and Compactness = 0.2 to segment SPOT imagery, and 20, 0.2, 0.2 to segment ASTER imagery in the process of object-oriented classification, the minimum dissimilarity could be obtained. Herein, the 'Scale' in Definiens' Developer is a unitless parameter that determines the size of objects. This means that pixels are merged if their values are within a user-defined threshold (Elmqvist et al., 2008). 'Shape' represents the shape information considered in the segmentation and is defined by the

compactness and smoothness heterogeneity of objects (Elmqvist et al., 2008). 'Compactness' equals the ratio of the perimeter of an object and the square root of the number of pixels forming that image object (Benz et al., 2004).

- Solution 3: The scaling relationships between landscape metrics and grain size, i.e. how pattern metrics change with scale in real landscapes of different kinds, have been revealed by many researchers, such as Benson and MacKenzie (1995), Cain et al. (1997), Wu et al. (2002), Saura (2004), and Wu (2004). Wu et al. (2002) grouped the effects of changing grain size into three general types: Type I, simple scale functions; Type II, staircase pattern; Type III, unpredictable behavior. Twelve of the nineteen landscape metrics we examined belonged to Type I, including the number of patches (NP), patch density (PD), total edge (TE), edge density (ED), landscape shape index (LSI), area-weighted mean shape index (AWMSI), area-weighted mean patch fractal dimension (AWMFD), patch size coefficient of variation (PSCV), mean patch size (MPS), square pixel index (SqP), patch size standard deviation (PSSD), and largest patch index (LPI). The relationships can help set up models to predict Landsat-based landscape pattern using alternatives, e.g. SPOT imagery.

2.6 Conclusions

Remote sensing provides significant information and plays a dominant role in large-area wildlife habitat mapping, although field data acquired by in situ methods are also indispensable for most studies. However, the limitations and uncertainties in remote sensing hinder the feasibility and reliability of remotely sensed data in large-area applications. Pioneering work has achieved promising results in addressing these issues, but a tremendous amount of research yet remains, especially regarding the limitations and uncertainties of Landsat-series data, clouds and cloud shadows in optical imagery, and landscape analysis and remote sensing. New optical and radar sensors, e.g. DMC and Radarsat-2, may provide answers to the above questions. Future research should explore the applicability of these sensors in large-area wildlife habitat mapping, and develop reliable and efficient methods for supporting diverse environmental, ecological and resource management applications. Key areas to address are: fusing the complementary optical and radar images to improve classification accuracy; diminishing the difference of classified maps from diverse sensors on landscape pattern analysis via adjusting object-oriented classification parameters; developing a cloud classification scheme according to their impacts on ground objects; and applying radar to remove cloud contamination in optical imagery.

2.7 References

Asner, G.P. 2001: Cloud cover in Landsat observations of the Brazilian Amazon. *International Journal of Remote Sensing* 22, 3855-62.

Benson, B.J. and MacKenzie, M.D. 1995: Effects of sensor spatial resolution on landscape structure parameters. *Landscape Ecology* 10, 113-20.

Benz, U.C., Hofmann, P., Willhauck, G., Lingenfelder, I. and Heynen, M. 2004: Multi-resolution, object-oriented fuzzy analysis of remote sensing data for GIS-ready information. *ISPRS Journal of Photogrammetry and Remote Sensing* 58, 239-58.

Bloom, A.L., Fielding, E.J. and Fu, X. 1988: A demonstration of stereophotogrammetry with combined SIR-B and Landsat TM images. *International Journal of Remote Sensing* 9, 1023-38

Buyantuyev, A. and Wu, J. 2007: Effects of thematic resolution on landscape pattern analysis. *Landscape Ecology* 22, 7-13.

Cain, D.H., Riitters, K. and Orvis, K. 1997: A multi-scale analysis of landscape statistics. *Landscape Ecology* 12, 199-219.

Canada Center for Remote Sensing 2008: Introduction to RADAR remote sensing. Retrieved 5 May 2009 from http://ccrs.nrcan.gc.ca/resource/tutor/gsarcd/downld_e. php

Carpenter, G.A., Gjaja, M.N., Gopal, S. and Woodcock, C. E. 1997: ART neural networks for remote sensing: vegetation classification from Landsat TM and terrain data. *IEEE Transactions on Geoscience and Remote Sensing* 35, 308-25.

Castilla, G., Larkin, K., Linke, J. and Hay, G.J. 2009: The impact of thematic resolution on the patch-mosaic model of natural landscapes. *Landscape Ecology* 24, 15-23.

Chander, G. 2007: Initial data characterization, science utility and mission capability evaluation of candidate Landsat mission data gap sensors (Draft pending final approval). *Landsat Data Gap Study, Technical Report — Version 1*, USGS and NASA. Retrieved 21 November 2008 from http://calval.cr.usgs.gov/documents/Landsat_ Data_Gap_Studies/Landsat_Data_Gap_Study_%20Technical_Report6.pdf

Chanussot, J., Benediktsson, J.A. and Fauvel, M. 2006: Classification of remote sensing images from urban areas using a fuzzy possibilistic model. *IEEE Geoscience and Remote Sensing Letters* 3, 40–4.

Chavez, P.S. 1987: Digital merging of Landsat TM and digitized NHAP data for 1:24,000 scale image mapping. *Photogrammetric Engineering and Remote Sensing* 56, 459-67.

Chen, J.M. and Black, T.A. 1992: Defining leaf area index for non-flat leaves. *Plant, Cell and Environment* 15: 421-29.

Chen, P. 2001: An improved cloud detection algorithm for monitoring agricultural growing conditions with NOAA AVHRR in Texas. PhD thesis. College Station, Texas: Texas A&M University.

Choi, H. and Bindschadler, R. 2004: Cloud detection in Landsat imagery of ice sheets using shadow matching technique and automatic normalized difference snow index threshold value decision. *Remote Sensing of Environment* 91, 237-242.

Cohen, W.B. and Goward, S.N. 2004: Landsat's role in ecological applications of remote sensing. *Bioscience* 54, 535−45.

Cohen, W.B., Maiersperger, T.K., Gower, S.T. and Turner, D.P. 2003: An improved strategy for regression of biophysical variables and Landsat ETM+ data. *Remote Sensing of Environment* 84, 561-71.

Collingwood, A. 2008: Satellite image classification and spatial analysis of agriculture areas for land cover mapping of grizzly bear habitat. MS thesis. Saskatoon, SK: University of Saskatchewan.

Congalton, R.G. and Plourde, L. 2002: Quality assurance and accuracy assessment of information derived from remotely sensed data. In J. Bossler (Ed.), *Manual of Geospatial Science and Technology*. London: Taylor & Francis.

Corbane, C., Faure, J-F., Baghdadi, N. and Petit, M. 2008: Rapid urban mapping using SAR/optical imagery synergy. *Sensors* 8, 7125-43.

Crowley, G. 2008: DMC data product manual. *DMC International Imaging Ltd*. Retrieved 5 May 2009 from http://www.dmcii.com/index.html

Dallemand, J., Lichtenegger, J., Raney, R. and Schumann, R. 1993: Lecture Notes. Rome: FAO Remote Sensing Center.

Definiens AG 2008: Definiens developer 7 - User guide. Retrieved 14 July 2009 from http://www.definiens.com/definiens-support-services_187_11_14.html

DMC International Imaging Ltd 2008: Price list. Retrieved 6 June 2009 from http://www.dmcii.com/pricing/DMCii_US_Prices_Oct2008.pdf

Draeger, W.C., Holm, T.M., Lauer, D.T. and Thompson, R.J. 1997: The availability of Landsat data - Past, present, and future. *Photogrammetric Engineering and Remote Sensing* 63, 869–75.

Elmqvist, B., Ardo, J. and Olsson, L. 2008: Land use studies in drylands: an evaluation of object-oriented classification of very high resolution panchromatic imagery. *International Journal of Remote Sensing* 29, 7129-40.

Esche, H.A., Franklin, S.E. and Wulder M.A. 2002: Assessing cloud contamination effects on K-means unsupervised classifications of Landsat data. In: *Proc. 2002 IEEE Int'l Geoscience and Remote Sensing Sym.*, Toronto, Canada, CD.

Fang, S., Gertner, G., Wang, G. and Anderson, A. 2006: The impact of misclassification in land use maps in the prediction of landscape dynamics. *Landscape Ecology* 21, 233-42.

Farah, I.R., Boulila, W., Ettabaa, K.S., Solaiman, B. and Ahmad, M.B. 2008: Interpretation of multisensory remote sensing images: Multiapproach fusion of uncertain information. *IEEE Transaction on Geoscience and Remote Sensing* 46, 4142-52.

Feng, C., Ma, J., Dai, Q. and Chen, X. 2004: An improved method for cloud removal in ASTER data change detection. In: Proc. IEEE Int. Geoscience and Remote Sensing Sym. (IGARSS 2004) 5, 3387–89.

Foody, G.M. 2002: Status of land cover classification accuracy assessment. *Remote sensing of Environment* 80, 185-201.

Franklin, S.E. and Wulder, M.A. 2002: Remote sensing methods in medium spatial resolution satellite data land cover classification of large areas. *Progress in Physical Geography* 26, 173−205.

Franklin, S.E., He, Y., Pape, A.D., Guo, X. and McDermid, G.J. 2009: Evaluation of the utility of SPOT and ASTER images for updating the Landsat-based landcover products in Alberta's Rocky Mountains. *International Journal of Remote Sensing* (In press).

Gamba, P. and Chanussot, J. 2008: Guest editorial: Foreword to the special issue on data fusion. *IEEE Transaction on Geoscience and Remote Sensing* 46, 1283-88.

Gao, F., Masek, J., Schwaller, M. and Hall, F. 2006: On the blending of the Landsat and MODIS surface reflectance: predicting daily Landsat surface reflectance. *IEEE Transactions on Geoscience and Remote Sensing* 44, 2207-18.

Garcia-Gigorro, S. and Saura, S. 2005: Forest fragmentation estimated from remotely sensed data: is comparison across scales possible? *Forest Science* 5, 51-63.

Garzelli, A. 2002: Wavelet-based fusion of optical and SAR image data over urban area. Retrieved 4 March 2009 from http://www.africover.org/download/manuals/ LCCSMS20.pdf

Gelautz, M., Paillou, P., Chen, C. W. and Zebker H. A. 2003: Radar stereo- and interferometry-derived digital elevation models: comparison and combination using Radarsat and ERS-2 imagery. *International Journal of Remote Sensing* 20, 5243-64.

Griffin, M.K., Hsiao-hua, K.B., Mandl, D. and Miller, J. 2003: Cloud cover detection algorithm for EO-1 Hyperion imagery. *Proceedings of SPIE* 5093, 483

Gutman, G.G. 1992: Satellite daytime image classification for global studies of earth's surface parameters from polar orbits. *International Journal of Remote Sensing* 13, 3295-304.

Guyenne, T.D. 1995: ERS-1/2 multitemporal tandem image: Helsinki (Finland). *Supplement to Earth Observation Quarterly* 48, 4.

Hall, L.S., Krausman, P.R. and Morrison, M.L. 1997: The habitat concept and a plea for standard terminology. *Wildlife Society Bulletin* 25, 173-82.

Hansen, M.J., Franklin, S.E., Woudsma, C.G., and Peterson, M. 2001: Caribou habitat mapping and fragmentation analysis using Landsat MSS, TM, and GIS data in the North Columbia Mountains, British Columbia, Canada. *Remote Sensing of Environment* 77, 50– 65.

Hegarat-Mascle, S.L., Bloch, I. and Vidal-Madjar, D. 1998: Introduction of neighborhood information in evidence theory and application to data fusion of radar and optical images with partial cloud cover. *Pattern Recognition* 31, 1811-23.

Huang, C., Geiger, E.L. and Kupfer, J.A. 2006: Sensitivity of landscape metrics to classification scheme. *International Journal of Remote Sensing* 27, 2927-48.

Hyde, P. 2005: Measuring and mapping forest wildlife habitat characteristics using LIDAR remote sensing and multi-sensor fusion. PhD Thesis. College Park, Maryland: University of Maryland.

Jensen, J.R. 2007: *Remote sensing of the environment: An Earth resource perspective.* Second edition. Upper Saddle River, NJ: Pearson Prentice Hall, 4 and 291-294.

Jin, Y. and Wang, D. 2009: Automatic detection of terrain surface changes after Wenchuan earthquake, May 2008, from ALOS SAR images using 2EM-MRF method. *IEEE Geoscience and Remote Sensing Letters* 6, 344-8.

Justice, C., Belward, A., Morisette, J., Lewis, P., Privette, J. and Baret, F. 2000: Developments in the ‘validation’ of satellite sensor products for the study of the land surface. *International Journal of Remote Sensing* 21, 3383-90.

Kansas, J.L. 2002: Status of the grizzly bear (Ursus arctos) in Alberta. *Alberta Wildlife Status Report No. 37.*

Kent, M. 2007: Biogeography and landscape ecology. *Progress in Physical Geography* 31, 345-55.

Keys, L.D., Schmidt, N.J. and Phillips, B.E. 1990: A prototype example of sensor fusion used for a siting analysis. *Technical Papers 1990, ACSM-ASPRS Annual Conference Image Processing and Remote Sensing* 4, 238-49.

Lam N.S.N. and Quattrochi, D.A. 1992: On the issues of scale, resolution, and fractal analysis in the mapping sciences. *Professional Geographer* 44, 88–98.

Leprince, S., Barbot, S., Ayoub, F. and Avouac, J. 2007: Automatic and precise orthorectification, coregistration, and subpixel correlation of satellite images, application to ground deformation measurements. *IEEE Transaction Geoscience and Remote Sensing* 45, 1529–58.

Li, H. and Wu, J. 2004: Use and misuse of landscape indices. *Landscape Ecology* 19, 389–99.

Li, Q., Hu, B. and Pattey, E. 2008: A scale-wise model inversion method to retrieve canopy biophysical parameters from hyperspectral remote sensing data. *Canadian Journal of Remote Sensing* 34, 311–19.

Lu, D. and Weng, Q. 2007: A survey of image classification methods and techniques for improving classification performance. *International Journal of Remote Sensing* 28, 823–70.

Lubis, A.M. and Isezaki, N. 2009: Shoreline changes and vertical displacement of the 2 April 2007 Solomon Islands earthquake Mw 8.1 revealed by ALOS PALSAR images. *Physics and Chemistry of the Earth* 34, 409-15.

McDermid, G.J. 2005: Remote sensing for large-area, multi-jurisdictional habitat mapping. PhD thesis. Waterloo, ON: University of Waterloo.

McDermid, G., McLane, A., Collingwood, A., Hird, J., Faraguna, A., Laskin, D., Linke, J., Cranston, J., Guo, X. and Franklin, S. 2008: Remote Sensing Mapping and Research Update. In: Stenhouse, G. and Graham, K. (eds). *Foothills Research Institute Grizzly Bear Program 2007 Annual Report.* Hinton, Alberta. 204 pp.

Meng, Q., Borders, B.E., Cleszewski, C.J. and Madden, M. 2009: Closest spectral fit for removing clouds and cloud shadows. *Photogrammetric Engineering and Remote Sensing* 75, 569-76.

Mitchell, S.C. 2005: How useful is the concept of habitat? – A critique. *Oikos* 110, 634-38.

Moody, A. and Woodcock, C.E. 1995: The influence of scale and the spatial characteristics of landscapes on land-cover mapping using remote sensing. *Landscape Ecology* 10, 363-79.

Morena, L.C., James, K.V. and Beck, J. 2004: An introduction to the RADARSAT-2 mission. *Canadian Journal of Remote Sensing* 30, 221-34.

Morrison, M.L., Marot, B.G. and Mannan, R.W. 2006: *Wildlife-habitat relationships: Concepts and application.* Third edition. Washington D.C.: Island Press, 3-128.

O'Neill, R.V., Krummel, J.R., Gardner, R.H., Sugihara, G., Jackson, B., DeAngelis, D.L., Milne, B.T., Turner, M.G., Zygnut, B., Christensen, S.W., Dale, V.H. and Graham, R.L. 1988: Indices of landscape pattern. *Landscape Ecology* 1, 152–62.

Osborne, P.E., Alonso, J.C. and Bryant, R.G. 2001: Modelling landscape-scale habitat use using GIS and remote sensing: a case study with great bustards. *Journal of Applied Ecology* 38, 458-71.

Paillou, P., Schuster, M., Tooth, S., Farr, T., Rosenqvist, A., Lopez, S. and Malezieux, J-M. 2009: Mapping of a major paleodrainage system in eastern Libya using orbital imaging radar: The Kufrah River. *Earth and Planetary Science Letters* 277, 327-33.

Pape, A.D. and Franklin, S.E. 2008: MODIS-based change detection for Grizzly Bear habitat mapping in Alberta. *Photogrammetric Engineering and Remote Sensing* 74, 973-85.

Pohl, C. and van Genderen, J.L. 1995: Image fusion of microwave and optical remote sensing data for map updating in the Tropics. *Image and Signal Processing for Remote Sensing, Proceedings EUROPTO 95, SPIE* 2579, 2-10.

Pohl, C. and van Genderen, J.L. 1998: Multisensor image fusion in remote sensing: concepts, methods and applications. *International Journal of Remote Sensing* 19, 823-54.

Pohl, C. and van Genderen, J.L. 1999: Multi-sensor image maps from SPOT, ERS and JERS. *Geocarto International* 14, 34-41.

Powell, R.L., Matzke, N., de Souza, Jr., C., Clark, M., Numata, I., Hess, L.L. and Roberts, D.A. 2004: Sources of error in accuracy assessment of thematic land-cover maps in the Brazilian Amazon. *Remote Sensing of Environment* 90, 221-34.

Qi, J., Kerr, Y.H., Moran, M.S., Weltz, M., Huete, A.R., Sorooshian, S. and Bryant, R. 2000: Leaf area index estimates using remotely sensed data and BRDF models in a semiarid region. *Remote Sensing of Environment* 73, 18-30.

Radarsat-2 Information 2009a: Applications. Retrieved 14 July 2009 from http://www.radarsat2.info/application/index.asp

Radarsat-2 Information 2009b: Features and benefits. Retrieved 14 July 2009 from http://www.radarsat2.info/about/features_benefits.asp

Ranchin, T. and Wald, L. 2000: Fusion of high spatial and spectral resolution images: The ARSIS concept and its implementation. *Photogrammetric Engineering and Remote Sensing* 45, 49-61.

Ranson, K.J., Kovacs, K., Sun, G. and Kharuk, V.I. 2003: Disturbance recognition in the boreal forest using radar and Landsat-7. *Canadian Journal of Remote Sensing 29*, 271-85

Rignot, E. 2008: Changes in West Antarctic ice stream dynamics observed with ALOS PALSAR data. *Geophysical Research Letter* 35, L12505, doi:10.1029/2008GL033365.

Rogers, R.H., and Wood, L. 1990: The history and status of merging multiple sensor data: an overview. *Technical Papers 1990, ACSM-ASPRS Annual Convention, Image Processing and Remote Sensing* 4, 352-60.

Rossi, R.E., Dungan, J.L. and Beck, L.R. 1994: Kriging in the shadows: Geostatistical interpolation for remote sensing. *Remote Sensing of Environment* 49, 32-40.

Rosenqvist, A., Shimada, M., Ito, N. and Watanabe, M. 2007: ALOS PALSAR: A pathfinder mission for global-scale monitoring of the environment. *IEEE Transactions on Geoscience and Remote Sensing* 45, 3307-16.

Rosenqvist, A., Shimada, M., Watanabe, M., Tadono, T. and Yamauchi, K. 2004: Implementation of systematic data observation strategies for ALOS PALSAR, PRISM and AVNIR-2. *IEEE Transactions on Geoscience and Remote Sensing* 7, 4527-30.

Roy, D.P., Ju, J., Lewis, P., Schaaf, C., Gao, F., Hansen, M. and Lindquist, E. 2008: Multi-temporal MODIS-Landsat data fusion for relative radiometric normalization, gap filling, and prediction of Landsat data. *Remote Sensing of Environment* 112, 3112-30.

Saura, S. 2004: Effects of remote sensor spatial resolution and data aggregation on selected fragmentation indices. *Landscape Ecology* 19, 197-209.

Simpson, J.J. and Stitt, J.R. 1998: A procedure for the detection and removal of cloud shadow from AVHRR data over land. *IEEE Transactions on Geoscience and Remote Sensing* 36, 880-97.

Shao, G. and Wu, J. 2008: On the accuracy of landscape pattern analysis using remote sensing data. *Landscape Ecology* 23, 505-11.

Stenhouse, G. 2008: Introduction. In: Stenhouse, G., and K. Graham (eds), 2008. *Foothills Research Institute Grizzly Bear Program 2007 Annual Report.* Hinton, Alberta. 204pp.

Takada, M., Mishima, Y., and Natsume, S. 2009: Estimation of surface soil properties in peatland using ALOS/PALSAR. *Landscape and Ecological Engineering* 5, 45-58.

Thanh, H.N., Ryutaro, T. and Dinh, D.N. 2008: Cloud removal of optical image using SAR data for ALOS applications - Experimenting on simulated ALOS data. *Proceedings of the Conference of the Remote Sensing Society of Japan* 41, 73-4.

Tseng, D.C., Tseng, H.T. and Chien, C.L. 2008: Automatic cloud removal from multi-temporal SPOT images. *Applied Mathematics and Computation* 205, 584-600.

Turner, M.G. 2005: Landscape ecology: what is the state of the science? *Annual Review of Ecology, Evolution, and Systematics* 36, 319-44.

Urban, D.L. 2005: Modeling ecological processes across scales. *Ecology* 86, 1996–2006.

Wang, B., Ono, A., Muramatsu, K. and Fujiwara, N. 1999: Automated detection and removal of clouds and their shadows from Landsat TM images. *IEICE TRANSACTIONS on Information and Systems* E82-D, 453-60.

Wang, Z., Jin, J., Liang, J., Yan, K. and Peng, Q. 2005: A new cloud removal algorithm for multi-spectral images, in: *Proc. of SPIE*, SAR and Multispectral Image Processing (MIPPR 2005), Vol. 6043.

Waske, B. and van der Linden, S. 2008: Classifying multilevel imagery from SAR and optical sensors by decision fusion. *IEEE Transaction on Geoscience and Remote Sensing* 46, 1457-66.

Weydahl, D.J. 1993: Multitemporal analysis of ERS-1 SAR images over land areas. Better Understanding of Earth Environment. *Proceedings 13th Annual IEEE International Geoscience and Remote Sensing Symposium (IGARSS 93)*, Tokyo, Japan, pp. 1459-61.

Wiens, J.A. 1989: Spatial scaling in ecology. *Functional Ecology* 3, 385–97.

Wong, A. and Clausi, D. 2007: ARRSI: Automatic registration of remote sensing images. *IEEE Transaction on Geoscience and Remote Sensing* 45, 1483-93.

Wu, J. 2004: Effects of changing scale on landscape pattern analysis: scaling relations. *Landscape Ecology* 19, 125-38.

Wu, J. and Hobbs, R. 2002: Key issues and research priorities in landscape ecology: an idiosyncratic synthesis. *Landscape Ecology* 17, 355–65.

Wu, J., Shen, W., Sun, W. and Tueller, P.T. 2002: Empiriacal patterns of the effects of changing scale on landscape metrics. *Landscape Ecology* 17, 761-82.

Wulder, M. A., White, J. C., Goward, S. N., Masek, J. G., Irons, J. R., Herold, M., Cohen, W. B., Loveland, T. R. and Woodcock, C. E. 2008: Landsat continuity: Issues and opportunities for land cover monitoring. *Remote Sensing of Environment* 112, 955–69.

Xu, M., Watanachaturaporn, P., Varshney, P.K. and Arora, M.K. 2005: Decision tree regression for soft classification of remote sensing data. *Remote Sensing of Environment* 97, 322-36.

Yamanouchi, T. and Kawaguchi, S. 1992: Cloud distribution in the Antarctic from AVHRR data and radiation measurements at the surface. *International Journal of Remote Sensing* 13, 111-27.

CHAPTER 3 - COMPARISON OF LANDSAT MULTISPECTRAL AND IRS PANCHROMATIC IMAGERY FOR LANDSCAPE PATTERN ANALYSIS OF GRIZZLY BEAR HABITAT IN AGRICULTURAL AREAS OF WESTERN ALBERTA[2]

3.1 Abstract

The grizzly bear (*Ursus arctos* L.) is listed as a moderately endangered species in Canada. Agricultural activities, oil and gas exploration and extraction, forestry, and recreation can all contribute to grizzly bear habitat fragmentation and loss. The purpose of this research was to compare two models of grizzly bear activity in agricultural areas of western Alberta, Canada, developed from landscape pattern metrics derived from Landsat- and IRS (Indian Remote Sensing)-based land cover classifications and assess if these models statistically converged on the same landscape metrics. Results were further explained by considering the influence of spatial, spectral and thematic resolution, along with previous knowledge on grizzly bear habitat preference. The Landsat- and IRS-based analyses were compared using relationships between landscape metrics and both grizzly bear presence/absence data and frequency of use data. Results indicated that landscape spatial structure had at least some role in determining whether or not grizzly bears would use an area in an agricultural landscape. It was concluded that the thematic

[2] The full citation of this published chapter is: Wang, K., Franklin, S.E., Guo, X., Collingwood, A., Stenhouse, G.B., and Lowe, S. 2010. Comparison of Landsat multispectral and IRS panchromatic imagery for landscape pattern analysis of grizzly bear habitat in agricultural areas of western Alberta. Canadian Journal of Remote Sensing, 36(1):36-47. This article is re-printed with permission from the Canadian Aeronautics and Space Institute. Herein, most of the "3.3 Methods" is derived from co-author, Collingwood, A's M.Sc. Thesis.

resolution represented the greatest impact on compositional metrics for both the grizzly bear presence/absence and frequency of use analyses; i.e., the Landsat-based product was more suited to revealing the function of the compositional metrics than IRS-based product. Configurational metrics, however, were more sensitive to the higher spatial resolution map derived from the IRS data. Landscape management recommendations are suggested in the context of these geospatial results.

3.2 Introduction

Landscape analysis, which refers to the process of accurately quantifying landscape pattern, is commonly used for resource management applications, environmental conservation, and examining the impacts of anthropogenic activity. A large number of metrics have been developed for quantifying landscape pattern since O'Neill et al. (1988). Specifically, landscape metrics have been shown to contribute to the explanation of species presence and abundance (McGarigal and McComb, 1995; Linke et al., 2005), habitat loss and fragmentation (Linke et al., 2005), and the effects of ecotones and corridors on species movement (Bowers et al., 1996). They have also been used extensively for describing habitat function and landscape pattern (Herzog and Lausch, 2001; Berland et al., 2008). Advances in remote sensing technologies have provided practical means for classified thematic maps which are the key inputs for most studies on landscape pattern analysis (Shao and Wu, 2008; Wang et al., 2009).

Landscape pattern is spatially correlated and scale-dependent (Wu, 2004). In particular, any measures of spatial heterogeneity in the landscape pattern, or of patch characteristics via metrics, will be scale-dependent (Wu and Hobbs, 2002; Li and Wu, 2004; Wu, 2004). For remotely sensed data, image spatial (Benson and MacKenzie, 1995; Wu et al., 2002) and radiometric resolution, applied thematic resolution (determined by the applied land cover classification scheme; Huang et al., 2006; Buyantuyev and Wu, 2007; Castilla et al., 2009), classification methods, and any other classification-relevant factors are deemed to have a direct and significant effect on the subsequent landscape pattern analysis. Moreover, the effects of these classification factors have been proven to be correlated and interactive both in theory and practice (Shao and Wu, 2008; Newton et al., 2009). However, it is difficult to clarify the internal statistical mechanism, as all classifications of remote sensing data are subject to different kinds of errors (Shao and Wu, 2008), such as position error, thematic error, uncertainty pertaining to class nomenclature, and uncertainty associated with classification accuracy assessment (Shao and Wu, 2008; Newton et al., 2009). These errors or uncertainties can be carried over or propagated in subsequent landscape pattern analysis (Shao and Wu, 2008).

The Foothills Research Institute Grizzly Bear Program (FRIGBP, formerly called Foothills Model Forest Grizzly Bear Research Program), initiated in 1999, is currently focusing on the relationships between landscape conditions, anthropogenic landscape changes, and health in grizzly bears (Stenhouse, 2008). Resource selection functions (RSF) and food-based habitat quality models have been developed to estimate the relative probability of grizzly bears occurring in west-central Alberta. However, the impact of agricultural activities has not yet been considered in the above models.

Agricultural activities, like other anthropogenic activities such as oil and gas exploration and extraction, forestry, and recreation, contribute to grizzly bear habitat fragmentation and loss (Garshelis et al., 2005). Modern agricultural methods fragment natural ecosystems, subsequently increasing isolation which typically leads to changes in community structure and function, such as loss of species in isolated islands and disruption of the food web (Kruess and Tscharntke, 1994). In a study of grizzly bear-human conflict on agricultural lands in Montana, Wilson et al. (2005, 2006) found that there were many different attractants for grizzly bears on private lands that are a part of the natural grizzly bear habitat. One of the most important factors was the use of riparian areas by grizzly bears as both habitat and transportation corridors (Wilson et al. 2005). The grizzly bears use these areas to reach anthropogenic attractants. The more attractants that were in an area and the closer that area was to wetlands or riparian areas, the more likely the grizzly bears were to use that area as habitat. When fences were introduced, the rate of grizzly bear use dropped considerably. Additionally, networks of roads and trail are correspondingly built up to accompany all of the aforementioned activities. These linear features allow access to otherwise remote areas by people, which Kansas (2002) listed as one of the primary limiting factors for grizzly bear populations in Alberta and elsewhere. Fragmentation not only changes the structure of the landscape, but also reduces the total area of available habitat, which may limit grizzly bear movement (Singleton et al., 2004).

Collingwood et al. (2009) classified agricultural areas in Alberta grizzly bear habitat using Landsat TM (Thematic Mapper) multispectral imagery, and Collingwood (2008) used the IRS-1C and -1D (Indian Remote Sensing) panchromatic imagery to classify the same location and derived the metrics based on the classification map (Table 3.1). However, the two classified maps were not effectively put in practice to help understand and preserve the threatened grizzly bear in Alberta. The purpose of this research was to compare two models of grizzly bear activity in agricultural areas of western Alberta, Canada developed from landscape pattern metrics derived from Landsat- and IRS-based classifications and assess if these models statistically converged on the same landscape metrics. Furthermore, we tried to explain results by considering the influence of spatial, spectral and thematic resolution and previous knowledge on grizzly bear habitat preference.

Table 3.1 Differences between Landsat- and IRS-based products

	Landsat-based	IRS-based
Spatial resolution	30 meters	5 meters
Spectral resolution	Multispectral (6 bands)	Panchromatic (1 band)
Thematic resolution	15 classes	4 classes

3.3 Methods

Methods used to generate the relationship model products consisted of image acquisition and preprocessing, image classification (including classification-accuracy validation) and landscape analysis for model building. In the following sections the key elements of map production and landscape analysis are presented.

3.3. 1 Study area

The study area for this project was the foothills region to the southwest of Calgary, Alberta. The area was chosen based on grizzly bear GPS location data that suggested that grizzly bears were present in agricultural areas in this part of the province. This landscape is dominated by agricultural grassland and cropland, with patches of forest, changing to largely forested areas further west in the foothills. Roads are a dominant feature in much of this landscape, with higher densities in the agricultural areas, and lower densities in the foothills.

The total study area covers 4494 km^2, which was sub-divided into 107 square sub-landscapes of 42 km^2 each (Figure 3.1), 71 of which contained grizzly bear occurrence points. The sub-landscapes were placed to cover agricultural fringe areas in the foothills that were within grizzly bear range. The selection of the 107 sub-landscapes was based on the combination of grizzly bear, agricultural areas, field data, and the available imagery. The range of the sub-landscapes in this research was based on the recommendations of Linke et al. (2005) and Nams et al. (2006), who found that grizzly bears move through and select habitat at a range of around 35 – 50 km^2. Nams et al. (2006) found a strong selection preference at a range of 16 – 64 km^2, with a peak preference at 36 km^2, while Linke et al. (2005) found a possible range from 31 – 49 km^2, and used a measure of 49 km^2. The use of sub-units of 42 km^2 is halfway (rounded down) between the two different recommended values of 36 km^2 and 49 km^2, and well within the given range of 35 – 50 km^2. It is important that this range be defined and representative of the organism being studied; otherwise, the landscape patterns detected will have little meaning, and the conclusions reached may not be accurate (McGarigal and Marks, 1995). Each sub-landscape was analyzed separately in the FRAGSTATS program (FRAGSTATS v3.3, Amherst, USA), and had its own landscape metrics generated.

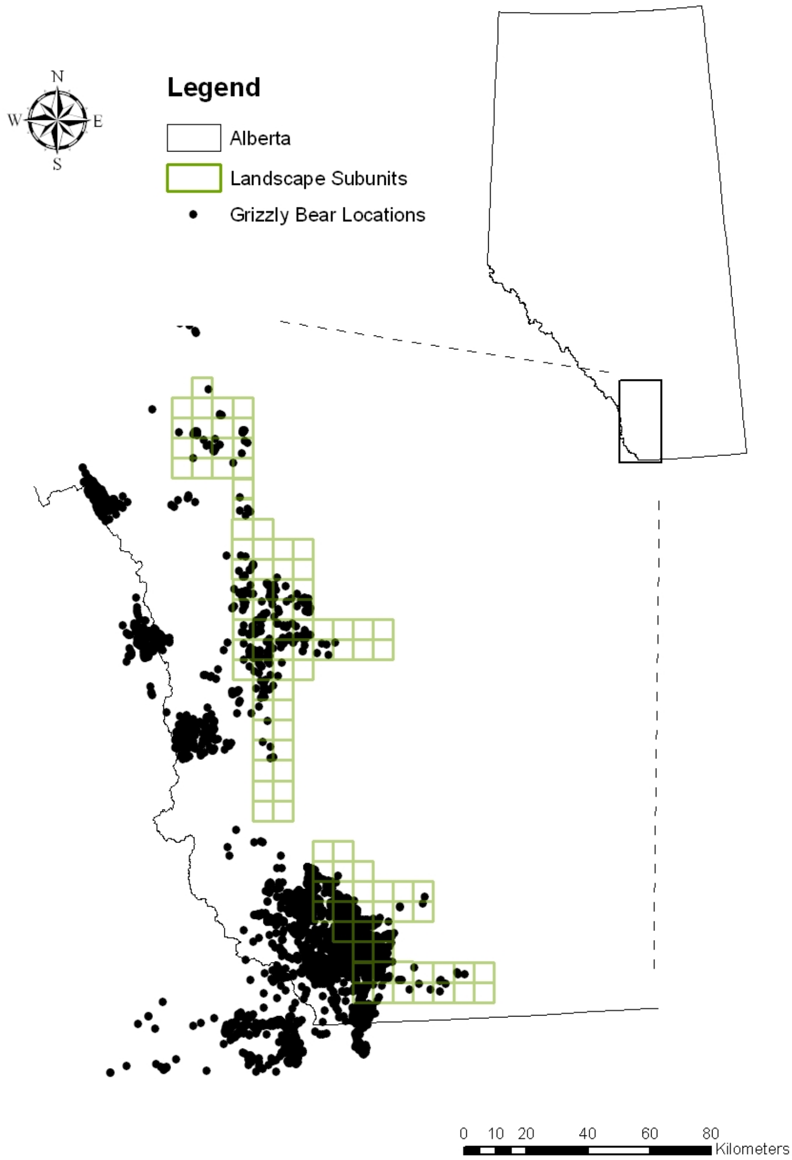

Figure 3.1 Study area map showing the distribution of the 107 sub-landscapes in western Alberta

3.3.2 Classification maps

The two classification maps derived from 30 m Landsat TM multispectral and 5 m IRS-1C and -1D panchromatic imagery were produced for the subsequent landscape pattern analysis. Both types of imagery were classified using an object-oriented approach in the Definiens Developer

7.0 software. The detailed procedure of Landsat- and IRS-based classification can be reviewed from Collingwood et al. (2009) and Collingwood (2008) respectively. The Supervised Sequential Masking (SSM) method was used to produce a 15-class map from the Landsat imagery, and a 4-class map from the IRS imagery. The classification schemes for these two maps are listed in Table 3.2. Regarding classification accuracy, the Landsat-based product obtained an overall accuracy of 88.0% (Collingwood et al., 2009), and the IRS-based product an overall accuracy of 81.0% (Collingwood, 2008).

Table 3.2 Classification scheme of Landsat and IRS

Landsat (15 classes)	IRS (4 classes)
Upland Trees, and Wetland Trees	Forest
Upland Herbs, Wetland Herbs, Shrubs, Grasses/Forage, Canola, Legumes, Small Grains, Bare Soil/Fallow, and Barren,	Agriculture
Water	Water
Shadow, Cloud, and Snow/Ice	Other

3.3.3 GIS data and grizzly bear location information

GIS data used in this study were provided by the FRIGBP. The data included vector data of roads and streams within the study area. The road and stream vector data were used to calculate the density of these features (km / km^2) within each sub-landscape. Stream density was included based on work by Nielsen et al. (2002) and Wilson et al. (2005, 2006) who demonstrated a relationship between grizzly bear habitat selection and distance to riparian areas. Road density was also included, as road density has been shown to play a large role in grizzly bear use or avoidance of an area (McLellan and Shackleton, 1988; Mace et al., 1996; Wielgus et al., 2002; Chruszcz et al., 2003; Waller and Servheen, 2005).

A grizzly bear point location database was also used in this analysis. In order to collect the grizzly bear GPS location data, the FRIGBP captured, immobilized, and radio-collared a sample of the grizzly bear population located throughout the grizzly bears' Alberta range. Collars were placed on both male and female grizzly bears. The resulting telemetry data from these collars were then transmitted to the FRIGBP through a satellite uplink, with locations being recorded every four hours or less (varies depending on year of capture). A detailed methodology and results from this program can be found in Hobson (2005, 2006). A total of 8 grizzly bears (5 male, 3 female) gave 1454 point locations (not evenly distributed among the grizzly bears or the study area) in the area of study. To reduce auto-correlation, over 85% of the data were selected with one or two locations per day per bear, approximately 10% of the data were selected with three locations per day per bear, and seldom were four locations selected. In addition, location data belonged to four different capture areas, and covered two capture years. Specific grizzly bear behavior, such as foraging or mating, was not accounted for, due to the nature of the available data.

3.3.4 Selection and calculation of spatial pattern metrics

A variety of configurational and compositional landscape metrics were chosen for this analysis based on their simplicity and accuracy in measuring different elements of the landscape. Metrics were computed at the landscape level in the FRAGSTATS program; landscape level analysis measures the aggregate properties of the entire landscape mosaic for each sub-landscape

(McGarigal et al., 2002). Individual grid cells of the same land cover type were merged to form discrete patches using the 8-cell patch neighbor rule (McGarigal et al., 2002), which could be placed with the help of the Minimum Mapping Unit (MMU) of polygons, and the sub-landscape borders were not counted as edges, which are the same parameters used by Linke et al. (2005). The metrics were chosen to try to limit redundancy in the physical characteristics being measured, and to represent each of four main categories: i) patch area, ii) edge and patch shape, iii) diversity, and iv) landscape configuration. The 'landscape configuration' category was further sub-divided into measures of isolation/proximity, contagion/interspersion, and connectivity (Table 3.3). In addition, the metrics were chosen based on expert advice and knowledge gained from field data collected from grizzly bears over the past 10 years of FRIGBP (McDermid et al., 2008). Some of the metrics were direct measures of some variables (e.g., Landscape Division Index), while others, such as the Shape Index, were aggregates of that metric across the entire sub-landscape in all classes. These aggregated metrics included the following distribution statistics of the measurement: mean (MN), area-weighted mean (AM), median (MD), range (RA), standard deviation (SD), and coefficient of variation (CV). Some of the metrics used (including the Euclidean Nearest Neighbor Distance, the Shape Index, and Simpson's Evenness Index) have shown promise in other studies (e.g., Linke et al., 2005) in describing the relationship between the spatial characteristics of the landscape and grizzly bear presence in that landscape.

Table 3.3 Configurational landscape metrics used in the landscape pattern analysis

Name	Abbreviation	Measure of	Description
Patch Density	PD	Area/Density/Edge	-# of patches per landscape area
Edge Density	ED	Area/Density/Edge	-Amount of edge per landscape area
Landscape Shape Index	LSI	Area/Density/Edge	-A measure of density that adjusts for the landscape size
Shape Index	SHAPE_ (distributions)	Shape	-A measure of overall patch shape complexity
Contiguity Index	CONTIG_ (distributions)	Shape	-Assesses the spatial connectedness (contiguity) of cells in a patch to provide an index of patch boundary configuration or shape
Euclidean Nearest Neighbor Distance	ENN_ (distributions)	Isolation/ Proximity	-A measure of patch context – the shortest straight line distance between a patch and its nearest neighbor of the same class
Contagion Index	CONTAG	Contagion / Interspersion	-Measures the degree of clumping of attributes on raster maps
Percentage of Like Adjacencies	PLADJ	Contagion / Interspersion	-Measures the degree of aggregation of patch types
Landscape Division Index	DIVISION	Contagion / Interspersion	-Measures the probability that 2 randomly chosen points in the landscape are not situated in the same patch
Connectance Index (100m)	CONNECT	Connectivity	-The number of functional joinings between patches of the same class that are within 100m of each other
Simpson's Evenness Index	SIEI	Diversity	-Measures the distribution of area among the different patch classes

Note: For more detailed information and formulas, see McGarigal and Marks (1995)

Compositional metrics were also used, and included the percent composition of each class type (Table 3.2), as well as road and stream density for each sub-landscape. Similar compositional components have been used in other grizzly bear landscape studies, with road density especially being seen as an important measurement to include (e.g., Apps et al., 2004; Singleton et al., 2004; Nams et al., 2006).

3.3.5 Statistical analysis

An Analysis of Variance (ANOVA) test (for normal distribution) and Mann–Whitney U test (for non-normal distribution) were conducted to find significant differences between identical variables with grizzly bear presence or absence as the controlling factor. Logistic regression based on presence/absence of grizzly bears was conducted, using a conditional forward stepwise method. Logistic regression was done to test predictions of the presence or absence of grizzly bears in a given area. An initial correlation analysis using Pearson's r was conducted to identify variables which may be related to grizzly bear frequency of use (location points/km^2, just including the presence data, without absence data). Frequency of use as used in this study refers to the number of grizzly bear GPS locations per km^2 in a specific sub-landscape. Finally, multiple regression analysis was conducted, using a stepwise approach, to see which metrics could be used to predict grizzly bear frequency of use, and how much of the variation could be explained by the given metrics. Cushman and McGarigal (2004) found that coding for frequency of use data generally produced a more descriptive model, but uncommon species with a low frequency of occurrence (such as grizzly bears) could be better represented by presence/absence data. They also found that presence/absence models were more sensitive to analysis of spatial metrics at the patch- and landscape-scale than frequency of use models were. The results of the statistical analysis could therefore be somewhat dependent on the scale of the landscape and the way in which the species-response data was coded (Cushman and McGarigal, 2004).

3.4 Results

3.4.1 Relationships between grizzly bear presence/absence and landscape metrics

The results of Landsat- and IRS-based analyses were compared below (Table 3.4). For the Landsat-based analysis, eight configurational metrics and 6 compositional metrics were significantly different when grizzly bear presence or absence in the sub-landscape was the controlling factor; for the IRS-based analysis, 15 configurational metrics and 1 compositional metric were significantly different. Patch Density (PD), Edge Density (ED), Land Shape Index (LSI), Area-weighted Mean and Median of Contiguity Index (CONTIG_AM and CONTIG_MD), Mean of Euclidean Nearest Neighbor Distance (ENN_MN), and Percentage of Like Adjacencies (PLADJ) were significantly correlated in both the Landsat- and IRS-based analyses. The compositional metrics for the IRS-based analysis only included %Forest, whereas the Landsat-based analysis consisted of the metrics not only related to the forest land cover, but also the agricultural land cover.

Table 3.4 Difference between Landsat- and IRS-based analyses in relationships between grizzly bear presence / absence and landscape metrics

	Landsat-based	IRS-based
Significantly correlated metrics [a]	Negative (-): %Upland Trees, %Upland Herbs, %Wetland Herbs, %Shrubs, PD, ED, and LSI Positive (+): %Grass/Forage, %Bare Soil/Fallow, CONTIG_AM, CONTIG_MD, ENN_MN, PLADJ, and CONTAG	Negative (-): %Forest, PD, ED, LSI, SHAPE_AM, SHAPE_RA, SHAPE_SD, SHAPE_C, CONTIG_MD, ENN_CV, and DIVISION Positive (+): CONTIG_AM, ENN_MN, ENN_SD, PLADJ, and CONNECT
Logistic regression models	$\ln\left(\frac{1-p_a}{p_a}\right) =$ 5.624+1.804*%WetlandHerbs+(-0.113)*%BareSoil/Fallow+(-0.074)*CONTAG	$\ln\left(\frac{1-p_a}{p_a}\right) = -$ 39.704+0.065*SHAPE_CV+41.954*CONTIG_MD+(-0.009)*ENN_MN+0.003*ENN_AM
Accuracy [b]	Absence: 47.2; Presence: 91.5; Overall: 76.6	Absence: 38.9; Presence: 87.3; Overall: 71.0

Note: [a] The minus sign indicates that the mean (or mean rank) was higher for bear presence; the plus sign indicates that the mean (or mean rank) was higher for bear absence; [b] The cut value of classification table is 0.500; p_a is the predicted probability.

Landscape metrics included in the logistic regression model (Table 3.4) by the conditional forward stepwise regression procedure were wetland herbs percentage (%Wetland Herbs), bare soil/fallow percentage (%Bare Soil), and Contagion Index (CONTAG) in the Landsat-based analysis. Coefficient of Variation of the Shape Index (SHAPE_CV), Median of Contiguity Index (CONTIG_MD), and Mean and Area-weighted Mean of the Euclidean Nearest Neighbor distance measure (ENN_MN and ENN_AM) were included in the IRS-based analysis. Because of the differences between what logistic regression and linear regression are predicting, there is no specific R^2 value in logistic regression that explains the percentage of variance explained, as for linear regression. There is, however, an 'R-Square' measure that approximates a normal R^2 value, based on likelihood estimates, called Nagelkerke R-Square. In addition, the Hosmer-Lemeshow Goodness-of-Fit, -2 Log Likelihood (-2LL), and Parameter Significance were used. If the Hosmer-Lemeshow Test statistic is greater than 0.5, it indicates the logistic model is a good fit. In the Landsat-based model, the values of these measures were 0.288 (Nagelkerke R-Square), 111.746 (-2LL), 0.511 (the Significance of Hosmer-Lemeshow Test), and the significance value of the three parameters were all below 0.05. In the IRS-based model, the values of these measures were 0.312 (Nagelkerke R-Square), 109.388 (-2LL), 0.655 (Hosmer-Lemeshow Test statistic), and the significance value of the four parameters were all below 0.05, except for ENN_AM (0.054).

From the coefficients for the logistic model, it would appear that grizzly bear presence is associated with an increase in wetland herbs percentage (%Wetland Herbs), and a decrease in bare soil/fallow percentage (%Bare Soil) and the Contagion Index (CONTAG) in the Landsat-based model; however, the presence seems to be associated with an increase in the Variation of the patch Shape Index (SHAPE_CV), a higher Median Contiguity Index (CONTIG_MD), a decrease in the Mean Euclidean Nearest Neighbor Distance between patches of the same class (ENN_MN), and an increase in the Area-weighted Mean Euclidean Nearest Neighbor Distance between patches of the same class (ENN_AM).

To test the multicollinearity between the independent variables in the logistic models, the Collinearity Diagnostics function was run in SPSS software (SPSS v16.0, Chicago, USA). For the Landsat-based model, the Variance Inflation Factor (VIF) values were 1.085, 1.098, and 1.017 for %Wetland Herbs, %Bare Soil/Fallow, and CONTAG respectively; for the IRS-based model, the VIF were 1.515, 1.152, 1.449, and 1.329 for SHAPE_CV, CONTIG_MD, ENN_MN, and ENN_AM respectively. There is no formal cutoff value to use with VIF for determining presence of multicollinearity. Generally, multicollinearity exists when VIF is greater than 10 (Allison, 1999). Therefore, no multicollinearity was indicated in either of the logistic models.

The logistic regression model (Table 3.4) predicted grizzly bear presence/absence with 91.5%/47.2% (Landsat-based) and 87.3%/38.9% (IRS-based) accuracy, and the overall prediction accuracy, including both presence and absence prediction, was 76.6% for the Landsat-based model and 71.0% for the IRS-based model. The prediction accuracy was based on the number of correctly predicted presence or absence values (using the regression equation) for each sub-landscape when compared to the observed values (the GPS locations). Figure 3.2 & 3.3 show the relationships between grizzly bear presence / absence and landscape metrics based on Landsat and IRS products.

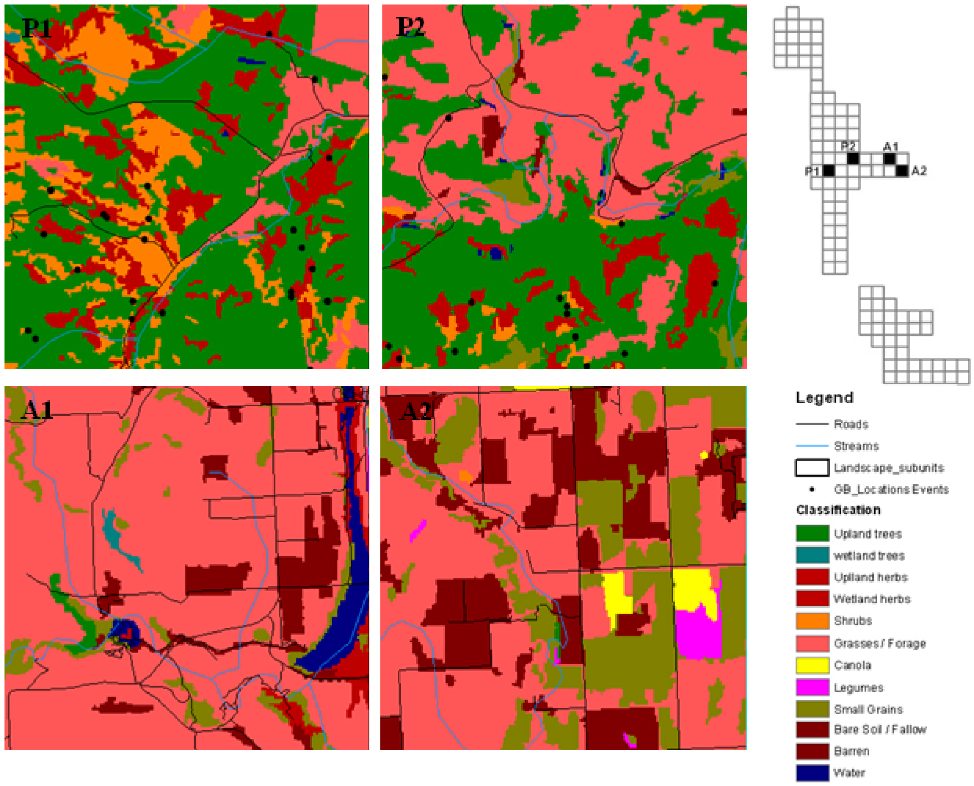

Figure 3.2 Relationships between grizzly bear presence/absence and landscape metrics based on Landsat product. P1 and P2 represent sub-landscapes with grizzly bears, and A1 and A2 stand for without grizzly bears.

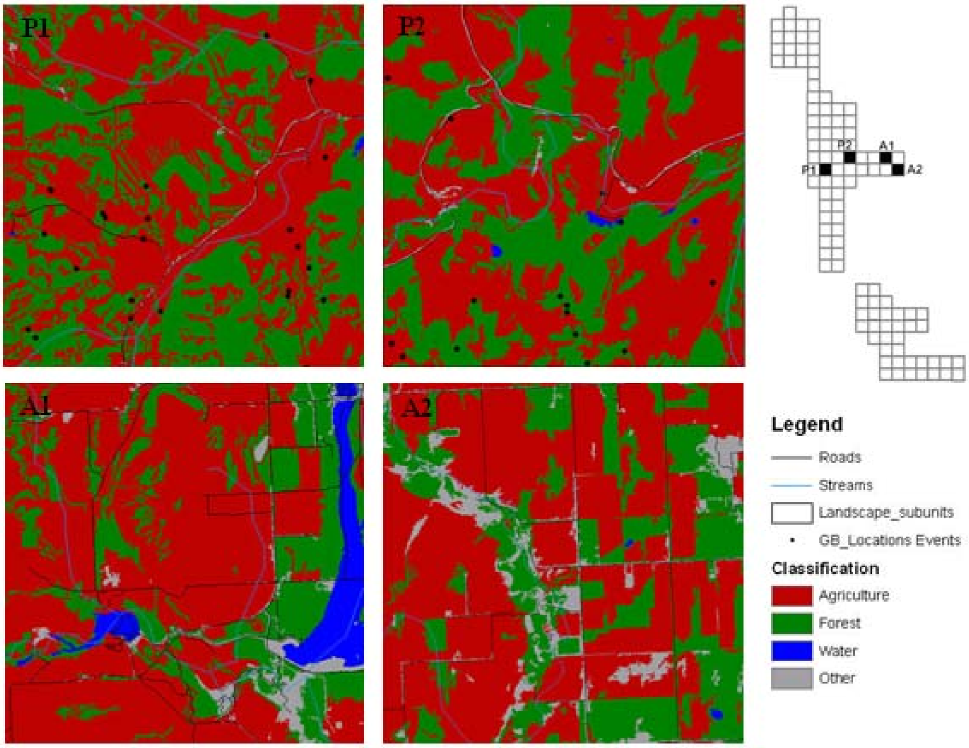

Figure 3.3 Relationships between grizzly bear presence/absence and landscape metrics based on IRS product. P1 and P2 represent sub-landscapes with grizzly bears, and A1 and A2 stand for without grizzly bears.

3.4.2 Relationships between grizzly bear frequency of use and landscape metrics

The Pearson correlation showed that a number of landscape metrics were significantly correlated ($p < 0.05$) with grizzly bear GPS location density (frequency of use) in each landscape unit. The results of Landsat- and IRS-based analysis were compared below (Table 3.5). Patch Density (PD), Edge Density (ED), Landscape Shape Index (LSI), Area-weighted Mean of Contiguity Index (CONTIG_AM), Percentage of Like Adjacencies (PLADJ), and Road Density were all significantly correlated with grizzly bear frequency of use data in both the Landsat- and IRS-based analysis.

Table 3.5 Difference between Landsat- and IRS-based analyses in relationships between grizzly bear frequency of use and landscape metrics

	Landsat-based	IRS-based
Significantly correlated metrics [a]	Negative (-): PD, ED, LSI, Road Density, and Stream Density	Negative (-): PD , ED, LSI, SHAPE_RA, and Road Density
	Positive (+): %Grass/Forage, CONTIG_MN, CONTIG_AM, CONTIG_MD, and PLADJ	Positive (+): CONTIG_AM, CONTIG_RA, ENN_MN, ENN_MD, ENN_SD, PLADJ, CONNECT, and SIEI
Multiple regression models	Y = 26.619 + (-0.829)*PD + (-0.662)*Road Density + (-0.254)*PLADJ (R square = 0.272)	Y = -12.181 + 0.005*ENN_MN + 6.497*CONTIG_RA + 4.170*SIEI (R square = 0.356)

Note: [a] The minus sign indicates the negative relationship between grizzly bear frequency of use and landscape metrics; the plus sign indicates the positive relationship.

Multiple regression analysis (Table 3.5) indicated that a model that included the Patch Density (PD), the Road Density and the Percentage of Like Adjacency (PLADJ) was likely to best explain grizzly bear location density in the Landsat-based model. The IRS-based model consisted of the Mean of the Euclidean Nearest Neighbor Distance (ENN_MN), the Road Density, and the Range of the Contiguity Index (CONTIG_RA). All of these metrics were significant ($P < 0.05$) in this model. R square values for the two models were 0.272 and 0.356 respectively, which indicates that about 27.2% and 35.6% of the variance seen in the grizzly bear location density could be explained by these metrics. The coefficients of the models suggest that grizzly bear use of an area increases with decreasing Patch Density (PD), Road Density, and Percentage of Like Adjacency (PLADJ) in the Landsat-based model, and grizzly bear use of an area increases with incremental Mean of Euclidean Nearest Neighbor Distance (ENN_MN), Range of the Contiguity Index (CONTIG_RA), and Simpson's Evenness Index (SIEI) in the IRS-based model. Similarly, to test the multicollinearity between the independent variables in the multiple regression models, Collinearity Diagnostics was run in SPSS software (SPSS v16.0, Chicago, USA). For the Landsat-based model, the VIF values were 5.881, 5.881, and 1.007 for PD, PLADJ, and Road Density respectively; for the IRS-based model, the VIF values were 1.222, 1.143, and 1.144 for ENN_MN, CONTIG_RA, and SIEI respectively. As previously mentioned, VIF values above 10 may be a cause for concern. Therefore, there is no indication of multicollinearity in either of the multiple regression models. Figure 3.4 & 3.5 show the relationships between grizzly bear frequency of use and landscape metrics based on Landsat and IRS products.

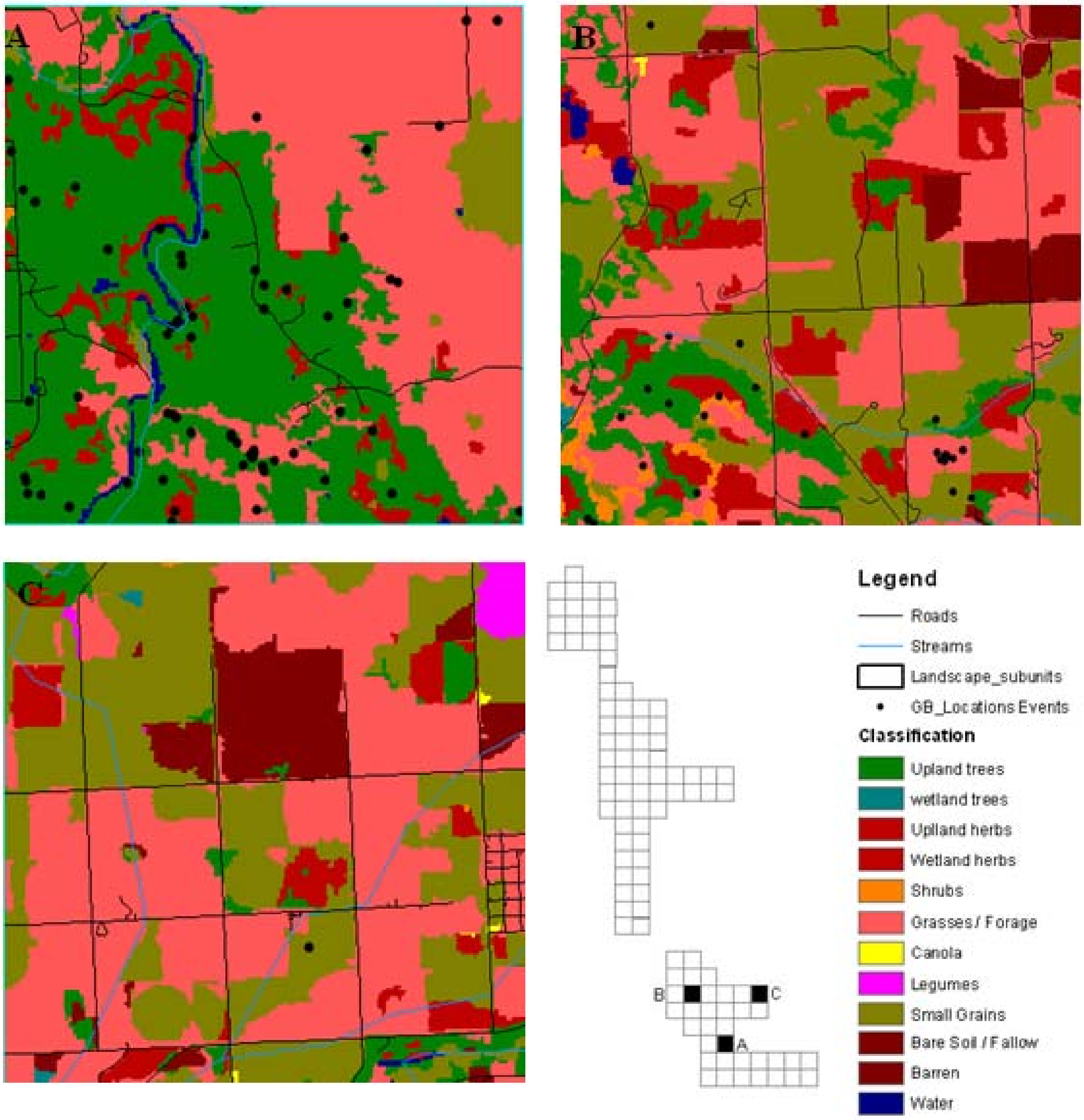

Figure 3.4 Relationships between grizzly bear frequency of use and landscape metrics based on Landsat product. A, B and C represent high, medium and low abundance respectively.

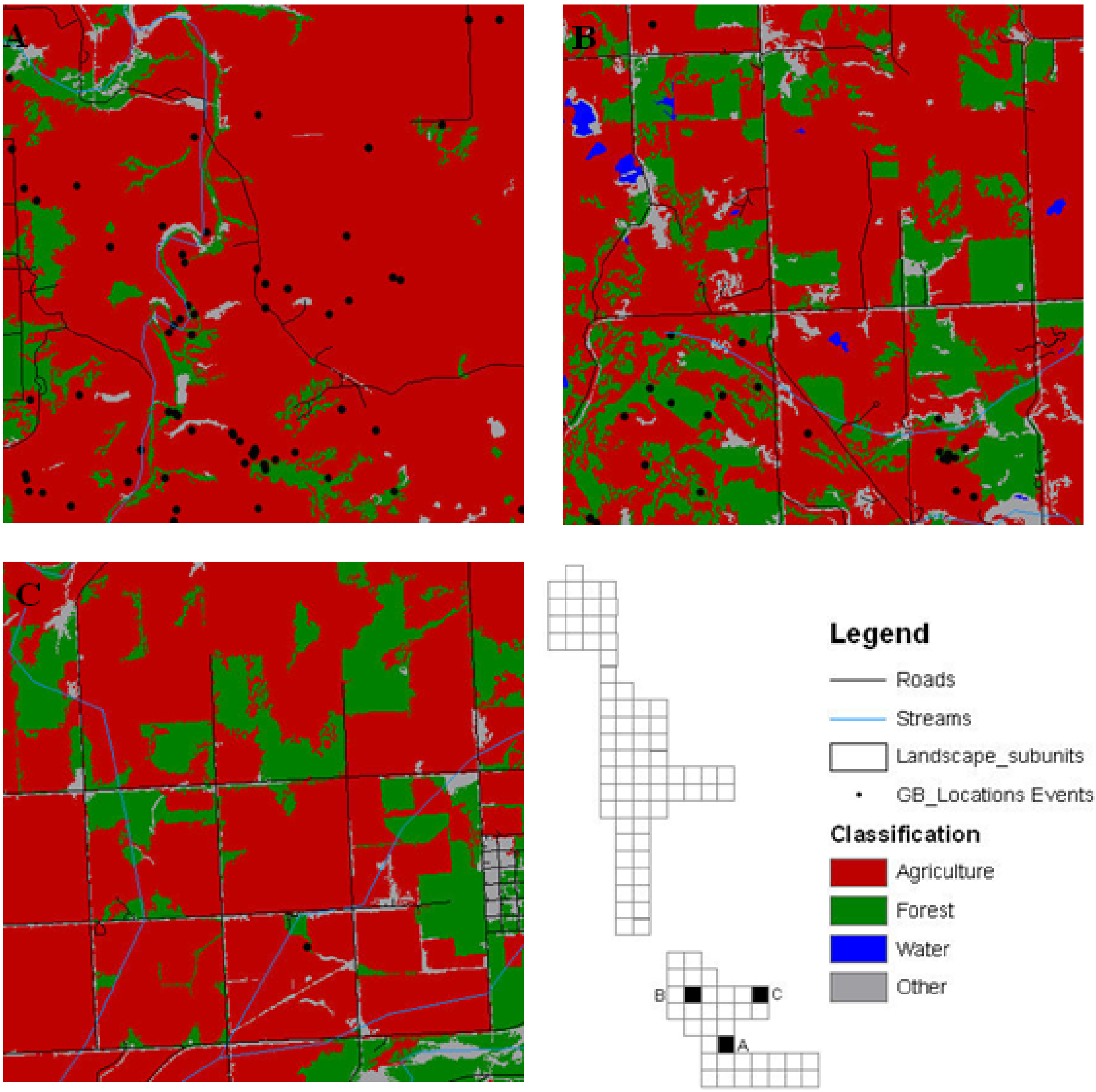

Figure 3.5 Relationships between grizzly bear frequency of use and landscape metrics based on IRS product. A, B and C represent high, medium and low abundance respectively.

3.5 Discussion

3.5.1 Presence/absence data and metrics

Six compositional metrics were significantly correlated with grizzly bear presence/absence, including upland trees percentage (%Upland Trees), upland herbs percentage (%Upland Herbs), wetland herbs percentage (%Wetland Herbs), shrubs percentage (%Shrubs), grass/forage percentage (%Grass/Forage), bare soil/fallow percentage (%Bare Soil/Fallow), in the Landsat-based analysis. Only one compositional metric, i.e. forest percentage (%Forest), had a significant correlation in the IRS-based analysis. The forest class of the IRS-based product refers to the upland trees and wetland trees classes of the Landsat-based product. In addition, upland trees were dominant in the study area. Overall, these results suggested both models converged in the forest environment, which is the main habitat of grizzly bears because it provides both food and shelter (Nielsen et al., 2003; Nielsen et al., 2004; Nielsen, 2005). The other five compositional metrics, i.e. %Upland Herbs, %Wetland Herbs, %Shrubs, %Grass/Forage, and %Bare Soil/Fallow, correspond to the agriculture class of the IRS-based products. However, the agriculture class was not significantly correlated with the grizzly bear presence/absence in the IRS-based analysis. Agriculture and its associated land cover have been proven to contribute to grizzly bear habitat fragmentation and loss (Garshelis et al., 2005), and have great impacts on grizzly bear use of an area (Wilson et al., 2005, 2006). Consequently, it implied that thematic resolution plays an important role in landscape analysis. Nevertheless, the thematic resolution is constrained by the combination of certain spatial and spectral resolution, and is the outcome of the designed classification scheme.

Six configurational metrics, including Patch Density (PD), Edge Density (ED), Landscape Shape Index (LSI), Area-weighted Mean of Contiguity Index (CONTIG_AM), Percentage of Like Adjacencies (PLADJ) and Median of Contiguity Index (CONTIG_MD), were also significantly correlated with grizzly bear presence/absence data in both landscape analyses. Moreover, the common metrics displayed analogic change trend, indicating the grizzly bear presence would be more likely in areas with a high percentage of natural cover (forest-related classes) and a low percentage of human-disturbed cover (agriculture-related classes). For example, grizzly bear presence resulted in higher mean values for patch area / edge metrics like Patch Density (PD), Edge Density (ED), and the Landscape Shape Index (LSI), which means that there were more patches with more irregular shapes and edges (i.e., more natural areas) in sub-landscapes where grizzly bears were present than in sub-landscapes where grizzly bears were not present. However, more configurational metrics were significantly correlated with presence/absence data in the IRS-based analysis than the Landsat-based one, i.e. 15 versus 8 metrics. When considering the properties of patch configuration, the IRS-based classification could delineate the boundary and shape of patches more precisely and was more sensitive to the configurational metrics because the IRS-based classification had a higher spatial resolution compared to the Landsat-based classification. Therefore, configuration metrics have more direct meaning when derived from higher spatial resolution data.

The results of the logistic regression specified that two compositional metrics and one configurational metric were used for the Landsat-based model, and four configurational metrics were used for the IRS-based model. Grizzly bear presence was associated with an increase in wetland herbs, and a decrease in bare soil/fallow and Contagion Index (CONTAG) in the Landsat-based analysis, with an overall accuracy of 76.6%. In the IRS-based analysis, the grizzly bear presence was linked to an increase in the Variation of the patch Shape Index (SHAPE_CV), a higher Median Contiguity Index (CONTIG_MD), a decrease in the Mean Euclidean Nearest Neighbor Distance between patches of the same class (ENN_MN), and an increase in the Area-weighted Mean Euclidean Nearest Neighbor Distance between patches of the same class (ENN_AM), with an overall accuracy of 71.0%. We could not identify any significant difference in the accuracy, and the results showed the uniqueness of the two different products; i.e., the

Landsat-based product could reveal balanced compositional and configurational landscape information with higher spectral and thematic resolution, while the IRS-based product had advantage in delineating the boundary and shape of patches with higher spatial resolution.

3.5.2 Frequency of use data and metrics

Only one of the ten significantly correlated metrics (%Grass/Forage) was a compositional metric in the Landsat-based analysis, and no compositional metrics were significantly correlated in the IRS-based analysis. This implies that grizzly bear frequency of use was guided by landscape configuration more than composition in both the Landsat- and IRS-based models. Bear presence/absence may be determined more by landscape composition or balance of composition/configuration versus the frequency of use that was determined more by landscape configuration. However, the advantage of Landsat multispectral imagery in describing land cover information was also implicitly exposed through grass/forage percentage, the only compositional metric significantly correlated with frequency of use data.

Patch Density (PD), Edge Density (ED), Landscape Shape Index (LSI), the area-weighted mean of Contiguity Index (CONTIG_AM), Percentage of Like Adjacencies (PLADJ) and Road Density were all significantly correlated with grizzly bear frequency of use in both analyses. Moreover, all the metrics displayed consistent effects on grizzly bear frequency of use. Patch Density (PD) is an index representing the number of patches per unit area and could serve as a good fragmentation index. Accordingly, higher grizzly bear frequency of use was more likely to occur within less fragmented agricultural areas in Alberta. Patch density gives a different relationship for frequency of use than for the presence/absence data, where the patch density was higher in areas of grizzly bear presence. This difference could be caused by the effects of coding the response variable differently. In terms of frequency of use data, lower fragmentation was more likely to be suitable for frequent bear activity. However, more patches indicate more attractants to grizzly bear presence. Further more, Edge Density (ED) and Landscape Shape Index (LSI) negatively correlated with frequency of use data which can further support this inference. The area-weighted mean of Contiguity Index (CONTIG_AM) and Percentage of Like Adjacency (PLADJ) were positively correlated with grizzly bear frequency of use, displaying that patch shape and patch aggregation degree had an incremental effect on frequency of use. High contiguity and like adjacency were analogous to low fragmentation. Roads were significantly ($p < 0.05$) negatively correlated with grizzly bear frequency of use, which is supported by most of the literature; high road densities are associated with increased fragmentation, which leads to loss of overall habitat and increased access and use by humans, all of which have been shown to have impacts on grizzly bear use and selection of an area (McLellan and Shackleton, 1988; Mace et al., 1996; Wielgus et al., 2002; Chruszcz et al., 2003; Waller and Servheen, 2005). Road density was quite high in agricultural areas which could relate to grizzly bear avoidance of anthropogenic landscapes. As well, traffic volume and speed can play a role in grizzly bear reactions to road density (Chruszcz et al., 2003; Waller and Servheen, 2005).

The R square of the multiple regression models was higher in the IRS-based analysis than the Landsat-based one (R^2: 0.356 versus 0.272). As mentioned earlier, the configurational metrics played the dominant role in explaining the variance seen in the grizzly bear frequency of use. The IRS-based classification map has 5 m spatial resolution, which can delineate the boundary and shape of patches more precisely than the 30 m Landsat-based map.

3.6 Conclusions

Knowledge about grizzly bear selection of habitat in agricultural areas is very limited. There were significant differences among landscapes that grizzly bears use versus those they do not use. Landscape spatial structure seems to have at least some role in determining whether or not grizzly bears will use an area in an agricultural landscape. The results of this research, while not definite, could be helpful in informing other grizzly bear resource selection models.

In this research, thematic resolution had a greater impact on compositional metrics in both grizzly bear presence/absence and frequency of use analyses, i.e. the Landsat-based product was more suitable for revealing the function of compositional metrics than IRS-based product. This could partly be because 30 m and 5 m spatial scales are both higher than the minimum scale required by grizzly bear ecology. A higher spatial resolution product has an advantage in accurately delineating the contour of patches. Therefore, configurational metrics were more sensitive to the higher spatial resolution IRS-based product. For landscape management, landscape analysis based on remotely sensed data should be performed and reported with explicit description of the attributes of the data. Furthermore, before applying the results of the analysis into further research and practice, the effect of attributes such as spatial, spectral, radiometric, and thematic resolutions need to be evaluated. For example, in the frequency of use analysis of the IRS-based product, no compositional metric was related to the grizzly bear location density. Nonetheless, it cannot be concluded that compositional metrics have no direct effect on the grizzly bear frequency of use, since the analysis was limited by the spectral and thematic resolution of the IRS imagery. In order to improve representation of landscape pattern, data fusion should be considered. For example, fusing Landsat and IRS data takes the advantages of spectral and spatial resolutions. However, the feasibility of data fusion would depend on issue of scale, data fusion technology, and the availability of imagery.

A concern may be raised due to the small size of grizzly bear samples used in this research. Therefore, it may be questionable to draw conclusions that are broadly applicable to grizzly bears in general. In addition, another potential limitation of this research is that it doesn't take the sex, age, reproductive state, nutritional state or previous experiences information of the grizzly bears into account. These factors may have effect on the presence/absence and frequency of use models, and thus limit the applicability of these two models.

This research demonstrated that agriculture and its associated land cover were related to an increase in grizzly bear habitat fragmentation and loss, which is consistent with previous research. It is known that grizzly bears generally tend to avoid anthropogenic disturbance despite agricultural areas having many food attractants such cattle, sheep, beehives and bone yards (Kansas, 2002; Nielsen et al., 2004; Linke et al., 2005; Berland et al., 2008). Because of this possibility of conflict between grizzly bears and humans, landscape managers should pay more attention to the effects of agricultural areas on grizzly bears.

3.7 References

Allison, P.D. 1999. *Logistic regression using the SAS system: theory and application.* SAS Institute Inc., Cary, N.C.

Apps, C.D., McLellan, B.N., Woods, J.G., and Proctor, M.F. 2004. Estimating Grizzly Bear Distribution and Abundance Relative to Habitat and Human Influence. *Journal of Wildlife Management* Vol. 68 No. 1, pp. 138–152.

Berland, A., Nelson, T., Stenhouse, G., Graham, K., and Cranston, J. 2008. The impact of landscape disturbance on grizzly bear habitat use in the Foothills Model Forest, Alberta, Canada. *Forest Ecology and Management*, Vol. 256, pp. 1875–1883.

Benson, B.J., and MacKenzie, M.D. 1995. Effects of sensor spatial resolution on landscape structure parameters. *Landscape Ecology*, Vol. 10, pp. 113–120.

Bowers, M.A., Gregario, K., Brame, C.J., Matter, S.F., and Dooley, J.L. 1996. Use of space and habitats by meadow voles at the home range, patch and landscape scales. *Oecologia*, 105: 107–115.

Buyantuyev, A., and Wu, J. 2007. Effects of thematic resolution on landscape pattern analysis. *Landscape Ecology*, Vol. 22, pp. 7–13.

Castilla, G., Larkin, K., Linke, J., and Hay, G.J. 2009. The impact of thematic resolution on the patch-mosaic model of natural landscapes. *Landscape Ecology*, Vol. 24, pp. 15–23.

Chruszcz, B., Clevenger, A.P. Gunson, K.E. and Gibeau, M.L. 2003. Relationships among grizzly bears, highways, and habitat in the Banff-Bow Valley, Alberta, Canada. *Canadian Journal of Zoology*, Vol.81, No. 8, pp. 1378–1391.

Collingwood, A. 2008. *Satellite Image Classification and Spatial Analysis of Agricultural Areas for Land Cover Mapping of Grizzly Bear Habitat*. M.Sc. thesis, University of Saskatchewan, Saskatoon, SK.

Collingwood, A., Franklin, S.E., Guo, X., and Stenhouse, G. 2009. A medium-resolution remote sensing classification of agricultural areas in Alberta grizzly bear habitat. *Canadian Journal of Remote Sensing*, Vol. 35, pp. 23–26.

Cushman, S. A. and McGarigal, K. 2004. Patterns in the species-environment relationship depend on both scale and choice of response variables. *Oikos*, Vol. 105, No. 1, pp. 117–124.

Garshelis, D.L., Gibeau, M.L. and Herrero, S. 2005. Grizzly bear demographics in and around Banff National Park and Kananaskis Country, Alberta. *Journal of Wildlife Management*, Vol. 69, pp. 277–297.

Herzog, F., and Lausch, A. 2001. Supplementing land-use statistics with landscape metrics: some methodological considerations. *Environmental Monitoring and Assessment*, Vol. 72, pp. 37–50.

Hobson, D. 2005. Bear capturing and handling. In *Foothills research institute grizzly bear program 1999-2003 final report*. Edited by G. Stenhouse and K. Graham. Foothills Research Institute, Hinton, Alberta.

Hobson, D. 2006. Summary of 2005 spring capture program. In *Foothills research institute grizzly bear program 2005 annual report*. Edited by G. Stenhouse and K. Graham. Foothills Research Institute, Hinton, Alberta.

Huang, C., Geiger, E.L., and Kupfer, J.A. 2006. Sensitivity of landscape metrics to classification scheme. *International Journal of Remote Sensing*, Vol. 27, 2927–2948.

Kansas, J.L. 2002. *Status of the Grizzly Bear* (Ursus arctos) *in Alberta*. Fish and Wildlife Division, Alberta Sustainable Resource Development, and Alberta Conservation Association, Edmonton, Alberta Wildlife Status Report 37. 43 pp.

Kruess, A., and Tscharntke, T. 1994. Habitat Fragmentation, Species Loss, and Biological control. *Science*, New Series, Vol. 264, pp. 1581–1584.

Li, H., and Wu, J. 2004. Use and misuse of landscape indices. *Landscape Ecology*, Vol. 19, pp. 389–399.

Linke, J., Franklin, S.E., Huettmann, F., and Stenhouse, G.B. 2005. Seismic Cutlines, Changing Landscape Metrics and Grizzly Bear Landscape Use in Alberta. *Landscape Ecology*, Vol. 20, No. 7, pp. 811–826.

Mace, R.D., Waller, J.S., Manley, T.L., Lyon, L.J., and Zuuring, H. 1996. Relationships among grizzly bears, roads and habitat in the Swan Mountains Montana. *Journal of Applied Ecology*, Vol. 33, No. 6, pp. 1395–1404.

Maehr, D.S., Noss, R.F., and Larkin, J.L. 2001. *Large Mammal Restoration: Ecological and Sociological Challenges in the 21st Century*. Island Press, Washington, D.C., pp. 71–72.

McDermid, G., McLane, A., Collingwood, A., Hird, J., Faraguna, A., Laskin, D., Linke, J., Cranston, J., Guo, X., and Franklin, S. 2008. Remote sensing mapping and research update. In *Foothills Research Institute Grizzly Bear Program 2007 Annual Report*. Edited by G. Stenhouse and K. Graham. Foothills Research Institute, Hinton, Alberta.

McGarigal, K., Cushman, S.A., Neel, M.C., and Ene, E. 2002. *FRAGSTATS: spatial pattern analysis program for categorical maps.* Computer software program produced by the authors at the University of Massachusetts, Amherst. Available from http://www.umass.edu/landeco/research/fragstats/fragstats.html [cited 21 March 2009].

McGarigal, K., and Marks, B.J. 1995. *FRAGSTATS: spatial pattern analysis program for quantifying landscape structure*. USDA For. Serv. Gen. Tech. Rep. PNW-351.

McGarigal, K., and McComb, W.C. 1995. Relationships between landscape structure and breeding birds in the Oregon Coast Range. *Ecological Monographs*, Vol. 65, pp. 235–260.

McLellan, B.N., and Shackleton, D.M. 1988. Grizzly bears and resource-extraction industries: effects of roads on behaviour, habitat use and demography. *Journal of Applied Ecology*, Vol. 25, No. 2, pp. 451–460.

Nams, V.O., Mowat, G., and Panian, M.A. 2006. Determining the spatial scale for conservation purposes – an example with grizzly bears. *Biological Conservation*, Vol. 128, pp. 109–119.

Nielsen, S.E. 2005. *Habitat ecology, conservation and projected population viability of grizzly bears* (Ursus arctos L.) *in west-central Alberta, Canada*. PhD Thesis, University of Alberta, Canada.

Nielsen, S.E., and Boyce, M.S. 2002. Resource selection functions and population viability analyses. In *Foothills model forest grizzly bear research program 2001 annual report*. Edited by G. Stenhouse and K Graham. Foothills Research Institute, Hinton, AB.

Nielsen, S.E., Boyce, M.S., Stenhouse, G.B., and Munro, R.H.M. 2003. Development and testing of phonologically driven grizzly bear habitat models. *Ecoscience*, Vol. 10, pp. 1–10.

Nielsen, S.E., Munro, R.H.M., Bainbridge, E., Boyce, M.S., and Stenhouse, G.B., 2004. Grizzly bear and forestry II: distribution of grizzly bear foods in clearcuts of west-central Alberta. *Forest Ecology and Management*, Vol. 199, pp. 67–82.

Newton, A.C., Hill, R.A., Echeverria, C., Golicher, D., Benayas, J.M.R., Cayuela, L., and Hinsley, S.A. 2009. Remote sensing and the future of landscape ecology. *Progress in Physical Geography*, Vol. 33, pp. 528–546.

O'Neill, R.V., Krummel, J.R., Gardner, R.H., Sugihara, G., Jackson, B., DeAngelis, D.L., Milne, B.T., Turner, M.G., Zygnut, B., Christensen, S.W., Dale, V.H., and Graham, R.L. 1988. Indices of landscape pattern. *Landscape Ecology*, Vol.1, pp. 152–162.

Shao, G., and Wu, J. 2008. On the accuracy of landscape pattern analysis using remote sensing data. *Landscape Ecology*, Vol. 23, pp. 505–511.

Singleton, P.H., Gaines, W.L., and Lehmkuhl, J.F. 2004. Landscape permeability for grizzly bear movements in Washington and southwestern British Columbia. *Ursus*, Vol. 15, Workshop Supplement, pp. 90–103.

Stenhouse, G. B. 2008. Introduction. In *Foothills research institute grizzly bear program 2007 annual report*. Edited by G. Stenhouse and K. Graham. Foothills Research Institute, Hinton, AB.

Waller, J.S., and Servheen, C. 2005. Effects of transportation infrastructure on grizzly bears in northwestern Montana. *Journal of Wildlife Management*, Vol. 69, No. 3, pp. 985–1000.

Wang, K., Franklin, S.E., Guo, X., He, Y., and McDermid, G.J. 2009. Problems in remote sensing of landscapes and habitats. *Progress in Physical Geography,* Vol. 33, pp. 747-768.

Wielgus, R.B., Vernier, P.R., and Schivatcheva, T. 2002. Grizzly bear use of open, closed, and restricted forestry roads. *Canadian Journal of Forest Research*, Vol. 32, No. 9, pp. 1597–1606.

Wilson, S.M., Madel, M.J., Mattson, D.J., Graham, J.M., Burchfield, J.A., and Belsky, J.M. 2005. Natural landscape features, human-related attractants, and conflict hotspots: a spatial analysis of human-grizzly bear conflicts. *Ursus*, Vol. 16, No. 1, pp. 117–129.

Wilson, S.M., Madel, M.J., Mattson, D.J., Graham, J.M., and Merrill, T. 2006. Landscape conditions predisposing grizzly bears to conflicts on private agricultural lands in the western USA. *Biological Conservation*, Vol. 130, No. 1, pp. 47–59.

Wu, J. 2004. Effects of changing scale on landscape pattern analysis: scaling relations. *Landscape Ecology*, Vol.19, pp. 125–138.

Wu, J. and Hobbs, R. 2002. Key issues and research priorities in landscape ecology: an idiosyncratic synthesis. *Landscape Ecology*, Vol. 17, pp. 355–365.

Wu, J., Shen, W., Sun, W., and Tueller, P.T. 2002. Empiriacal patterns of the effects of changing scale on landscape metrics. Landscape Ecology, Vol.17, pp. 761–782.

CHAPTER 4 - THE APPLICABILITY OF SMALL-SATELLITE CONSTELLATION IN CLASSIFICATION FOR LARGE-AREA HABITAT MAPPING: A CASE STUDY OF DMC MULTISPECTRAL IMAGERY IN WEST-CENTRAL ALBERTA[3]

4.1 Abstract

The small-satellite constellation (SSC) has the outstanding advantage of efficient operation and cost, global surveying, and increased revisit frequency, such that it has become the cutting edge of development in remote sensing for recent years. The Disaster Monitoring Constellation (DMC) is the first successful application of the concept of an earth-observation constellation. Its mission is to address the issue of large-area habitat mapping and to display the capability of SSC. The DMC provides 32 m spatial resolution imagery with one-day revisit frequency and 600 km swath width. The objective of this research was to demonstrate the applicability of SSC in large-area habitat mapping, i.e., by applying DMC multispectral imagery in the classification of grizzly bear habitat in west-central Alberta. An object-oriented classification method was selected to classify the DMC imagery into a hierarchical land cover classification scheme composed of three levels of detail. An error matrix was tabulated based on ground reference data to assess the accuracy of the DMC-based classification. In order to learn about the capability of

[3] The full citation of this chapter is: Wang, K., Franklin, S.E., and Guo, X. 2010. The applicability of small-satellite constellation in classification for large-area habitat mapping: a case study of DMC multispectral imagery in west-central Alberta. Canadian Journal of Remote Sensing, in press. This article is re-printed with permission from the Canadian Aeronautics and Space Institute.

DMC imagery as objectively as possible, the DMC-based and Landsat-based classifications were compared. The overall accuracies of DMC-based classification were 95.6% in the most general Level I, and 82.4% in the most detailed Level III classifications. However, the DMC-based classification was inferior to the Landsat-based classification in accuracy, and the difference was gradually widened from the Level I to Level III. It is believed that the DMC multispectral imagery can be a good candidate of remotely sensed data sources to describe the physiognomy of earth's surface with more than 80% accuracy, especially for large areas.

4.2 Introduction

According to the recognized satellite classification scheme, small satellite commonly refers to a mass in the range of 1-500 kg and satellite constellation is defined as groups of satellites working in concert (Xue et al., 2008). Since 1997, dozens of symposia on small satellites have been organized in Europe and North American. Kramer and Cracknell (2008) reviewed the development of small satellites, and predicted that more small satellites are likely to be dedicated to a particular mission objective in the future. With the launch of DMC (Disaster Monitoring Constellation, Table 4.1), the concept of the earth-observation constellation of low-cost small satellites was first put into action, with the capability of obtaining multispectral images for any part of the world every day (Goward et al., 2009). Other future systems, such as HJ-1 (Huan Jing-1, also called Environment-1, operated by China), RapidEye, and Sentinel 2, are constellation-based small-satellite programs, using the multiplicity of sensors to achieve both global surveying and increased revisit frequency (Goward et al., 2009). Moreover, it is declared that the upcoming RADARSAT series, developed by the Canadian Space Agency (CSA) and MacDonald Dettwiler and Associates Ltd (MDA), has been designed as a constellation.

Table 4.1 Disaster Monitoring Constellation (DMC) on orbit (adapted from DMC International Imaging Ltd)

Designation	Type	Imager	Launch	Waveband
Alsat-1	DMC	32m MS	2002	✓ MS
UK-DMC	DMC	32m MS	2003	NIR: 0.77-0.90 μm
Nigeriasat-1	DMC	32m MS	2003	Red: 0.63-0.69 μm
Beijing-1	DMC+4	32m MS / 4m Pan	2005	Green:0.52-0.60 μm
Deimos-1	DMC	22m MS	2008	✓ Pan
UK-DMC2	DMC	22m MS	2008	0.50-0.80 μm

Note: MS = Multispectral; Pan = Panchromatic

Aplin (2005) has predicted a bright future for small-satellite constellation (SSC) imagery, but still researchers of ecology, biodiversity, and conservation seldom apply this type of imagery. Only several papers discussed the potential of the imagery of SSC, or proposed applications. For instance, the results from Yan et al. (2006) revealed the potential of remote sensing applications of the HJ-1 (Huan Jing-1, also called Environment-1, operated by China) on water quality monitoring. Qian et al. (2009) demonstrated that simulated HJ-1B satellite data performed better on smaller and cooler fires than MODIS (Moderate Resolution Imaging Spectroradiometer) or AVHRR (Advanced Very High Resolution Radiometer) data, offering a great opportunity for the fire detection.

The DMC was initially proposed in 1996 and led by SSTL (Surrey Satellite Technology Limited), which is a world leader in high performance small satellites (Xue et al., 2008). Surrey Linear Imager - 6 Channels (SLIM-6) is a dual bank linear push broom imager utilizing the orbital motion of the DMC platform to capture radiation reflected from the Earth's surface (Crowley, 2008). SLIM-6 has 32 m spatial resolution with 3 bands (Table 4.1), which are equivalent to Landsat Thematic Mapper (TM) or Enhanced Thematic Mapper Plus (ETM+) band 4, band 3 and band 2 respectively. In addition, the DMC has two obvious advantages in remote sensing applications: one-day revisit frequency and 600 km swath width. A one-day temporal resolution can not only satisfy the application of detecting rapid surface changes, such as crop-growth monitoring and detecting intraseasonal ecosystem disturbance, but also promotes the acquisition of imagery with limited cloud-contamination. Wang et al. (2009) discussed the issue of clouds and cloud shadows in the context of environmental remote sensing, and have advised researchers to seek for good solutions to this unavoidable problem in optical remote sensing. It is believed that the development of a constellation of low-cost small satellites makes a significant contribution to addressing this issue. Furthermore, DMC imagery is especially suitable for large-area land cover mapping due to its 600 km swath width. In theory, the combination of the aforementioned sensor characteristics has potential to support DMC imagery use for extensive practical applications (Wang et al., 2009), such as forest, agriculture, land cover and habitat mapping, and flood or fire monitoring. However, its applicability should be tested in practice. One concern is whether DMC-based classification could achieve commonly accepted accuracy.

Habitat, defined as 'the sum of specific resources that are needed by an organism for survival and reproduction' (including biotic and abiotic entities; Hall et al., 1997; McDermid et al., 2005), has become the cornerstone concept of applied ecology, forest management, biodiversity science, and conservation (Kerr and Ostrovsky, 2003; Turner et al., 2003; Wulder et al., 2004; Mitchell, 2005; Morrison et al., 2006). For large-area habitat mapping, because of the limitations of in situ observation in aspects of spatial extent, time, cost and labor, remote sensing has long been identified as a feasible and effective technology for large scale measurement (i.e., regional or global scale) (Kerr and Ostrovsky, 2003; Turner et al., 2003; Alpine, 2005). A good example of large-area habitat mapping is the Foothills Research Institute Grizzly Bear Program (FRIGBP, formerly called Foothills Model Forest Grizzly Bear Research Program), initiated in 1999, which focuses on the relationships between landscape conditions, landscape change (human-caused), and health in grizzly bears (*Ursus arctos* L.) (Stenhouse, 2008). The grizzly bear is a species of concern in Alberta, because it has been identified as a wilderness-quality indicator species (Maehr et al., 2001). The FRIGBP has mapped the 228,000 km^2 that comprise the grizzly bear range in province of Alberta, including Landsat-derived products of land cover, crown closure, species composition, and MODIS-derived products of phenology (McDermid et al., 2008). Furthermore, these products support subsequent habitat-related applications, such as landscape change analysis, and resource selection functions, and food-based habitat quality models, which are used for grizzly bear habitat assessments and mapping. However, Wang et al. (2009) suggested that some of the Landsat satellite characteristics restrict the applications of Landsat-based products in large-area habitat mapping. For example, the 185 × 185 km image size is not always suitable for large-area applications. Mosaic methods were developed in the FRIGBP (McDermid et al., 2008) to combine land cover maps from different years forming a large map of the whole study area. As a consequence, the maps as a whole cannot present the updated information of landscape (Wang et al., 2009). Other problems still probably remain, such as a 16-day temporal resolution and the possible gap of Landsat continuity (Wulder et al., 2008; Wang et al., 2009). Accordingly, DMC may provide solution to the above problem.

As mentioned before, the main concern is the capability of DMC multispectral imagery in land cover classification. For remote sensing imagery, a pixel is the smallest operational unit. The per-pixel analysis, which is based on the statistical analysis of single pixels, dominated in the early stage of image processing. The typical algorithms include nearest-neighbor (e.g., Hardin and Thomson, 1992), maximum likelihood (e.g., Mather, 1985), decision tree (e.g., Hansen et al., 1996), artificial neural network (e.g., Chen et al., 1995), etc. However, more and more critiques question the applicability of the per-pixel analysis (Blaschke, 2010), because of its neglect of image semantics, i.e., characteristic texture of image data, which reflects attributes of pattern of reality in scales (Baatz and Schäpe, 2000; Blaschke and Strobl, 2001). Baatz and Schäpe (2000) underlined the semantic information can be represented in meaningful image objects, which coincide with spatial patchiness in ecosystems, and suggested image segmentation can be the bridge from pixels to objects.

In contrast to per-pixel analysis, object based image analysis (OBIA) is based on segmented image objects and their mutual relations. Blaschke (2010) stated that the number of OBIA-related peer-reviewed papers has increased sharply since the year 2005, especially in studies using fine spatial resolution satellite images, e.g., IKONOS, QuickBird, etc. Recently, OBIA methods have also been applied to studies using medium or coarse spatial resolution data, e.g., Landsat (Myint et al. 2008) or SPOT (Satellite Pour l'Observation de la Terre)-VEGETATION (Bontemps et al., 2008) data. Besides the aforementioned, two other significant advantages of OBIA are: 1) to bridge image processing and GIS functionality in order to utilize spectral and contextual information in an integrative way (Blaschke, 2010); and 2) to overcome the problem of salt-and-pepper effects found in traditional per-pixel analysis (Blaschke et al., 2000; Yu et al., 2006).

The objective of this research was to examine the applicability of small-satellite constellation in large-area habitat mapping, i.e., to apply DMC multispectral imagery in the classification of grizzly bear habitat in west-central Alberta. Besides presenting classification accuracy of DMC imagery itself, a Landsat-based classification was chosen as a reference to evaluate the applicability of the DMC imagery.

4.3 Study area and data

4.3.1 Study area

The FRIGBP covers sections, with a study area greater than 228,000 km^2, within the natural range of the grizzly bear in western-central Alberta, Canada. This research was conducted as part of the FRIGBP, and its study area is located on the eastern slopes of the Rocky Mountains (Figure 4.1). The study area lies approximately 50 km northeast of the town of Nordegg. It is located at the transitional zone from the Upper Foothills Natural Subregion to the Lower Foothills Natural Subregion affiliated to the Foothills Natural Region (Natural Regions Committee, 2006). This transition can be noticeably seen from mixedwood and deciduous stands in the Lower Foothills Natural Subregion to conifer-dominated forests in the Upper Foothills Natural Subregion (Natural Regions Committee, 2006). It consists of pure and mixed stands of trembling aspen (*Populus tremuloides*), balsam poplar (*Populus balsamifera*), white birch (*Betula pubescens*), lodgepole pine (*Pinus contorta*), white spruce (*Picea glauca*) and black spruce (*Picea mariana*), and scattered areas of shrubby grasslands, woody shrubs, and treed and non-treed wetlands (Natural Regions Committee, 2006). This area is experiencing significant human-disturbance, such as forestry practices (e.g., harvesting, plantations), oil and gas exploration, and recreational development (Stenhouse, 2008). All of these disturbances are contributing to grizzly bear habitat fragmentation and loss (Garshelis et al., 2005).

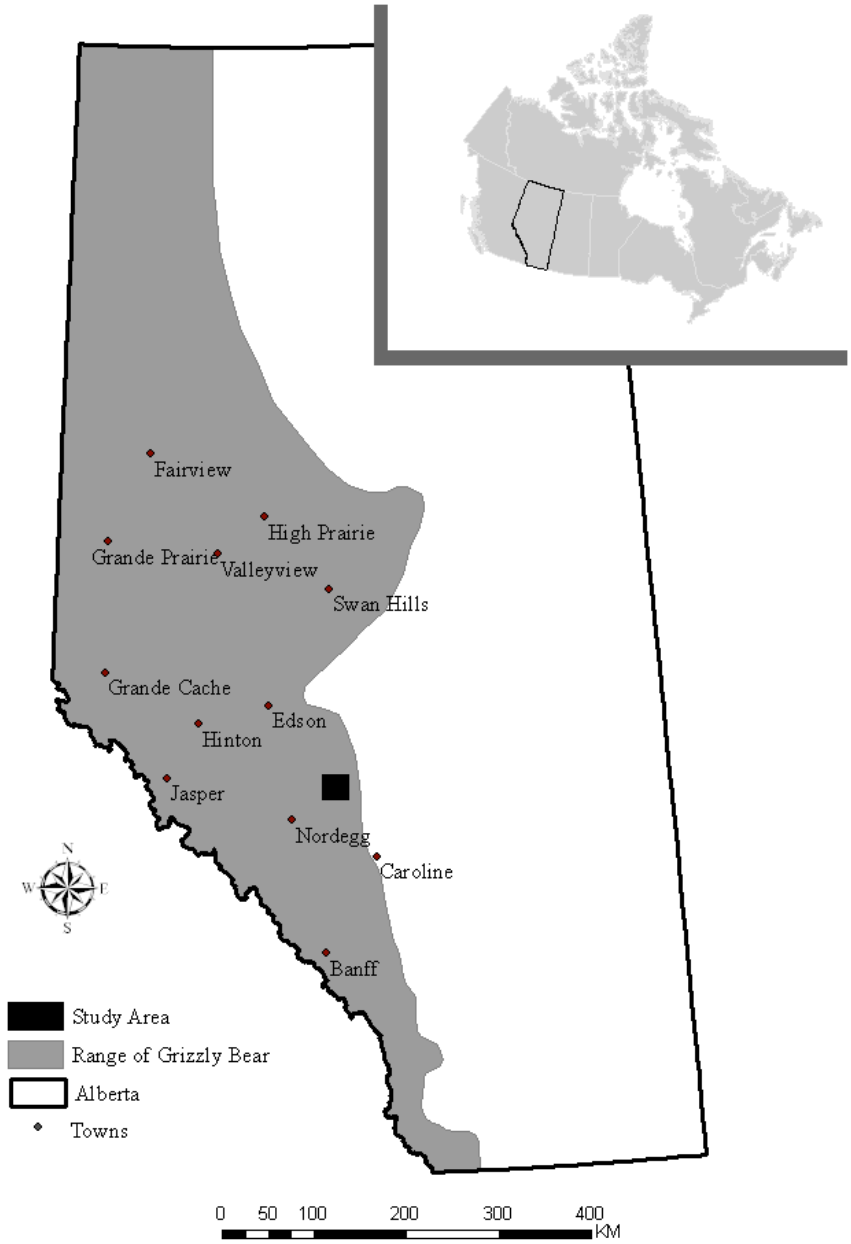

Figure 4.1 Location of the study area and the natural range of grizzly bear in Alberta

4.3.2 Imagery and ancillary data

The images used in this study consist of DMC Beijing-1 32 m multispectral imagery and Landsat 5 TM 30 m multispectral imagery. The DMC image was acquired July 12, 2008 by DMC International Imaging Ltd. Its footprint nearly covers the whole range of the FRIGBP study site. The spectral specification of DMC image can be seen in Table 4.1. The Landsat imagery includes three scenes of Path/Row 44/23: one from August 17, 2008 for comparison with DMC-based classification, and another two from July 10, 2003 and September 17, 2005 for field sample generation. The TM sensor has six optical spectral bands that cover visible, near-infrared, and mid-infrared portions of the electromagnetic spectrum (band 6, that measures emitted thermal energy, was not used in this study).

In addition, 30 m resolution Digital Elevation Model (DEM) data were used to assist land cover classification, including the information of aspect, slope and elevation. Existing field data and Landsat-based classification maps from the FRIGBP were used to produce training samples and validation samples (See detail in the section of field sample generation below).

4.4 Methods

Data and methods used to test the applicability of DMC imagery consist of image preprocessing, object-oriented classification, validation including accuracy assessment, and comparison of DMC- and Landsat-based classification. Figure 4.2 provides the flowchart of the processing chain. In the following sections the key elements of the process are presented.

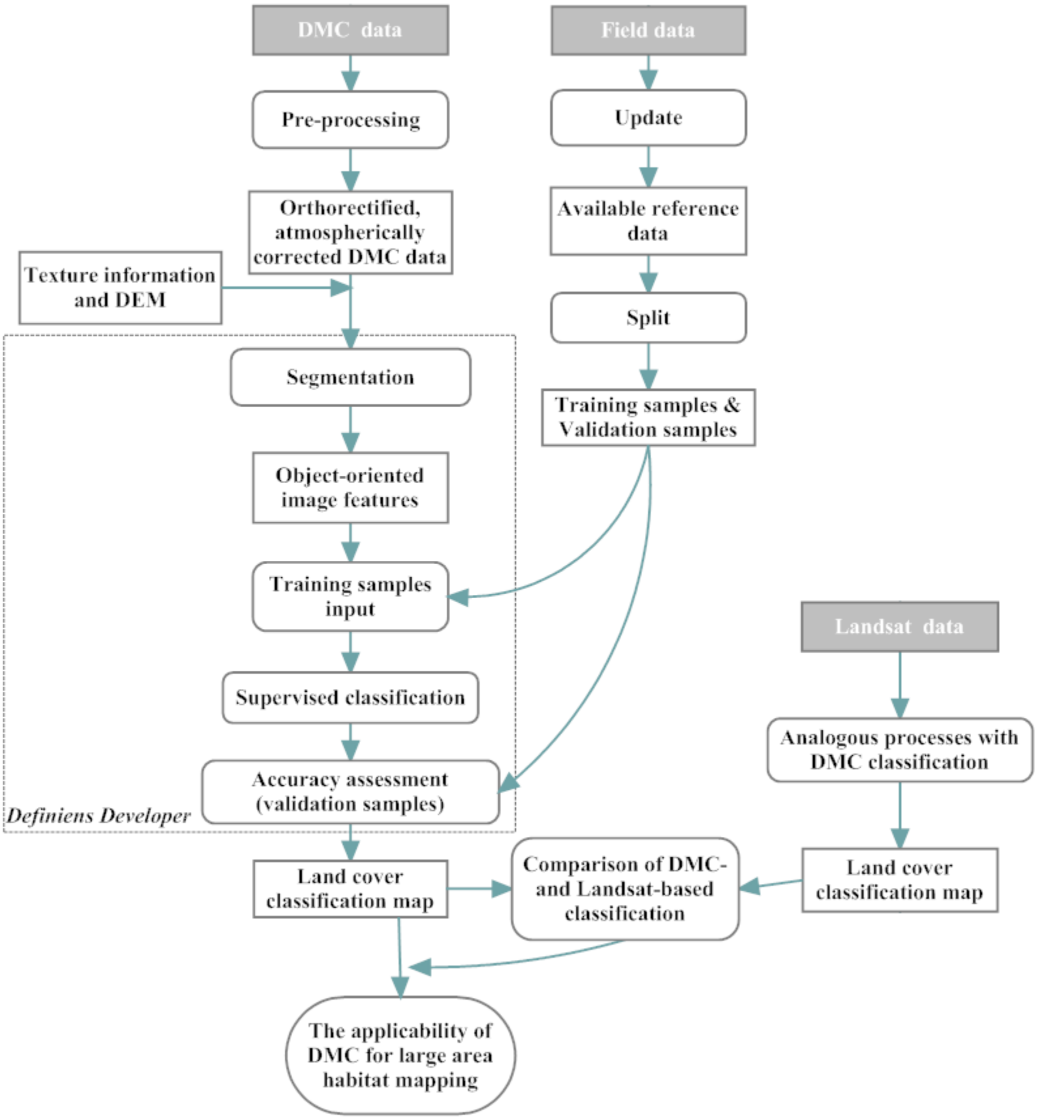

Figure 4.2 Flowchart of processing chain

4.4.1 Sample data

The DMC and Landsat images were acquired in 2008, but the available field data were collected in 2003 and the existing classification map of the FRIGBP was created in 2005. Therefore, samples for classification training and assessment can not be directly produced from the existing data set. The method introduced below was designed to produce the samples for classification training and assessment.

Of the field data regarding land cover, some are changed from the year 2003 to 2008, but some are not. The unchanged points can be used as the classification samples. Two criteria were set up to identify the unchanged points. One is that they should have very similar spectral reflectance in the 2003 and 2008 Landsat images. The other is that the points should not be located at the edge of landscape patches because the edge of patches is prone to influence by neighbor patches and anthropogenic disturbances. In reality, a high percentage of the study area remained stable and unchanging because it is located in the reserved forest environment of the Rocky Mountains, although the study area is still undergoing succession and human-induced change. Likewise, the classification samples can be extracted from the existing classification map in 2005 by comparing the 2005 and 2008 Landsat images. Finally, 530 points were selected out as the classification samples. Of the total, 70% were randomly selected for training and 30% were saved for assessment.

4.4.2 Image preprocessing

For comparison purposes, the DMC image was georeferenced based on the Landsat map products of the FRIGBP. Specifically, orthorectification was run using the satellite orbital math-model approach with an available DEM in PCI OrthoEngine (Version 10.2). A root mean square error (RMSE) <0.5 pixel was estimated based on 30 ground control points. Atmospheric correction of the DMC image was performed using the Improved Dark-Object Subtraction technique developed by Chavez (1988), in order to remove the effects of the atmosphere (mainly haze) and to convert digital numbers to scaled surface reflectance. The Landsat image was corrected using the ATCOR-2 algorithm (Richter, 2008) in PCI Geomatica 10.2.

After geometric and atmospheric correction, the Normalized Difference Vegetation Index (NDVI) was calculated to assist the classification of the DMC and Landsat images. In addition, the tasseled cap transformation (Crist and Cicone, 1984) was used to generate the standard orthogonal components brightness, greenness, and wetness from the Landsat image. The tasseled cap components were applied to the Landsat-based classification in two aspects: to reduce data volume without a loss of information (Crist and Cicone, 1984), and to be useful in discriminating between vegetation types and vegetation conditions (Jin and Sadar, 2005).

4.4.3 Object-oriented classification

Compared with traditional pixel-based classification methods, object-oriented classification methods have had promising results in improving classification accuracy for medium spatial resolution remotely sensed data, e.g., Landsat images (Dorren et al., 2003; Jobin et al., 2008; Collingwood et al., 2009). In addition, the FRIGBP has successfully applied Landsat imagery and object-oriented methods to produce land cover maps (McDermid et al., 2008). Due to the similarity of DMC and Landsat imagery in spatial resolution and spectral bands, an object-oriented method was selected to classify DMC imagery. The basic processing units of object-oriented classification are segments, or the so-called image objects (Benz et al., 2004) that represent a relatively homogenous unit on the ground. Classification is performed on the image objects. The advantages of object-oriented classification are that it makes full use of texture calculations, uncorrelated shape information (e.g., length-to-width ratio, direction and area of an object, etc.) and topological features (e.g., neighbor, super-object, etc.), and the close relation between real-world objects and image objects (Benz et al., 2004). In this study, the object-oriented approach included image segmentation and object-oriented classification performed in the Definiens Developer software (Version 7.0, Definiens AG).

Detailed parameters are listed in Table 4.2 regarding object-oriented classification of DMC and Landsat imagery. The FRIGBP has developed a general procedure to generate standard map products. The parameters for the Landsat imagery were chosen mainly based on previously empirical experience (see McDermid, 2005), but a small change was adopted according to the testing results. Since DMC imagery has similar characteristics as Landsat TM imagery, DMC's parameters were derived from tests based on the Landsat's parameters. More specifically, for DMC-based classification, input channels included three image bands (NIR, Red and Green), DEM data, and two texture measures (NIR and Green Contrast). Texture analysis has been demonstrated to improve classification accuracy of remotely sensed data (Gong et al., 1992; Franklin et al., 2000; Franklin et al., 2001; Kim et al., 2009). Therefore, after extensive testing, NIR and Green Contrast (see Haralick et al., 1973) were selected to offset the weaknesses of the DMC limited spectral resolution. However, for Landsat imagery, no texture measures were selected, but brightness, greenness and wetness were applied in order to reduce the processing time required for segmentation. The multiresolution segmentation method was applied to both the DMC and Landsat imagery. However, different scale values were selected for the DMC and Landsat images, due to their different spatial resolutions. The applied method was a nearest neighbor (NN) classification using an automated feature space optimization based on selected training samples (see Definiens AG, 2008).

Table 4.2 Parameters of object-oriented classification of DMC and Landsat imagery

	DMC	Landsat
Input channels	NIR, Red and Green bands; DEM; NIR and Green Contrast	TM 1-5 and 7 bands; DEM; Brightness, Greenness and Wetness
Segmentation	Multiresolution segmentation (scale: 7.5, shape: 0.2, compactness: 0.2)	Multiresolution segmentation (scale: 9, shape: 0.2, compactness: 0.2)
Classification methods	Nearest Neighbor classification	

In order to fully test the applicability of DMC imagery, a hierarchical land cover classification scheme composed of three levels of detail was adopted from McDermid (2005; Table 4.3). Beginning at the most general Level I, training, classification, and refinement were iteratively processed until an acceptable accuracy (>80%, if possible) had been achieved. Once the process was complete, all original objects within a class were merged into a composite region for the next level of classification. In this way, a hierarchical classification was created ending with the most detailed Level III classes. The hierarchy provided a mechanism for tracking of accuracy at multiple land cover levels, as well as providing a means to compare DMC-based classification with Landsat-based classification at the different scales.

Table 4.3 Class hierarchy used in object-oriented land cover classification

Level I	Level II	Level III
A. Vegetation	1. Trees	a. Upland Trees
		b. Wetland Trees
	2. Herbs	c. Upland Herbs
		d. Wetland Herbs
	3. Shrubs	e. Shrubs
B. Non-vegetation	4. Water	f. Water
	5. Barren Land	g. Barren Land

4.4.4 Validation

In this research, accuracy assessment was undertaken with image objects as the units of analysis. The error matrix was selected to assess the accuracy of the DMC-based classification, and in order to learn about the capability of DMC imagery as objectively as possible, the DMC-based and Landsat-based classifications were compared. Quantitative accuracy assessment was implemented to identify and measure map errors (Congalton and Plourde, 2002). The error matrix, currently at the core of the accuracy assessment literature (Foody, 2002), was created to construct user's, producer's and overall accuracies, which were estimated by the difference between the image classification result and the ground referenced data (obtained from the assessment samples). The kappa index of agreement (KIA) was calculated to statistically evaluate the accuracy of the classification maps and error matrices. In addition, the corresponding Landsat-based classification was produced as a reference to investigate the applicability of DMC imagery in practice.

4.5 Results and discussion

4.5.1 Visual comparison of DMC and Landsat TM

The spectral bands of DMC SLIM-6 are equivalent to Landsat TM bands 4, 3, and 2. Additionally, due to their comparable spatial resolution, their standard false color composites are visualized similarly in the overview (Figure 4.3). However, the variation of the two sensors is exposed as well. By comparison, Landsat imagery had obvious advantages in sharpness and contrast. For instance, Landsat imagery was able to better delineate the boundary of patches, especially the common boundary in contrast, and linear features, such as cut blocks, well sites, trail systems, and waterways. In addition, more detail was observed within different patches.

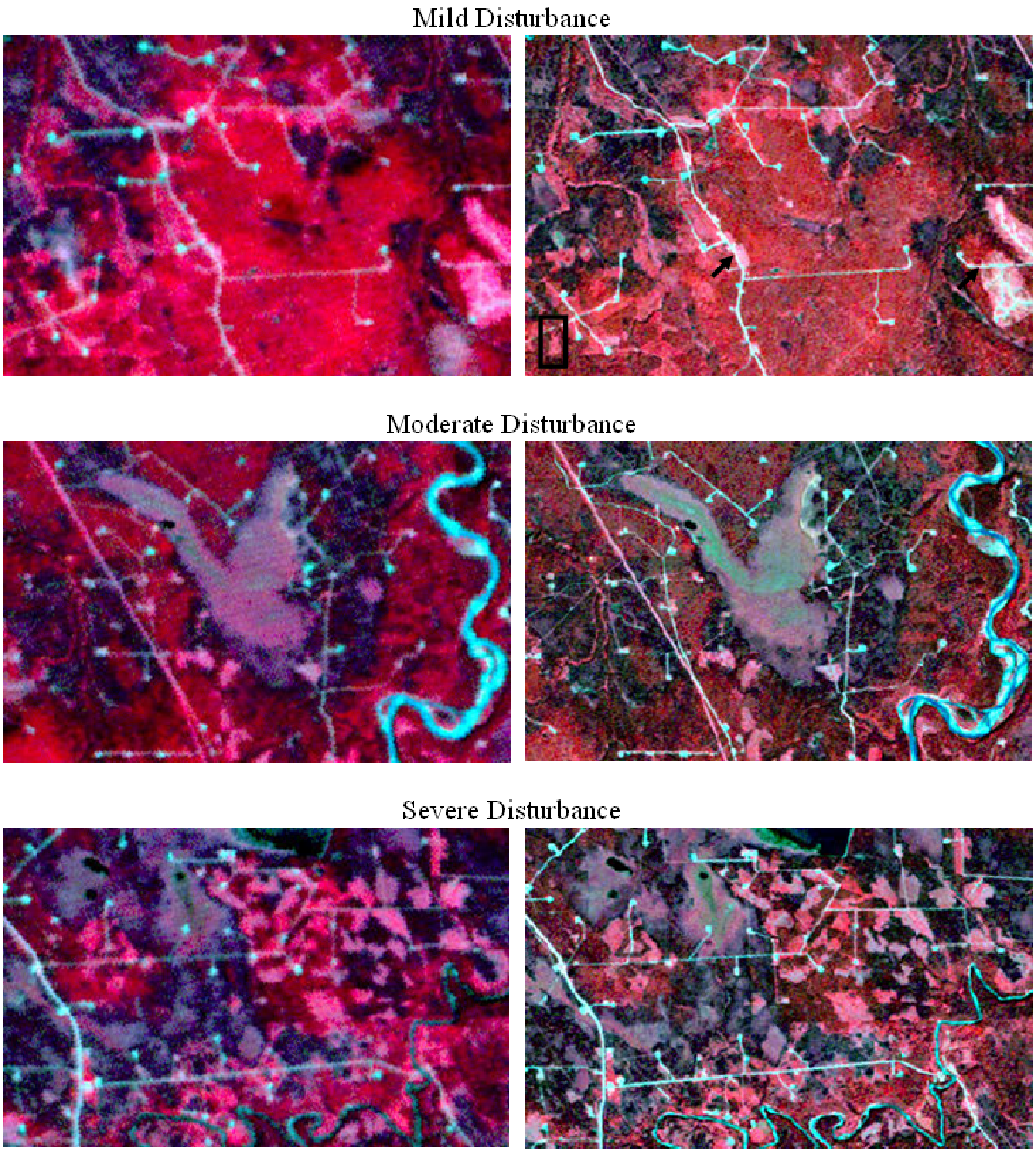

Figure 4.3 Visual comparison of standard false color composite DMC (left) and Landsat (right) under different human-induced disturbance (DMC: RGB = bands 1, 2, 3; Landsat: RGB = bands 4, 3, 2). Arrow sign indicates linear disturbance, and rectangle sign indicates cut-block disturbance.

4.5.2 Nearest neighbor-based classification results for the DMC imagery

Land cover classification results are summarized in Table 4.4. The object-oriented classification approach to DMC imagery proved very effective for performing the relatively simple task of separating vegetation class from non-vegetation class, with an overall accuracy of 95.6% (KIA=86.8%). Only the producer's accuracy of non-vegetation class was inferior to 90% accuracy (85.7%). The results of the level II classification showed that the overall accuracy decrease to 84.9% (KIA=78.6%) with the increase in classes from 2 to 5. Of the individual classes, the accuracy of trees class remained relatively stable, comparable with the vegetation class at Level I. However, the accuracy of herbs class and shrubs class decreased dramatically, with producer's accuracy of 70.0% and 77.3%, and user's accuracy of 72.4% and 81.0%, respectively. Barren land class and water class, corresponding to the non-vegetation class category of Level I, inherited the analogous accuracy from the previous level. The main objective of level III analysis was to separate wetland vegetation surfaces from upland vegetation surfaces. A distinction was considered to be important from a habitat perspective (Wilson et al., 2005; 2006). As an extension of Level II, the overall accuracy was not significantly decreased, reaching 82.4% (KIA=78.6%). The new classes introduced substantial error of omission and commission, with producer's accuracy of 62.5% for upland herbs class and user's accuracy of 61.1% for wetland herbs class, respectively.

Table 4.4 DMC-based Classification at Level I, II, and III

	Producer's	User's	Overall	KIA
		Level I		
Vegetation	98.4%	96.1%	95.6%	86.8%
Non-vegetation	85.7%	93.8%		
		Level II		
Trees	93.1%	87.0%	84.9%	78.6%
Herbs	70.0%	72.4%		
Shrubs	77.3%	81.0%		
Barren Land	86.4%	90.5%		
Water	84.6%	100%		
		Level III		
Upland Trees	95.3%	80.4%	82.4%	78.6%
Wetland Trees	75.9%	84.6%		
Upland Herbs	62.5%	90.9%		
Wetland Herbs	78.6%	61.1%		
Shrubs	77.3%	81.0%		
Barren Land	86.4%	90.5%		
Water	84.6%	100%		

From a producer's standpoint, non-vegetation class exhibited confusion with vegetation class. Confusion probably resulted from two aspects: one was that mixed pixels emerged at the overlapping zones between vegetation and non-vegetation, which mainly happened in the barren land; the other was the spectral signal of water with high-density organic material, especially where water flowed through vegetational zones. All of the vegetated categories displayed confusion with one another in varying degrees. The study area was located in the disturbed and regenerating areas formed by cut blocks, burns, and other natural and anthropogenic processes. Therefore, vegetated land cover changed frequently and considerably. As a result, it was hard to precisely describe the land cover from field and remotely sensed data. Similar perceptions have been experienced in previous research by the FRIGBP. For instance, McDermid (2005) pointed out that field records revealed common field classification errors between shrub and herbaceous classes – particularly in the abundant wetland zones in the northern and central portions of west-central Alberta. Under the tree class, the upland/wetland tree confusion reflects the spectral similarity of high-crown-closure treed wetlands and adjacent uplands (McDermid, 2005).

4.5.3 Comparison of DMC and Landsat NN-based classification

The comparison of DMC- and Landsat-based classification is summarized in Table 4.5. In Level I, all statistics of both classifications were comparable, except the producer's accuracy of the non-vegetation class, and the consequent KIA. With the increase in detail and class with Level II, the Landsat-based classification still retained a high overall accuracy and KIA, whereas the DMC-based classification accuracy decreased considerably, the overall accuracy from 95.6% to 84.9%, and the KIA from 86.8% to 78.6%. The most significant difference occurred in the herbs class. The corresponding producer's and user's accuracies of DMC-based classification decreased by 30% and 20.5% respectively, compared with the Landsat-based classification. Likewise, the producer's accuracy of wetland trees class, upland herbs class and wetland herbs class, and the user's accuracy of wetland herbs class in the DMC-based classification were inferior to the Landsat-based classification at Level III. The disparities were 24.1%, 37.5%, 21.4%, and 22.2% respectively. Differences correspond to the characteristics of the imagery as displayed in Figure 4.4.

Table 4.5 Difference between DMC-based and Landsat-based Classification at Level I, II, and III

	Producer's	User's	Overall	KIA
		Level I		
Vegetation	+1.8%	-0.5%	-0.1%	-4.2%
Non-vegetation	-8.7%	-0.6%		
		Level II		
Trees	-6.9%	-3.9%	-8.7%	-13.2%
Herbs	-30.0%	-20.5%		
Shrubs	+4.0%	-29.0%		
Barren Land	-8.3%	+0.5%		
Water	-9.5%	Zero		
		Level III		
Upland Trees	+1.2%	-3.8%	-10.2%	-12.5%
Wetland Trees	-24.1%	-8.3%		
Upland Herbs	-37.5%	-9.1%		
Wetland Herbs	-21.4%	-22.2%		
Shrubs	+4.0%	-29.0%		
Barren Land	-8.3%	+0.5%		
Water	-9.5%	Zero		

Note: Results refer to the calculation of DMC minus Landsat. The plus sign indicates the accuracy was higher for DMC-based classification; the minus sign indicates the accuracy was higher for Landsat-based classification; zero indicates no difference in the accuracy.

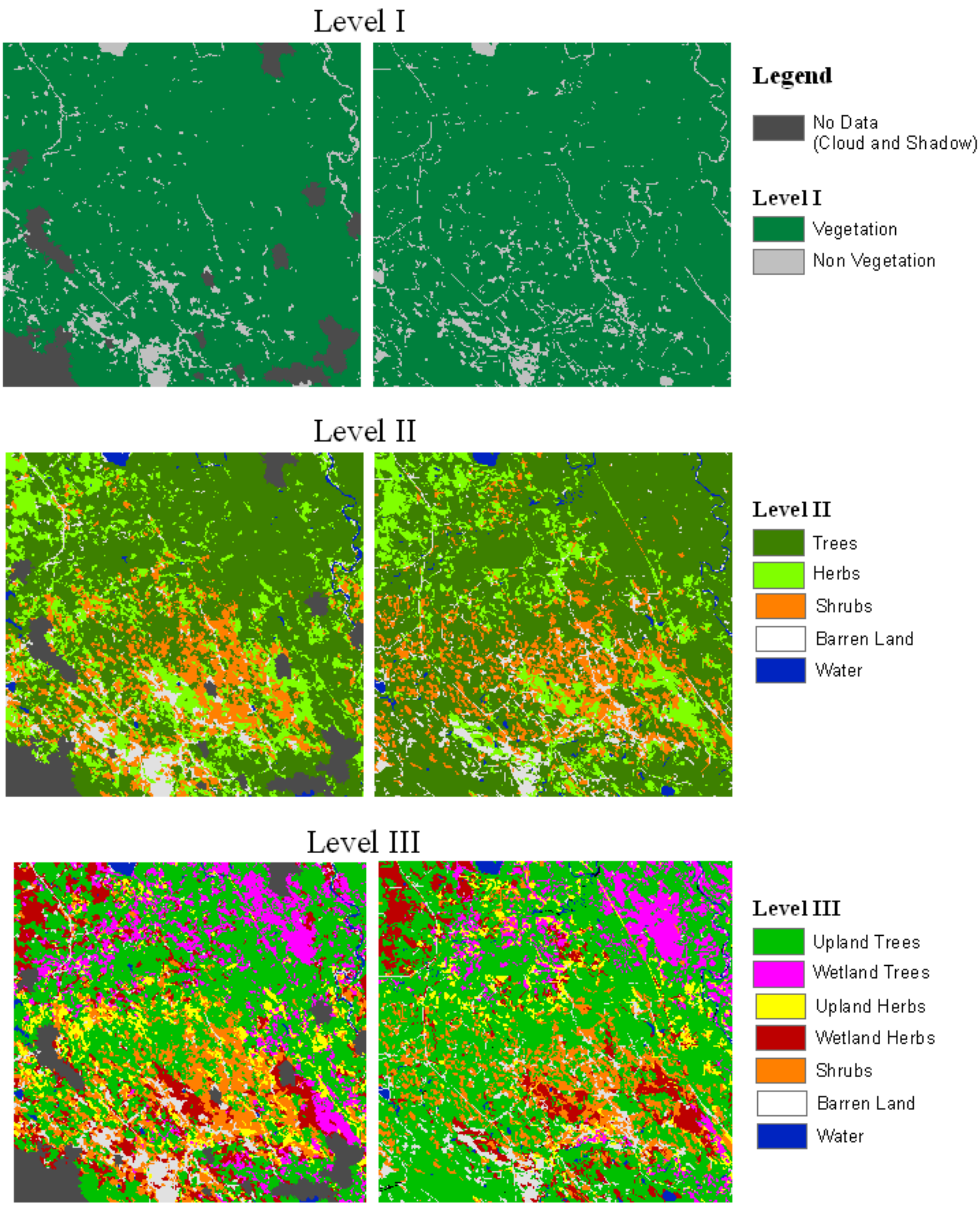

Figure 4.4 Classification comparison of DMC (left) and Landsat (right) imagery at three hierarchical levels

4.6 Conclusion

The objective of this research was to preliminarily exploit the applicability of constellation of low-cost small satellite in large-area habitat mapping, through exemplifying DMC multispectral imagery in the classification of grizzly bear habitat in west-central Alberta. The overall accuracy was 95.6% in the most general Level I (2 classes) classification, and 82.4% in the most detailed Level III (7 classes) classification. Therefore, the DMC multispectral imagery has acceptable capability of describing the physiognomy of earth's surface with more than 80% accuracy, especially for large areas. For example, the accepted overall accuracy of the FRIGBP is no less than 80% in order to ensure the aforementioned applications. Accordingly, cloud-free or cloud-limited DMC imagery is capable of being applied to the program with affordable cost. Simultaneously, the advantages of DMC on temporal resolution and footprint can be applied to better support large-area habitat mapping. However, it is worth noting that the practical applicability depends on the objective of specific research. In contrast to the results of Landsat-based classification, only in Level I were both classifications comparable in their overall accuracies, whereas in Level II and III, the DMC-based classification was inferior to Landsat-based classification by 8.7% and 10.2%, respectively. This is mainly due to the advantage of Landsat TM multispectral imagery in spectral resolution. However, the advantage of DMC multispectral imagery in footprint and temporal resolution cannot be ignored. The relatively broad footprint is suitable for large-area applications, and the high temporal resolution can benefit rapid change detection and increase the possibility of obtaining cloud-free or low cloud-covered imagery.

It is possible to improve the classification accuracy of DMC imagery by applying advanced object-oriented techniques or the fusion of optical and radar imagery. For example, supervised sequential masking (SSM) method has been proven to perform better than NN methods in theory and practice (Turker and Arikan, 2005; Collingwood et al., 2009). It is because the SSM method integrates expert knowledge into the classification. But it is worth noting that the SSM method is image analyst-dependent, and time-consuming to run. Another improved hybrid method, called post-classification refinement, can also improve classification results. It is advised to run the NN method first, and then refine confused, low-accuracy classes based on rule sets. This can simplify the SSM method to be more efficient. Fusion of optical and radar imagery, e.g., DMC multispectral and Radarsat-2 imagery, is another solution for increasing the classification accuracy of DMC imagery (Boyd and Danson, 2005; Li and Chen, 2005; Wang et al., 2009), because the disparate information from radar imagery, such as structure, surface roughness and moisture, may be able to offset the deficit of DMC in spectral resolution. Therefore, future research can focus on the fusion of DMC and other remotely sensed data to improve the applicability of DMC-based products on large-area habitat mapping.

4.7 References

Aplin, P. 2005. Remote sensing: ecology. *Progress in Physical Geography,* Vol. 29, pp. 104-113.

Baatz, M., and Schäpe, M. 2000. Multiresolution segmentation – an optimization approach for high quality multi-scale image segmentation. In *Angewandte Geographische Informationsverarbeitung XII.* Edited by J. Strobl, T. Blaschke and G. Griesebner, Wichmann Verlag, Karlsruhe, pp. 12-23.

Benz, U.C., Hofmann, P., Willhauck, G., Lingenfelder, I. and Heynen, M. 2004: Multi-resolution, object-oriented fuzzy analysis of remote sensing data for GIS-ready information. *ISPRS Journal of Photogrammetry and Remote Sensing,* Vol. 58, pp. 239–258.

Blaschke, T. 2010. Object based image analysis for remote sensing. *ISPRS Journal of Photogrammetry and Remote Sensing,* Vol. 62, pp. 2-16.

Blaschke, T., Lang, S., Lorup, E., Strobl, J., and Zeil, P. 2000. Object-oriented image processing in an integrated GIS/remote sensing environment and perspectives for environmental applications. In *Environmental Information for Planning, Politics and the Public, Vol. 2.* Edited by A. Cremers and K. Greve, Metropolis Verlag, Marburg, pp. 555-570.

Blaschke, T., and Strobl, J. 2001. What's wrong with pixels? Some recent developments interfacing remote sensing and GIS. *GIS – Zeitschrift für Geoinformationssysteme,* Vol.14, pp. 12-17.

Bontemps, S., Bogaert, P., Titeux, N., and Defourny, P. 2008. An object-based change detection method accounting for temporal dependences in time series with medium to coarse spatial resolution. *Remote Sensing of Environment,* Vol. 112, pp. 3181-3191.

Boyd, D.S., and Danson, F.M. 2005. Satellite remote sensing of forest resources: three decades of research development. *Progress in Physical Geography,* Vol. 29, pp. 1-26.

Chavez, P.S. 1988. An improved dark-object subtraction technique for atmospheric scattering correction of multispectral data. *Remote Sensing of Environment,* Vol. 24, pp. 459-479.

Chen, K.S., Tzeng, Y.C., Chen, C.F., and Kao, W.L. 1995. Land-cover classification of multispectral imagery using a dynamic learning neural network. *Photogrammetric Engineering and Remote Sensing,* Vol. 61, pp. 403-408.

Collingwood, A., Franklin, S.E., Guo, X., and Stenhouse, G. 2009. A medium-resolution remote sensing classification of agricultural areas in Alberta grizzly bear habitat. *Canadian Journal of Remote Sensing,* Vol. 35, pp. 23-36.

Congalton, R.G., and Plourde, L. 2002. Quality assurance and accuracy assessment of information derived from remotely sensed data. In *Manual of Geospatial Science and Technology.* Edited by J. Bossler, Taylor & Francis Group, London.

Crist, E.P., and Cicone, R.C., 1984. A physically based transformation of Thematic Mapper data-the TM Tasseled Cap. *IEEE Transactions on Geoscience and Remote Sensing,* Vol. GE-22, No. 3, pp. 256-263.

Crowley, G. 2008. *DMC data product manual.* DMC International Imaging Ltd. Retrieved 5 May 2009 from http://www.dmcii.com/index.html.

Definiens AG 2008. *Definiens Developer 7 – user guide.* Retrieved 14 July 2009 from http://www.defi niens.com/definiens-support-services_187_11_14.html

Dorren, L.K., Maier, B., and Seijmonsbergen, A.C. 2003. Improved Landsat-based forest mapping in steep mountainous terrain using object-based classification. *Forest Ecology and Management,* Vol. 183, pp. 31-46.

Franklin, S.E., Hall, R.J., Moskal, L.M., Maudie, A.J., and Lavigne, M.B. 2000. Incorporating texture into classification of forest species composition from airborne multispectral images. *International Journal of Remote Sensing,* Vol. 21, pp. 61-79.

Franklin, S.E., Maudie, A.J., and Lavigne, M.B. 2001. Using spatial co-occurrence texture to increase forest structure and species composition classification accuracy. *Photogrammetric Engineering and Remote Sensing,* Vol. 67, pp. 849-855.

Foody, G.M., 2002. Status of land cover classification accuracy assessment. *Remote Sensing of Environment,* Vol. 80, pp. 185-201.

Garshelis, D.L., Gibeau, M.L., and Herrero, S. 2005. Grizzly bear demographics in and around Banff National Park and Kananaskis Country, Alberta. *Journal of Wildlife Management*, Vol. 69, pp. 277–297.

Gong, P., Marceau, D.J., and Howarth, P.J. 1992. A comparison of spatial feature extraction algorithms for land-use classification with SPOT HRV data. *Remote Sensing of Environment,* Vol. 40, pp. 137-151.

Goward, S.N., Arvidson, T., Williams, D.L., Irish, R., and Irons, J.R. 2009. Moderate spatial resolution optical sensors. In *The SAGE handbook of remote sensing.* Edited by T.A. Warner, M.D. Nellis, and G.M. Foody, SAGE Publications.

Hall, L., Krausman, P., and Morrison, M. 1997. The habitat concept and a plea for standard terminology. *Wildlife Society Bulletin,* Vol. 25, pp.173-182.

Hansen, M., Dubayah, R., and DeFries, R. 1996. Classification trees: an alternative to traditional land cover classifiers. *International Journal of Remote Sensing,* Vol. 17, pp. 1075-1081.

Haralick, R.M., Shanmugam, K., and Dinstein, I. 1973. Textural features for image classification. *IEEE Transactions on Systems, Man and Cybernetics,* Vol. 3, pp. 610-620.

Hardin, P.J., and Thomson, C. 1992. Fast nearest neighbor classification methods multispectral imagery. *The Professional Geographer,* Vol. 44, pp. 191-201.

Jensen, J.R. 2007. *Remote sensing of the environment: an earth resource perspective, second edition.* Prentice Hall, Upper Saddle River, N.J.

Jin, S., and Sader, R.A. 2005. Comparison of time series tasseled cap wetness and the normalized difference moisture index in detecting forest disturbance. *Remote Sensing of Environment*, Vol. 94, pp. 364-372.

Jobin, B., Labrecque, S., Grenier, M., and Falardeau, G. 2008. Object-based classification as an alternative approach to the traditional pixel-based classification to identify potential habitat of the grasshopper sparrow. *Environmental Management*, Vol. 41, pp. 20-31.

Kerr, J.T., and Ostrovsky, M. 2003. From space to species: ecological applications for remote sensing. *Trends in Ecology and Evolution,* Vol. 18, pp. 299-305.

Kim, M., Madden, M., and Warner, T.A. 2009. Forest type mapping using object-specific texture measures from multispectral Ikonos imagery: segmentation quality and image classification issues. *Photogrammetric Engineering and Remote Sensing*, Vol. 75, pp. 819-829.

Kramer, H.J., and Cracknell, A.P. 2008. An overview of small satellites in remote sensing. *International Journal of Remote Sensing*, Vol. 29, pp. 4285-4337.

Li, J. and Chen, W. 2005. A rule-based method for mapping Canada's wetlands using optical, radar, and DEM data. *International Journal of Remote Sensing,* Vol. 26, pp. 5051–5069.

Maehr, D.S., Noss, R.F., and Larkin, J.L. 2001. *Large mammal restoration: ecological and sociological challenges in the 21st century.* Island Press, Washington, D.C., pp. 71-72.

Mather, P.M. 1985. A computationally-efficient maximum-likelihood classifier employing prior probabilities for remotely sensed data. *International Journal of Remote Sensing,* Vol. 6, pp. 369-376.

McDermid, G.J. 2005. *Remote Sensing for large-Area, multi-jurisdictional habitat mapping*. Ph.D. Thesis, Department of Geography, University of Waterloo, Waterloo, Ontario, Canada.

McDermid, G.J., Franklin, S.E., and LeDrew, E.F. 2005. Remote sensing for large-area habitat mapping. *Progress in Physical Geography,* Vol. 29, pp. 449-474.

McDermid, G.J., McLane, A., Collingwood, A., Hird, J., Faraguna, A., Laskin, D., Linke, J., Cranston, J., Guo, X., and Franklin, S.E. 2008. Remote sensing mapping and research update.

In *Foothills research institute grizzly bear program 2007 annual report.* Edited by G. Stenhouse and K. Graham. Foothills Research Institute, Hinton, Alberta.

Mitchell, S., 2005. How useful is the concept of habitat?–a critique. *Oikos,* Vol.110, pp. 634-638.

Morrison, M., Marot, B., and Mannan, R. 2006. *Wildlife-habitat relationships: concepts and application, third edition.* Island Press, Washington D.C., USA.

Myint, S.W., Yuan, M., Cerveny, R.S., and Giri, C.P. 2008. Comparison of remote sensing image processing techniques to identify tornado damage areas from Landsat TM data. *Sensors,* Vol. 8, pp. 1128-1156.

Natural Regions Committee 2006. *Natural Regions and Subregions of Alberta.* Compiled by D.J. Downing and W.W. Pettapiece. Government of Alberta, Pub. No. T/852. Retrieved 30 June 2011 from http://www.tpr.alberta.ca/parks/heritageinfocentre/docs/NRSRcomplete%20May_06.pdf

Qian, Y.G., Yan, G.J., Duan, S.B., and Kong, X.S. 2009. A contextual fire detection algorithm for simulated HJ-1B imagery. *Sensors,* Vol. 9, pp. 961-979.

Richter, R. 2008. *Atmospheric-topographic correction for satellite imagery: ACTOR-2/3 user guide, version 6.4.* German Aerospace Center, Wessling, Germany. DLR-1B 565-01/08.

Stenhouse, G. 2008. Introduction. In *Foothills research institute grizzly bear program 2007 annual report.* Edited by G. Stenhouse and K. Graham. Foothills Research Institute, Hinton, Alberta.

Turker, M., and Arikan, M. 2005. Sequential masking classification of multi-temporal Landsat 7 ETM+ images for field-based crop mapping in Karacabey, Turkey. *International Journal of Remote sensing*, Vol. 26, No. 17, pp. 3813-3830.

Turner, W., Spector, S., Gardiner, N., Fladeland, M., Sterling, E., and Steininger, M. 2003. Remote sensing for biodiversity science and conservation. *Trends in Ecology and Evolution,* Vol. 18, pp. 306-314.

Wang, K., Franklin, S.E., Guo, X., He, Y., and McDermid, G.J. 2009. Problems in remote sensing of landscapes and habitats. *Progress in Physical Geography,* Vol. 33, pp. 747-768.

Wilson, S.M., Madel, M.J., Mattson, D.J., Graham, J.M., Burchfield, J.A., and Belsky, J.M. 2005. Natural landscape features, human-related attractants, and conflict hotspots: a spatial analysis of human – grizzly bear conflicts. *Ursus,* Vol. 16, pp. 117-129.

Wilson, S.M., Madel, M.J., Mattson, D.J., Graham, J.M., and Merrill, T. 2006. Landscape conditions predisposing grizzly bears to conflicts on private agricultural lands in the western USA. *Biological Conversation,* Vol. 130, pp. 47-59.

Wulder, M.A., Hall, R.J., Coops, N.C., and Franklin, S.E. 2004. High spatial resolution remotely sensed data for ecosystem characterization. Bioscience, Vol. 54, pp. 511-521.

Wulder, M.A., White, J.C., Goward, S.N., Masek, J.G., Irons, J.R., Herold, M., Cohen, W.B., Loveland, T.R., and Woodcock, C.E. 2008. Landsat continuity: issues and opportunities for land cover monitoring. *Remote Sensing of Environment,* Vol. 112, pp. 955–969.

Xue, Y., Li, Y., Guang, J., Zhang, X., and Guo, J. 2008. Small satellite remote sensing and applications – history, current and future. *International Journal of Remote Sensing,* Vol. 29, pp. 4339-4372.

Yan, F.L., Wang, S.X., Zhou, Y., Xiao, Q., Zhu, L.Y., Wang, L.T., and Jiao, Y.Q. 2006. Monitoring the water quality of Taihu Lake by using Hyperion hyperspectral data. *Journal of Infrared and Millimeter Waves,* Vol. 25, pp. 460-464.

Yu, Q., Gong, P., Chinton, N., Biging, G., Kelly, M., and Schirokauer, D. 2006. Object-based detailed vegetation classification with airborne high spatial resolution remote sensing imagery. *Photogrammetric Engineering and Remote Sensing,* Vol. 72, pp. 799-811.

CHAPTER 5 - EVALUATION OF TEXTURAL INFORMATION ON THE APPLICATION OF SAR IMAGERY IN NORTHERN BOREAL FOREST

5.1 Abstract

Textural information plays a key role in the interpretation of Synthetic Aperture Radar (SAR) imagery. However, some uncertainties and challenges such as window size, the effect of speckle filtering on texture measures, and the combination of two types of texture are still not fully solved. These issues should be addressed to be able to apply SAR imagery for large-area wildlife habitat mapping. The study area is located within the natural range of the grizzly bear in west-central Alberta, Canada. The object-oriented classification was performed on a RADARSAT-2 Standard Dual-Pol image to evaluate two disparate types of texture, namely the grey level co-occurrence matrix (GLCM) based texture and probability density function (PDF) based SAR texture. Results show that 1) 25 and 5 are the best window size to extract GLCM-based and PDF-based SAR texture measures for classification; 2) speckle filtering has significant effect on GLCM-based texture measures with smaller window size; and 3) promising results are achieved regarding the combination of GLCM-based texture and PDF-based SAR texture.

5.2 Introduction

Synthetic Aperture Radar (SAR) imagery has been commonly used for a variety of applications, especially environment-related fields, such as sea ice discrimination (Barber and LeDrew, 1991; Soh and Tsatsoulis, 1999), wetland mapping (Arzandeh and Wang, 2002), vegetation biomass estimation (Kuplich et al., 2005; Wang et al., 2006). Tone and texture are two major elements for interpreting SAR imagery (Barber and LeDrew, 1991). Given that tone only provides limited information, which is often insufficient for applications, texture plays a key role in quantitatively explaining SAR data.

Among many algorithms of texture extraction, the grey-level co-occurrence matrix (GLCM) is the most popular statistical algorithm. The derived texture measures are the co-occurrence of grey-level values which are calculated from the probability of combination of two grey values at a defined inter-pixel distance and orientation within a defined moving window. Accordingly, four parameters should be taken into account when GLCM-based texture measures are extracted: kernel size; inter-pixel angle or orientation; inter-pixel distance or displacement; and quantization level. A large number of research papers have been published evaluating the practical effect of the four parameters under certain circumstances (See Ulaby et al., 1986; Barber and LeDrew, 1991; Soh and Tsatsoulis, 1999; Arzandeh and Wang, 2002; Clausi, 2002; Ndi Nyoungui et al., 2002; Zhang et al., 2010). In order to generate meaningful texture features, an appropriate kernel size has to be determined. Theoretically, the kernel size should be smaller than the objects in the image, which will determine the usefulness of the texture measure for classification, yet large enough to include the characteristic variability of the objects (Wang et al., 2006; Hall-Beyer, 2007). For example, Arzandeh and Wang (2002) reported that the preferred window size of 17×17 pixel maximizes the overall accuracy of classification for wetland mapping; however, a 5×5 pixel kernel size is the optimal choice to estimate the biomass of regenerating tropical forests (Kuplich et al., 2005). Inter-pixel angle and inter-pixel distance describe the spatial relationship of the two involved neighboring pixels in the computation of GLCM. The conclusion varied in different studies (Clausi, 2002); however, many studies preferred the set of angle (0˚) and distance (1 pixel). This set was also proclaimed to perform significantly better than others (Barber and LeDrew, 1991) and selected to investigate the statistical meaning of six GLCM parameters (Baraldi and Parmiggiani, 1995). Regarding the quantization level, a similar conclusion has been revealed that a grey level value greater than twenty-four is recommended (Clausi, 2002).

It is well-known that the occurrence of speckle in SAR imagery has a significant impact on GLCM-based texture measures. However, the effect of speckle is a controversial issue in the literature (Arzandeh and Wang, 2002). Speckle is defined as "statistical fluctuation or uncertainty associated with the brightness of each pixel in the image of a scene" (Canadian Center for Remote Sensing, 2008). It appears as a multiplicative random process specifically determined by SAR systems. Due to the speckle considered as "noise", speckle suppression technology (also called speckle filtering) is developed to facilitate the interpretation of SAR data, such as feature extraction and classification. Accordingly, some researchers advised to use speckle filtering before texture extraction; however, to some extent speckle, which cannot be simply considered as image noise, contains statistically useful information that can be applied to understanding SAR data. Besides, speckle suppression techniques may not preserve all scene texture details; consequently, others claimed that texture extraction should be implemented before speckle filtering. Therefore, it is worth noting that the practical effect of speckle filtering on texture measures derived from different algorithms for applications.

Another type of texture measures, namely probability density function (PDF) based SAR texture, was proposed specifically for SAR data (Oliver and Quegen, 2004), which includes VI (a ratio of the mean of squared intensity to the mean intensity squared), VA (a ratio of mean intensity to the squared mean amplitude), VL (a difference of the mean value of the squared intensity logarithm and the square of the mean intensity logarithm), and U (a normalized log measure of texture). The PDF-based SAR texture measures account for radar image formation and statistical properties of radar speckle. Therefore, it is mandatory that no prior speckle filtering has been performed on the input SAR data. Oliver (2000) classified the rain forest based on PDF-based SAR texture and achieved promising results. In addition, it is suggested that PDF-based SAR and GLCM-based texture have potential to offer complementary information. The combinations of texture features have been applied to improve the interpretation of SAR images, such as the fusion of co-occurrence, Gabor and Markov Random Field (MRF) texture features (Clausi, 2001), and the first- and second-order texture measures (Kurvonen and Hallikainen, 1999). However, few studies are done on the combination of PDF-based SAR texture and GLCM-based texture.

In this context, this research aims to address the following questions: 1) What is the effect of texture window size on classification accuracy and what is the preferred texture window size for the classification? 2) What is the effect of speckle filtering on GLCM-based texture measures, and which one (before or after speckle filtering) obtains higher accuracy or does the performance vary? 3) Does the GLCM-based texture or PDF-based SAR texture achieve higher classification accuracy? 4) Does the combination of GLCM-based texture and PDF-based SAR texture perform better than the individual texture and what is the preferred configuration of the combination?

5.3 Texture features

In this research, two categories of texture measures were chosen. The first is computed from the GLCM, and the other is the PDF-based SAR texture proposed by Oliver and Quegan (2004).

The GLCM-based texture measures fall into three groups according to the purpose of weights in texture calculation equations (Hall-Beyer, 2007): the contrast group, the orderliness group, and the stats group (Table 5.1). Arzandeh and Wang (2002) concluded that the number of texture measures has a significant effect on the textural classification of land cover. Meanwhile, a set of three or four texture measures was recommended. Clausi (2002) demonstrated the set of contrast, entropy and correlation is optimal for increasing classification accuracy. Therefore, contrast, entropy and correlation were calculated before and after speckle filtering with window size 5, 11, and 25. A window size 3 is too small to capture the intrinsic texture information, and sizes larger than 25 are computationally expensive and so, harder to apply to large-area mapping in practice.

Table 5.1 Groups of GLCM-based texture measures

Groups	Texture measures
Contrast Group	Contrast, Dissimilarity, and Homogeneity
Orderliness Group	Angular Second Moment, MAX Probability, and Entropy
Stats Group	Mean, Variance (or Standard Deviation), and Correlation

PDF-based SAR texture measures account for radar image formation and statistical properties of radar speckle, including VI, VA, VL, and U. Through test and their correlation analysis, VI, and U were selected because VI, VA, and VL display high correlation. The two measures were calculated with window size 3, 5, 11, and 25.

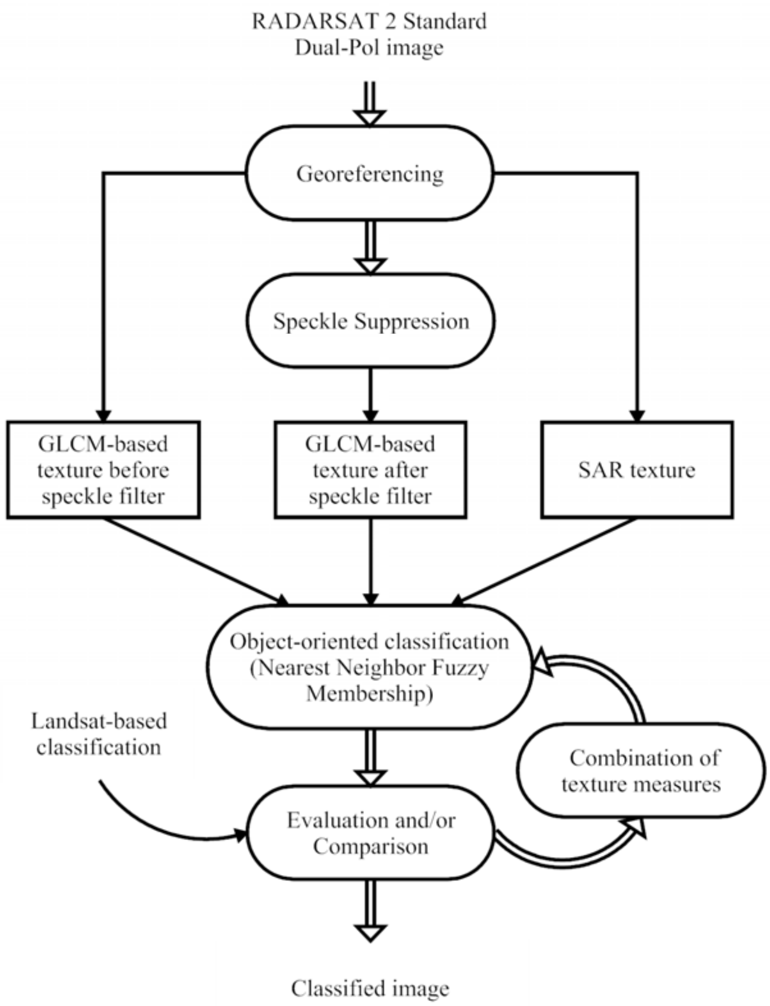

Figure 5.1 Flowchart of methodology for processing of SAR image

5.4 Methodology

The flowchart of the proposed methodology is shown in Figure 5.1. First, the raw SAR image is georeferenced. Then GLCM-based and PDF-based SAR texture measures, explained in Section II, are extracted before speckle suppression. Next speckle filtering is run and GLCM-based texture measures are extracted again. Three sets of the texture measures plus filtered SAR image channels are available as an input for object-oriented classification. Finally, the classified results is compared and evaluated to select an optimal combination of texture measures. Specific details are provided below.

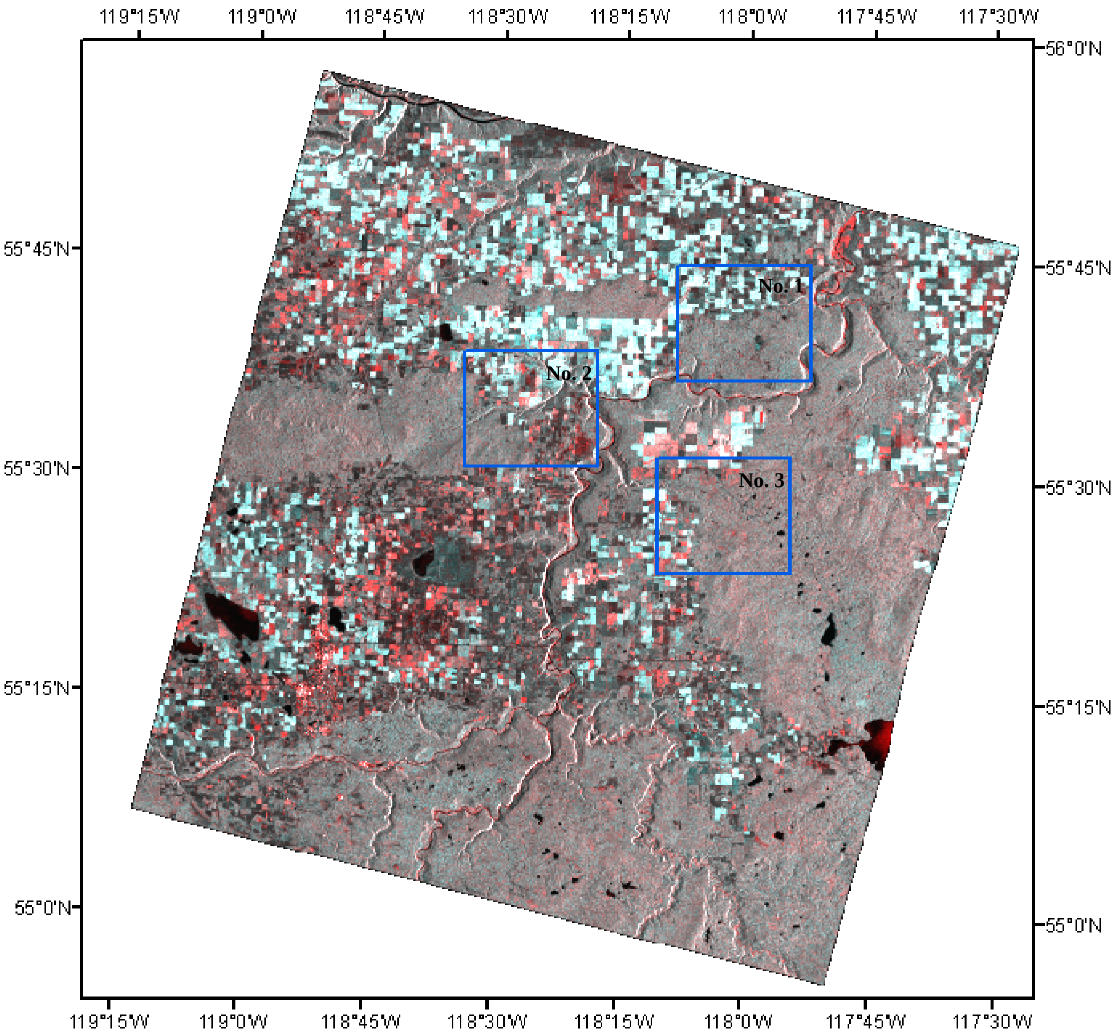

Figure 5.2 The RADARSAT 2 Standard Dual-Pol image covering the study area and three test sites (blue squares). RGB: VV, VH, and VH.

5.4.1 Data set and study area

Three test sites were chosen from a RADARSAT 2 Standard Dual-Pol image (Figure 5.2), which was acquired on August 10th, 2008 with the beam mode of VV+VH (S1) and the product format of SGX (Path Image Plus). The image is georeferenced to a Landsat TM scene used as a reference for geographic information. The presence of multiplicative speckle in SAR image interrupts the interpretation of the image. A MAP Gamma filter is applied to reduce speckle effects with a window size of 5×5. The referenced Landsat TM image is the scene of Path/Row 46/21 from August 6th, 2008. The TM sensor has six optical bands (Band 1-5 and 7) that cover visible, near-infrared, and mid-infrared portions of the electromagnetic spectrum (Band 6 that measures emitted thermal energy was not used in this study).

The study area is located around the town of Grand Prairie at the foothills of the Rocky Mountains, within the natural range of grizzly bear in west-central Alberta, Canada. Most of the study area belongs to the Dry Mixedwood Natural Subregion affiliated to the Boreal Forest Natural Region (Natural Regions Committee, 2006). Natural Regions Committee (2006) summarized that this subregion is "characterized by aspen forests and cultivated landscapes, with fens commonly occurring in low-lying areas". Similarly, this area is experiencing significant human-disturbance, such as forestry practices (e.g., harvesting, plantations), oil and gas exploration, and recreational development (Stenhouse, 2008), which all contribute to grizzly bear habitat fragmentation and loss (Garshelis et al., 2005). Kansas (2002) stated that agriculture and its associated activities increased human-grizzly bear conflicts, and caused a decline in bear populations. Within the three test sites, both natural forest and anthropogenic activities were included. However, the ratio varies. No. 2 test site has the most human-induced disturbance, and No. 3 has the least.

5.4.2 Object-oriented classification and evaluation, and optimal combination

As mentioned before, the object-oriented classification method was selected for this experiment. Blaschke (2010) claimed that critiques are showing up to question the applicability of the per-pixel analysis, because of its neglect of image semantics (i.e. characteristic texture of image data). Conversely, the advantages of object-oriented classification are that it makes full use of meaningful statistics and texture calculations, uncorrelated shape information, topological features, and the close relation between real-world objects and image objects (Benz et al., 2004). Baatz and Schäpe (2000) stated that radar data, such textured data, should be analyzed based-on object-oriented methods. Every set of texture measures, and filtered intensities (i.e. VV and HV), were used as input layers to the Definiens Developer, the software in support of object-oriented classification. The Foothills Research Institute Grizzly Bear Program (FRIGBP) developed a hierarchical land cover classification scheme composed of three levels of detail for mapping grizzly bear habitat (see McDermid, 2005). Only the most general Level I including Vegetation and Non-vegetation classes was used for this research. Fifty samples of 30×30 meters (25 vegetation and 25 non-vegetation samples) were selectively collected as the ground reference for each test site. That is, 150 reference samples (50 samples each site and 3 test sites) were used in total. Theoretically, reference samples were needed to create an error matrix to assess classification accuracy. To some extent, the accuracy of classification depends on the location of assessment samples, especially for the relatively low accuracy classification generated in this research. If another set of assessment samples was chosen, a different classification accuracy would result, even though the classification map is consistent throughout. Thus, to avoid this issue, a classified Landsat TM image was used as a reference to assess the RADARSAT-2 classification accuracy. For Landsat classification, two thirds of the 150 reference samples were used to train the classifier, and another one third (50 reference samples) was used to create an error matrix for the purpose of the accuracy assessment. An overall accuracy of 98.2% was obtained for this Landsat classification.

Through assessing the classification accuracy of each texture type, possible combinations of texture measures were selected out, and then applied to the classification to obtain optimal combination.

5.5 Results and discussion

5.5.1 Effect of texture window size

Table 5.2, 5.3 and 5.4 show the effect of window size on the three sets of texture measures, i.e. the GLCM-based texture measures extracted after speckle filtering (GLCM-Tex A), the GLCM-based texture measures extracted before speckle filtering (GLCM-Tex B), and the PDF-based SAR texture measures (SAR-Tex). The three display different response tendencies. In GLCM-Tex A (Table 5.2), the classification accuracy decreases from Size 5 to 11, and then increases to Size 25. The highest accuracy appears in Size 25 in Sites 1 and 3, but it is Size 5 in Site 2. It is constant that Size11 has the lowest value. The average represents the response tendency very well. The texture information from the Size 5 and 25 provides more accurate description than that from the Size 11, and the Size 25 is slightly better. GLCM-Tex B (Table 5.3) shows that the change is more consistent. The accuracy has a positive relationship with window size, i.e. the biggest Size 25 achieves the best classification accuracy. This result is roughly consistent with the results of the GLCM-Tex A; however, dissimilar change can be observed in SAR-Tex (Table 5.4). The best Size is 3 or 5 in Site 1, 25 in Site 2, and 11 in Site 3. The average increases from Size 3 to 5, and then dramatically decreases to 11, but increases again to 25. Nonetheless, the Size 5 plays a dominant role in accurately extracting PDF-based SAR texture measures in support of classification.

Regardless of whether GLCM-based texture measures are extracted before or after speckle filtering, the largest window Size 25 is the most suitable option. However, the optimal window size is 5 in PDF-based SAR texture. Two types of texture are based on two different algorithms, which lead to the diverse optimal window size. Furthermore, appropriate window size must be a concern in applying the combination of texture measures derived from different algorithms.

Table 5.2 Effect of window size on GLCM-based texture measures extracted after speckle filtering

Test site	Window size		
	5×5	11×11	25×25
No. 1	73.8	72.1	75.4
No. 2	67.6	63.1	66.5
No. 3	81.9	80.9	82.1
Average	74.5	72.0	74.7

Note: The value refers to classification accuracy in percentage; Average stands for the average value of No. 1, No. 2 and No. 3.

Table 5.3 Effect of window size on GLCM-based texture measures extracted before speckle filtering

Test Site	Window Size		
	5×5	11×11	25×25
No. 1	70.6	73.1	74.0
No. 2	64.3	65.9	68.6
No. 3	80.0	83.7	84.2
Average	71.6	74.2	75.6

Table 5.4 Effect of window size on PDF-based SAR texture measures extracted before speckle filtering

Test Site	Window Size			
	3×3	5×5	11×11	25×25
No. 1	72.8	72.8	68.8	71.2
No. 2	67.8	70.4	68.4	70.6
No. 3	84.3	84.9	86.0	84.1
Average	75.0	76.0	74.4	75.3

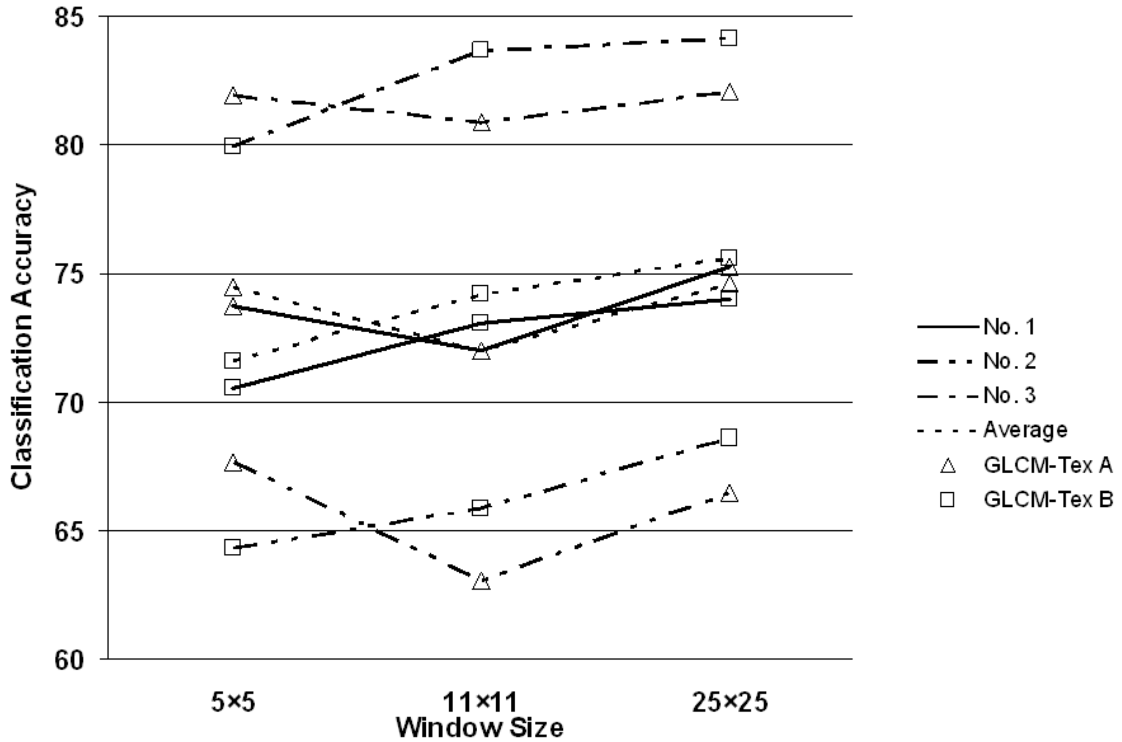

Figure 5.3 Comparison of before-filtering and after-filtering GLCM-based texture. GLCM-Tex A refers to the after-filtering texture, and GLCM-Tex B corresponds to the before-filtering texture.

5.5.2 Comparison of before- and after-filtering GLCM-based texture

The comparison is visualized in Figure 5.3, where the horizontal axis is categorized by window size and the vertical axis represents the value of classification accuracy. Four pairs of comparison are shown, i.e. Test Site No. 1, No. 2, No. 3, and the average of each window size. Their specific values can be seen in Table 5.2 and 5.3. The four pairs have nearly consistent pattern: GLCM-Tex B achieves lower accuracy than GLCM-Tex A in Size 5, but higher in Size 11 and 25, except for the values of No. 1 in Size 25, where the GLCM-Tex A obtained higher accuracy. Therefore, window size influences the effect of the MAP Gamma speckle filter on GLCM-based texture measures. The after-filtering texture (GLCM-Tex A) performs better in smaller size, but the before-filtering texture (GLCM-Tex B) does better in larger size. From the perspective of selecting out the optimal combination, the before-filtering texture is preferred because Size 25 is the most suitable option to extract GLCM-based texture measures.

5.5.3 Comparison of GLCM-based and PDF-based SAR texture

It is listed in Table 5.5 that the highest classification accuracy is obtained using GLCM-based and PDF-based SAR texture respectively. GLCM-based texture has higher accuracy in No. 1, but PDF-based SAR texture accuracy is higher in No. 2 and 3. Consequently, a conclusion cannot be made on their comparison; however, to some extent, the uncertainty of the comparison demonstrates it is necessary to combine diverse types of texture to achieve better accuracy.

Table 5.5 Comparison of GLCM-based and PDF-based SAR texture on highest classification accuracy

Test Site	Texture	
	GLCM-based	SAR
No. 1	75.4 (GLCM-Tex A, Size 25)	72.8 (Size 3 or 5)
No. 2	68.6 (GLCM-Tex B, Size 25)	70.6 (Size 25)
No. 3	84.2 (GLCM-Tex B, Size 25)	86.0 (Size 11)

5.5.4 Optimal combination

Due to the ambiguity of best window size on PDF-based SAR texture, measures of the first two window sizes, which correspond to the first and second highest accuracy, are selected to combine with the best GLCM-based texture measures (Table 5.6). Accordingly, there are two sets of combination per test site. If all measures from GLCM-based and PDF-based SAR texture are simply put together, there will be 12 input channels for the classification in total (10 texture channels plus two intensity channels). Many channels therefore did not achieve satisfactory results through testing, and the large data volume slows down processing in practice. Consequently, the best performing GLCM-based texture measures – Entropy, and VI and U from PDF-based SAR texture are picked out as input to represent the combination of the two types of texture. The accuracy of the combinations is %77.0 in No. 1 and %86.9 in No. 3, and increases by %1.6 and %0.9 respectively. However, in No. 2 is only %69.4, and decreases by %1.2. Also it is worth noting that the optimal combination does not always come from individual texture with highest accuracy. For example, in No. 2, the best individual texture should be GLCM-Tex B Size 25 and SAR-Tex Size 25 (Table 5.5), but it is seen in Table 5.6 that the combination with SAR-Tex Size 5 achieved better accuracy than that with SAR-Tex Size 25.

Table 5.6 Classification accuracy of the combinations of GLCM-based and PDF-based SAR texture under selected window size

Test Site	Configuration		Accuracy	Highest Accuracy of Individual texture
	GLCM-Tex	SAR-Tex		
No. 1	A, Size 25	Size 3	74.6	75.4
		Size 5	77.0	
No. 2	B, Size 25	Size 5	69.4	70.6
		Size 25	68.2	
No. 3	B, Size 25	Size 5	83.5	86.0
		Size 11	86.9	

5.6 Conclusions

In this research, it is explicit that No. 3 has the highest classification accuracy, and No. 2 has the lowest accuracy regardless of texture algorithm, window size, or applying speckle filtering or not. This should result from the ratio of natural area to humanly disturbed area (i.e. agricultural area in this research). If the ratio is relatively low, due to the regularly shaped agricultural area and the tillage orientation, the textural information extracted from these areas does not contribute to improve the classification of vegetation and non-vegetation, whereas it can impair the functionality of textural information on classification.

Several key but still uncertain parameters regarding GLCM-based and PDF-based SAR texture extraction from RADARSAT-2 were examined in a northern boreal forest setting, which is the dominant habitat of the grizzly bear habitat in west-central Alberta, Canada. Our results indicate that window size has at least some effect on classification results regardless of speckle filtering, or applied algorithms (GLCM-based or PDF-based SAR texture). Even though the effect varies with different situations, a preferred window size, Size 25 in our case, can be explicitly determined on GLCM-based texture. However, the effect of window size is not that clear for PDF-based SAR texture. Size 5 should be the preferred window size according to the entire set of test sites. In addition, Size 5 was justified by the result of optimal combination. Therefore, it can easily be seen that the two algorithms portray texture information on a dissimilar scale.

The evaluation of speckle filtering on GLCM-based texture measures indicates that the MAP Gamma filter has some effect on smaller window size, such as Size 5, but not on larger size, such as Size 11 and 25. This result is probably because a smaller window size is mores easily affected by speckle, like the speckle that is prone to represent as random noise in smaller coverage. However, with the increase in window size, speckle appears to be more "expectable and explainable", which can somewhat represent a part of the texture information. Therefore, if window size is large enough, no speckle filter is preferred to extract texture information as much as possible. In our case, the preferred Size 25 is large enough so a better performance is seen in before-filtering GLCM-based texture (GLCM-Tex B).

Based on the results of this research, it is tough to evaluate the comparison between GLCM-based and PDF-based SAR texture. Fortunately, the combination of the two types of texture has shown promising result: the optimal combination is likely to achieve better classification accuracy than each individual texture in large-area applications, or at least, the combination accuracy is equivalent with the highest individual accuracy. Consequently, it is operationally convenient to use the combination rather than to first compare between the different textures and then select the best. In our case, the recommended configuration of optimal combination for the whole study area is GLCM-Tex B with Size 25 and SAR-Tex of Size 5.

Concerns may be raised regarding the "non-significant" difference of the classification accuracy among window sizes, before/after speckle filtering, and GLCM and PDF-based algorithms. Theoretically, the difference should exist, but be slight and thus have limited effect on improving classification accuracy. In addition, the textural information is designed as additional information to assist optical imagery for better accuracy. Therefore, the obtained conclusions will play some role in the application of SAR data for large-area habitat mapping. In the meantime, it is noteworthy that SAR data users should balance the computer capability and the parameter configuration of texture extraction. In general, larger window size consumes more computation resources, and requires superior hardware configuration.

5.7 References

Arzandeh, S., and Wang, J. 2002. Texture evaluation of RADARSAT imagery for wetland mapping. *Canadian Journal of Remote Sensing*, Vol. 28, pp. 653–666.

Baatz, M., and Schäpe, M. 2000. Multiresolution segmentation – an optimization approach for high quality multi-scale image segmentation. In *Angewandte Geographische Informationsverarbeitung XII.* Edited by J. Strobl, T. Blaschke and G. Griesebner, Wichmann Verlag, Karlsruhe, pp. 12-23.

Baraldi, A., and Parmiggiani, F. 1995. An investigation of the textural characteristics associated with gray level cooccurrence matrix statistical parameters. *IEEE Transactions on Geoscience and Remote Sensing*, Vol. 33, pp. 293–304.

Barber, D.G., and LeDrew, E.F. 1991. SAR sea ice discrimination using texture statistics: A multivariate approach. *Photogrammetric Engineer & Remote Sensing,* Vol. 57, pp. 385–395.

Blaschke, T. 2010. Object based image analysis for remote sensing. *ISPRS Journal of Photogrammetry and Remote Sensing*, Vol. 65, pp. 2–16.

Benz, U.C., Hofmann, P., Willhauck, G., Lingenfelder, I., and Heynen, M. 2004. Multi-resolution, object-oriented fuzzy analysis of remote sensing data for GIS-ready information. *ISPRS Journal of Photogrammetry and Remote Sensing*, Vol. 58, pp. 239–258.

Canadian Center for Remote Sensing 2008. *Tutorial: Radar remote sensing.* Retrieved 5 August 2010 from http://www.ccrs.nrcan.gc.ca/resource/tutor/gsarcd/downld_e.php.

Clausi, D.A. 2001. Comparison and fusion of co-occurrence, Gabor and MRF texture features for classification of SAR sea-ice imagery. *Atmosphere-Ocean*, Vol. 39, pp. 183–194.

Clausi, D.A. 2002. An analysis of co-occurrence texture statistics as a function of grey level quantization. *Canadian Journal of Remote Sensing*, Vol. 28, pp. 45–62.

Collingwood, A., Franklin, S.E., Guo, X., and Stenhouse, G. 2009. A medium-resolution remote sensing classification of agricultural areas in Alberta grizzly bear habitat. *Canadian Journal of Remote Sensing*, Vol. 35, pp. 23–36.

Garshelis, D.L., Gibeau, M.L., and Herrero, S. 2005. Grizzly bear demographics in and around Banff National Park and Kananaskis Country, Alberta. *Journal of Wildlife Management*, Vol. 69, pp. 277–297.

Hall-Beyer, M. 2007. *Tutorial: GLCM texture.* Retrieved 5 August 2010 from http://www.fp.ucalgary.ca/mhallbey/tutorial.htm.

Kansas, J.L. 2002: Status of the grizzly bear (Ursus arctos) in Alberta. *Alberta Wildlife Status Report No. 37.*

Kuplich, T.M., Curran, P.J., and Atkinson, P.M. 2005. Relating SAR image texture to the biomass of regenerating tropical forests. *International Journal of Remote Sensing*, Vol. 26, pp. 4829–4854.

Kurvonen, L., and Hallikainen, M.T. 1999. Textural information of multitemporal ERS-1 and JERS-1 SAR images with applications to land and forest type classification in boreal zone. *IEEE Transactions on Geoscience and Remote Sensing,* Vol. 37, pp. 680–689.

McDermid, G.J. 2005. *Remote Sensing for large-Area, multi-jurisdictional habitat mapping*. Ph.D. Thesis, Department of Geography, University of Waterloo, Waterloo, Ontario, Canada.

Natural Regions Committee 2006. *Natural Regions and Subregions of Alberta.* Compiled by D.J. Downing and W.W. Pettapiece. Government of Alberta, Pub. No. T/852. Retrieved 30 June 2011 from http://www.tpr.alberta.ca/parks/heritageinfocentre/docs/NRSRcomplete%20May_06.pdf

Oliver, C.J. 2000. Rain forest classification based on SAR texture. *IEEE Transactions on Geoscience and Remote Sensing*, Vol. 38, pp. 1095–1104.

Oliver, C., and Quegan, S. 2004. *Understanding Synthetic Aperture Radar Images*. SciTech Publishing, Raleigh, NC.

Soh, L.-K., and Tsatsoulis, C. 1999. Texture analysis of SAR sea ice imagery using gray level co-occurrence matrices. *IEEE Transactions on Geoscience and Remote Sensing*, Vol. 37, pp. 780–795.

Stenhouse, G. 2008. Introduction. In *Foothills research institute grizzly bear program 2007 annual report.* Edited by G. Stenhouse and K. Graham. Foothills Research Institute, Hinton, Alberta.

Wang, H., Ouchi, K., Watanabe, M., Shimada, M., Tadono, T., Rosenqvist, A., Romshoo, S.A., Matsuoka, M., Moriyama, T., and Uratsuka, S. 2006. In search of the statistical properties of high-resolution polarimetric SAR data for the measurements of forest biomass beyond the RCS saturation limits. *IEEE Geoscience and Remote Sensing Letters*, Vol. 3, pp. 495–499.

CHAPTER 6 – SUMMARY AND CONCLUSIONS

Wildlife habitat mapping strongly supports applications in natural resource management, environmental conservation, impacts of anthropogenic activity, perturbed ecosystem restoration, species-at-risk recovery and species inventory. The year of 2011 marks the twelfth year in which remote sensing has contributed products and services in the ambitious FRIGBP. Beyond any doubt, this program can be stated as a successful and productive practice of wildlife and resource management, in which large-area grizzly bear habitat mapping plays an important role. However, there are still a number of challenges and opportunities in large-area wildlife habitat mapping, especially in the grizzly bear program. The development of science and technology provides remote sensing specialists more possibilities and opportunities to sharpen the large-area habitat mapping, especially with the launch of innovative optical and radar earth observation satellites.

The overall hypothesis is that optical and radar remote sensing can reliably and effectively generate wildlife-habitat information over large-areas. More specifically, this study was built on three hypotheses. The first hypothesis is that the alternate imagery with medium spatial resolution can be used as the primary resource for large-area habitat mapping. The second hypothesis is that the alternative imagery with medium spatial resolution can produce reliable products compared with those based on Landsat. The last hypothesis is that the landscape pattern analysis can be further characterized via the comparison of presence/absence and frequency of use models based on diverse remote sensing products. The first and the last hypotheses have been fully validated, and the second has been partly validated.

The overall goal of this research was to explore the optical and radar imagery to address the existing and potential challenges (or uncertainties) in remote sensing of large-area habitat mapping. In summary, three main research objectives were formulated to address this goal:

1) Review problems in remote sensing of landscapes and habitats, and provide theoretically possible solutions;

2) Investigate the applicability of Disaster Monitoring Constellation (DMC) and Radarsat-2 imagery for large-area wildlife habitat mapping; and

3) Identify the response of landscape pattern analysis to diverse remote sensing products.

The following paragraphs briefly summarize the successful achievement of these goals.

1) Problems in remote sensing of landscape and habitats, and possible solutions were reviewed from three aspects: current challenges and opportunities in remote sensing; possible sensors and methods to deal with these challenges and opportunities; and the application issue - landscape analysis and remote sensing.

2) Satellite imagery has its own characteristics, theoretically representing relative advantages and disadvantages of the imagery. Thus, it is important to determine the appropriate data source based on the specific research question. For grizzly bear habitat mapping in west Alberta conducted by the FRIGBP, DMC and RADARSAT-2 were chosen to address the existing and potential challenges (or uncertainties) according to their own unique characteristics and literature review. However, their advantages in theory can not ensure their success in reality. Due to the disparity of optical and radar remotely sensed data in imaging and the status of their usage, two types of sub-framework were designed to investigate the feasibility and applicability of DMC and RADARSAT-2 for large-area wildlife habitat mapping. The overall accuracy of DMC-based classification was 95.6% in the most general Level I (2 classes) classification, and 82.4% in the most detailed Level III (7 classes) classification. Therefore, the DMC multispectral imagery has acceptable capability of

describing the physiognomy of earth's surface with more than 80% accuracy, especially for large areas. I investigated the textural information for the application of RADARSAT-2 imagery. In the study, the recommended configuration is performed by combining before-filtering GLCM-based texture of window size 25 and PDF-based SAR texture of window size 5.

3) Landscape analysis refers to the process of accurately quantifying landscape pattern, which is spatially correlated and scale-dependent. For remotely sensed data, image spatial and radiometric resolution, applied thematic resolution (determined by the applied land cover classification scheme), classification methods, and any other classification-relevant factors are deemed to have a direct and significant effect on the subsequent landscape pattern analysis. Moreover, the effects of these classification factors have been proven to be correlated and interactive both in theory and practice. In order to identify the response of landscape pattern analysis to diverse remote sensing products, we compared two models of grizzly bear activity in agricultural areas of western Alberta, Canada. The two models were developed from landscape pattern metrics derived from Landsat- and IRS-based classifications and assessed if these models statistically converged on the same landscape metrics. In this research, thematic resolution had a greater impact on compositional metrics in both grizzly bear presence/absence and frequency of use analyses, i.e. the Landsat-based product was more suitable for revealing the function of compositional metrics than IRS-based product. This could partly be because 30 m and 5 m spatial scales are both higher than the minimum scale required by grizzly bear ecology. A higher spatial resolution product has an advantage in accurately delineating the contour of patches. Therefore,

configurational metrics were more sensitive to the higher spatial resolution IRS-based product. In order to improve representation of landscape pattern, data fusion should be considered. For example, fusing Landsat and IRS data takes the advantages of spectral and spatial resolutions. However, the feasibility of data fusion would depend on issue of scale, data fusion technology, and the availability of imagery.

6.1 Research contributions

The entire research focuses on the challenges and opportunities in remote sensing of large-are wildlife habitat, and studies several key concerns in the large-area habitat mapping, including methodology of habitat mapping, technical issues of remote sensing, and relevant ecological applications. With the support of conclusions obtained in this research, a number of research contributions have been accomplished. First, a comprehensive review regarding problems in remote sensing of landscapes and habitats was published (Wang et al., 2009). The work articulated the current challenges and opportunities in remote sensing for large-area wildlife habitat mapping, and possible solutions and directions for further research, and forms a significant contribution to the literature of large-area wildlife habitat mapping. In addition, another review was compiled from a broader perspective of ecology, biodiversity and conservation in the context of state-of-the-art remote sensing technology, including instruments and techniques (Wang et al., 2010a).

The applicability of DMC and RADARSAT-2 was assessed and promising results were obtained to better accommodate large-area habitat mapping. The work on the applicability of DMC was published as Wang et al. (in press) in Canadian Journal of Remote Sensing. Both remote sensing and ecological societies are extremely interested in the response of landscape pattern analysis to diverse remote sensing products because it is straightforwardly linked with scale issue. The relationship of landscape metrics and image spatial resolution, and landscape metrics and thematic resolution was stated in Wang et al. (2010b).

6.2 Suggestions for future research

While this thesis contains a number of substantial contributions, some specific research limitations still remain, and a large number of potential research issues exist. The limitations and relevant future research issues and applications are suggestions below.

This study does have several limitations that need to be taken into account or addressed in future studies. First, the applicability of RADARSAT-2 needs to be further investigated, especially the use of PolSAR (Polarimetric SAR) and PolInSAR (SAR Polarimetric Interferometry) technology (e.g. Lee et al., 2001; McNairn et al., 2009; Shimoni et al., 2009), which have obtained promising results in many environmental researches, and will be the future direction of SAR applications. Secondly, the fusion of DMC and RADARSAT-2 has not yet been brought into action. Theoretically, it ought to improve the accuracy of remote sensing products a lot, especially products on vertical vegetation structure, such as crown closure, biomass, etc. Lastly, the substantial products of habitat mapping are not generated based on obtained conclusions. It is partly because more studies are needed to exploit the applicability of RADARSAT-2, and funding issue will become a bottleneck to hamper the implementation because RADARSAT-2 imagery is expensive, and restricted to obtain sufficient data due to the conflict of orders. Further studies need to focus on these aspects.

6.3 References

Lee J.S., Grunes, M.R., and Pottier, E. 2001. Quantitative comparison of classification capability: fully polarimetric versus dual and single-polarisation SAR. IEEE Transactions on Geoscience and Remote Sensing, 39(11): 2343-2351.

McNairn, H., Shang, J., Jiao, X., and Champagne, C. 2009. IEEE Transactions on Geoscience and Remote Sensing, 47(12): 3981-3992.

Shimoni, M., Borghys, D., Heremans, R., Perneel, C. and Acheroy, M. 2009. Fusion of PolSAR and PolInSAR data for land cover classification. International Journal of Applied Earth Observation and Geoinformation, 11: 169-180.

Wang, K., Franklin, S.E., and Guo, X. 2010. The applicability of small-satellite constellation in classification for large-area habitat mapping: a case study of DMC multispectral imagery in west-central Alberta. Canadian Journal of Remote Sensing, in press.

Wang, K., Franklin, S.E., Guo, X., and Cattet, M. 2010a. Remote sensing of ecology, biodiversity and conservation: a review from the perspective of remote sensing specialists. Sensors, 10(11): 9647-9667.

Wang, K., Franklin, S.E., Guo, X., Collingwood, A., Stenhouse, G.B., and Lowe, S. 2010b. Comparison of Landsat multispectral and IRS panchromatic imagery for landscape pattern analysis of grizzly bear habitat in agricultural areas of western Alberta. Canadian Journal of Remote Sensing, 36(1):36-47.

Wang, K., Franklin, S.E., Guo, X., He, Y., and McDermid, G.J. 2009. Problems in remote sensing of landscapes and habitats. Progress in Physical Geography, 33(6): 747-768.